RHODES UNIVERSITY
Where leaders learn

Design, Synthesis, Characterization and Evaluation of Chitosan-based hydrogel for controlled drug delivery system.

A thesis submitted to Rhodes University in fulfilment of the requirements for the degree of

Master of Science (Chemistry)

By

JUSTIN BAZIBUHE SAFARI
B. Pharm. (Official University of Bukavu)
https://orcid.org/0000-0002-8940-9552

Supervised by Professor RUI WERNER MAÇEDO KRAUSE

March 2022

ACKNOWLEDGEMENT

I would like to express my gratitude to all the amazing people who supported me during the achievement of this work.

Mainly, I am so grateful to the following:

Professor Rui Werner Maçedo Krause, my supervisor, who accepted to take me on his shoulders during this scientific adventure and without his thorough remarks and supportive guidance, this work would not have been possible,

The NGO Förderverein Uni Kinshasa e.V./Else-Kroener Fresenius Stiftung for all the intellectual and financial support of my studies through the "Bourse d'Excellence Bringmann aux Université Congolaise" (BEBUC),

Mr. Alain Bapolisi, for mentoring me since day one, for his thoughtful advice, guidance, critics, and for being a good friend,

Marvin Randall for his help on SEM and EDS analysis and Michelle Isaacs for helping with cytotoxicity studies,

The staff members of the Chemistry Department at Rhodes University,

The Chemistry Lab F22 members for being good collaborators,

My family, especially my parents Adolphe Bulibirha and Aimercianne Mapendo, my brothers and sisters Fiston Bazibuhe, Chrispin Bazibuhe, Joelle Bazibuhe, Josué Bazibuhe, Marie Bazibuhe and Josephine Bazibuhe

My unconditional friends and companions, Aliane Naweza, Urbain Ndagano, Bafokeng Sekaleli, Yolande Openda, Christian Nkanga, Baa Ebenezer, Choonzo Chiyumba, Andile Zitha, Christian Irenge, Gracien Misenga, Grady Mukubwa, Bienfait Kabuyaya, Nelson Hendwa, Mihlali Stoffels, and Siphamandla Ruiters.

ABSTRACT

Hepatitis B infection is a deadly infectious disease caused by the hepatitis B virus and is responsible for many deaths every year worldwide. Despite medication and vaccines against hepatitis B infection, it still presents high morbidity and mortality among populations. This is partly due to factors such as a long medication period of the existing treatments, resulting in poor patient compliance and leading to treatment failure. In addition, this situation can be responsible for the observed emerging drug resistance. Hence, novel drugs and drug delivery systems are needed to tackle this matter.

Many strategies have been used to develop long-acting drug delivery systems treatment for several infectious diseases. Hydrogel drug delivery systems have shown interesting results as controlled drug delivery systems for several drugs.

Therefore, the present study aimed to develop chitosan grafted poly (acrylamide-*co*-acrylic acid) hydrogel and apply it as a pH-sensitive controlled delivery system of tenofovir disoproxil fumarate (TDF). TDF is a nucleoside reverse transcriptase inhibitor used as first-line treatment of hepatitis B chronic infection and in the treatment of other viral infections.

The free-radical polymerization method was utilized to modify chitosan by grafting acrylamide and acrylic acid and using *N*, *N*'-methylene bisacrylamide as the crosslinking agent to prepare the hydrogel, followed by an optimization of parameters that could affect the swelling capacity. The prepared chitosan-*g*-poly(acrylamide-*co*-acrylic acid) hydrogel was characterized using Fourier Transmission Infra-red spectroscopy (FTIR), X-Ray Diffraction (XRD), Thermal Gravimetric Analysis (TGA), Differential Scanning Calorimetry (DSC), Energy-dispersive X-ray spectroscopy (EDS), Scanning Electron Microscopy (SEM), and was evaluated for cytotoxicity using a HeLa cell assay. TDF was used as a drug model, it was loaded by the swelling equilibrium method, following by the investigation of the release profile of TDF-loaded hydrogel at pH 1.2 and 7.4.

A successful synthesis of chitosan grafted poly(acrylamide-*co*-acrylic acid) hydrogel was confirmed by Fourier Transmission Infra-red spectroscopy (FTIR), X-Ray Diffraction Spectroscopy (XRD), Thermal Gravimetric Analysis (TGA), Differential Scanning Calorimetry (DSC), Energy-dispersive X-ray spectroscopy (EDS) and Scanning Electron Microscopy (SEM).

Optimization results showed that the ratio of monomers impacted the swelling ratio of the hydrogel and both the concentration of the crosslinking agent, and the reaction initiator also affected the swelling ratio. The synthesized hydrogels were sensitive to pH and ionic strength. Hydrogel swelling was lower in acidic solutions and higher in neutral and basic solutions and decreased with the increasing ionic strength.

Furthermore, SEM results revealed that hydrogel have a rough and fibrous surface structure with numerous pores. Cytotoxicity studies demonstrated that the hydrogel was non-cytotoxic at 50 µg/ml against HeLa cells which suggested a good biocompatibility of the material.

TDF was loaded and released from the hydrogels and showed an encapsulation efficiency and drug loading percentage ranging from 81-96% and 8-10%, respectively. TDF release profile was found to be low in buffer solution of pH 1.2 (in the range of 5-10%) and much higher (38-53%) at pH 7.4 within 96 hours. TDF maintained its chemical integrity after release and the hydrogels can therefore be proposed as a new controlled-release drug delivery system for hepatitis B treatment.

RESUME

L’hépatite B est une maladie infectieuse mortelle causée par le virus de l’hépatite B et est responsable de plusieurs décès chaque année dans le monde. Malgré la disponibilité des médicaments et les vaccins contre cette infection, elle présente toujours une morbidité et une mortalité élevées au sein des populations. Ceci est en partie dû à des facteurs tels qu’une longue période de traitement des médicaments existants, entraînant une mauvaise compliance au traitement par les patients et conduisant ainsi à l’échec du traitement. En outre, cette situation peut être responsable de l’émergence observée de la résistance aux médicaments. Par conséquent, de nouveaux médicaments et systèmes de libération de médicaments sont nécessaires pour résoudre ce problème.

De nombreuses stratégies ont été utilisées pour développer des nouveaux systèmes de libération de médicaments à action prolongée pour le traitement de plusieurs maladies infectieuses. Les systèmes de libération de médicaments utilisant les hydrogels ont montré des résultats intéressants en tant que systèmes de libération contrôlée de plusieurs médicaments.

Par conséquent, la présente étude visait à développer un hydrogel à base du chitosane greffé au poly (acrylamide-*co*-acide acrylique) et à l’appliquer comme système de libération contrôlée sensible au pH du fumarate de ténofovir disoproxil (TDF). Le TDF est un inhibiteur nucléosidique de la transcriptase inverse utilisé comme traitement de première ligne de l'infection chronique par l’hépatite B.

La méthode de polymérisation radicalaire a été utilisée pour modifier le chitosane en greffant l’acrylamide et l’acide acrylique et en utilisant le *N, N′*-méthylène bisacrylamide comme agent de réticulation pour préparer l’hydrogel. Cela a été suivi d’une optimisation des paramètres qui pourraient affecter la capacité de gonflement. L’hydrogel de chitosan-*g*-poly (acrylamide-*co*-acide acrylique) préparé a été caractérisé par la spectroscopie infrarouge à transmission de Fourier (FTIR), la diffraction des rayons X (XRD), l’analyse thermogravimétrique (TGA), la calorimétrie différentielle à balayage (DSC), la spectroscopie des rayons X à dispersion d’énergie (EDS), la microscopie électronique à balayage (SEM), et sa cytotoxicité a été évaluée à l'aide d’un test sur cellules HeLa. Le TDF a été utilisé comme médicament modèle et a été chargé par la méthode de

l'équilibre de gonflement, puis le profil de libération du TDF chargé dans l'hydrogel a été étudié à pH 1,2 et 7,4.

La synthèse de l'hydrogel chitosan-*g*-poly (acrylamide-*co*-acide acrylique) a été confirmée par la spectroscopie infrarouge à transmission de Fourier (FTIR), la spectroscopie de diffraction des rayons X (XRD), l'analyse thermogravimétrique (TGA), la calorimétrie différentielle à balayage (DSC), la spectroscopie des rayons X à dispersion d'énergie (EDS) et la microscopie électronique à balayage (MEB).

Les résultats de l'optimisation ont montré que le rapport des monomères avait un impact sur le taux de gonflement de l'hydrogel et que la concentration de l'agent de réticulation et l'initiateur de la réaction avaient également un impact sur le taux de gonflement. Les hydrogels synthétisés étaient sensibles au pH et à la force ionique. Le gonflement de l'hydrogel était plus faible dans les solutions acides et plus élevé dans les solutions neutres et basiques et diminuait avec l'augmentation de la force ionique.

De plus, les résultats du MEB ont révélé que l'hydrogel a une surface rugueuse et fibreuse avec de nombreux pores. Les études de cytotoxicité ont démontré que le matériau synthétisé était non cytotoxique à 50 µg/ml contre les cellules HeLa, ce qui suggère une bonne biocompatibilité.

Le TDF a été chargé et libéré des hydrogels et a montré une efficacité d'encapsulation et un pourcentage de chargement du médicament allant de 81-96% et 8-10%, respectivement. La libération de TDF s'est avérée faible dans les solutions tampons de pH 1.2 (5-10%) et beaucoup plus élevée (38-53%) à pH 7,4 en 96 heures. Le TDF a conservé son intégrité chimique après la libération et les hydrogels peuvent donc être proposés comme un nouveau système pour une libération contrôlée de TDF pour le traitement de l'hépatite B.

GRAPHICAL ABSTRACT

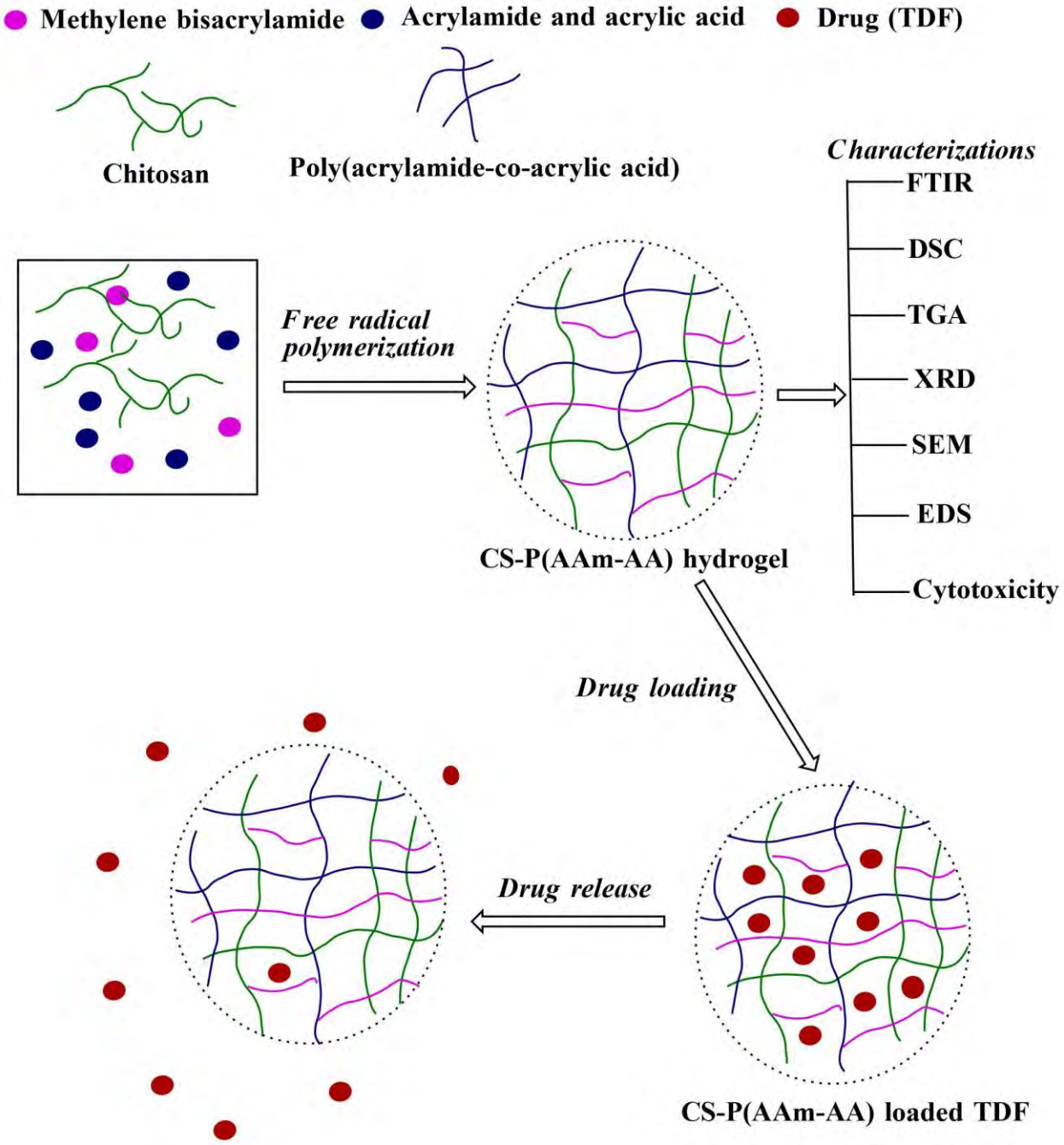

TABLE OF CONTENTS

TABLE OF FIGURES

TABLE OF TABLES

Chapter One

General Introduction

1. GENERAL INTRODUCTION

1.1 Hepatitis B

1.1.1 Introduction

A hepatitis B infection is a liver inflammation caused by the hepatitis B virus (HBV). Chronic infections with HBV are a global public health threat because of its worldwide distribution and potential complications, including cirrhosis, end-stage liver disease, and hepatocellular carcinoma (HCC) (Pastergiou et al., 2015). Regardless of the availability of effective HBV vaccines and antiviral therapies, HBV infection remains a significant cause of death and morbidity in the world in general and particularly in Africa and Asia-Pacific regions. The World Health Organization (WHO), through its global health strategy on viral hepatitis, established in 2016, aims to achieve 90% and 65% reduction of new cases and mortality, respectively caused by hepatitis B in the endemic regions by 2030 (Lemoine and Thursz, 2017; Spearman et al., 2017).

1.1.2 Epidemiology and transmission

According to the most recent estimations of the Global Burden of Disease Study (GBD) and WHO, in 2017, 257 million people were infected with chronic HBV infection, corresponding to a prevalence of 3,9%. The same organizations estimated that in 2017, at least 887 000 people died from chronic HBV infection worldwide (Tan et al., 2021). The overwhelming majority of HBV cases (96.5%) are from low- and middle-income countries. HBV infections are highly concentrated in Asia and Sub-Saharan Africa (**Figure 1.1**). Immigrants from these regions also represent the greatest number of cases of HBV infections in Europe and North America. Just four countries (China, India, Nigeria, and Indonesia) account for almost 50% of all HBV infections (Razavi-Shearer et al., 2018; Razavi, 2020).

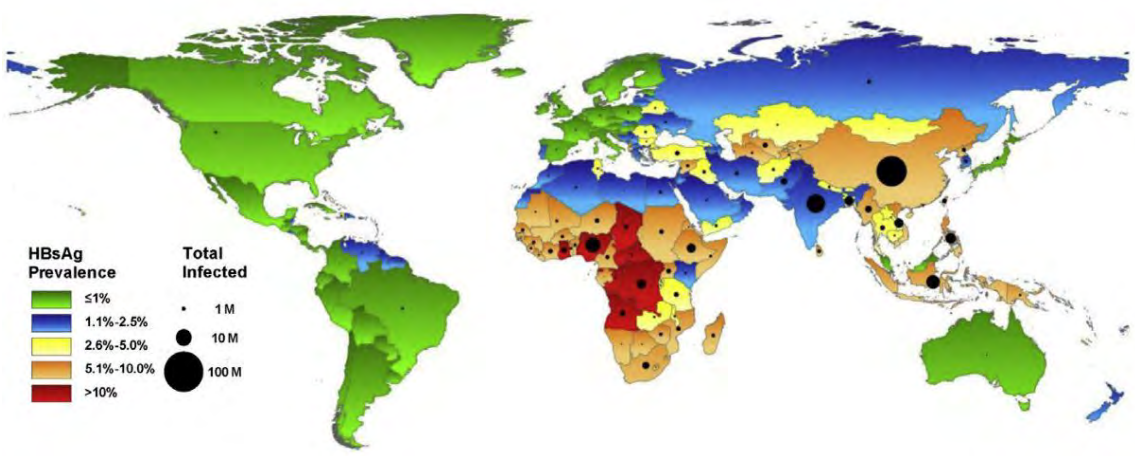

Figure 1. 1: Global distribution of HBV infection 2016 (Razavi, 2020).

The hepatitis B virus is transmitted principally by percutaneous or mucosal contact with infected blood or other biological fluid. The prevalence of the disease determines the predominant mode of transmission. In high endemic areas, HBV is transmitted chiefly vertically from infected mothers to their children around birth, while in low-endemic regions, the virus is transmitted during adolescence and adulthood through high-risk behavior like unprotected sexual intercourse and drug injections (Pastergiou et al., 2015).

1.1.3 Pathogen and pathogenesis

1.1.3.1 Pathogen

The human hepatitis B virus is a DNA virus and is considered the prototype of the genus of orhohepadnavirus. Orthohepadnaviruses are members of the family of Hepadnaviridae, a family of small, enveloped viruses that cause hepatotropic infections. Hapadnaviridae comprise two genera, including avihepadnavirus that infect birds, and orthohepadnaviruses, which infect mammals (Valaydon and Locarnini, 2017).

Hepatitis B virus is a 30-42 nm diameter virion consisting of an envelope and a nucleocapsid containing a circular DNA molecule, a DNA polymerase, a protein kinase enzyme, and a DNA-linked protein (**Figure 1.2**). The envelope carries the hepatitis B surface antigen (HBsAg) and the capsid, the hepatitis B core antigen (HBcAg). An additional antigen related to capsid, hepatitis B e antigen (HBeAg), is detected in the serum when virions are present in the blood (Tiollais et al., 1985).

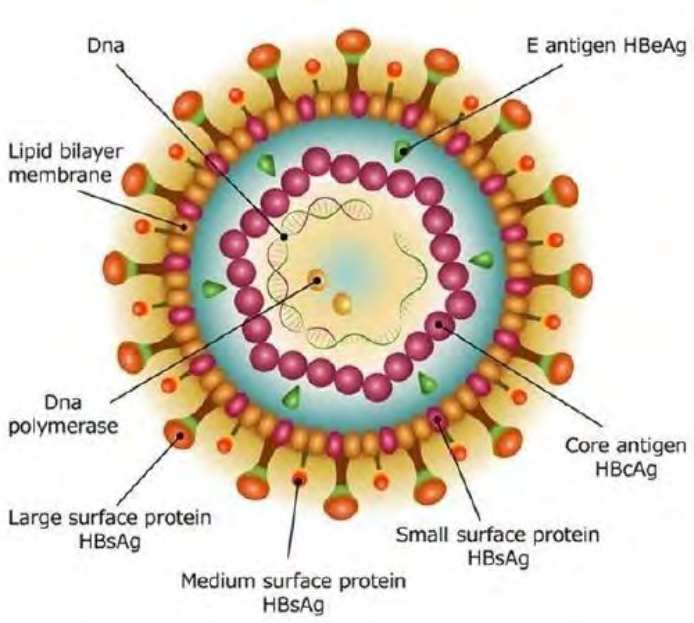

Figure 1. 2: Hepatitis B virus structure (Mckenzie and Logan, 2019)

1.1.3.2 Pathogenesis and virus-host interaction

As a hepatotropic DNA virus that replicates in the liver, (**Figure 1.3**), the totality of liver cells can be infected. The immune system mediates the liver damage induced during HBV infections, making the virus an indirect cytopathic agent. Infection by HBV does not generate the innate immune response; thus, its clearance and pathogenesis are primarily explained by the adaptative immune system (Peppa and Maini, 2012).

In general, replication of virus results in the induction of the innate immune response that is expressed by rapid induction of interferon-alpha/beta (INF α/β) by the infected cell, this production of INF α/β induces the transcriptional expression of several interferon-inducible genes (ISGs). Infection by HBV does not induce any cellular gene expression which makes HBV acting as a stealth virus early after infection (Chisari et al., 2010; Zhang and Hu, 2015).

The adaptive immune response of HBV is expressed through antibodies, CD4 T cells, and CD8 T cells responses. Anti-envelope antibodies play a crucial role in the clearance of the HBV by complexing with free viral particles and removing them from the circulation or by inhibiting their attachment and uptake by hepatocytes. They are usually detectable in patients who clear and recover from acute HBV infection while undetectable in patients with acute HBV infection.

Patients with acute hepatitis who ultimately clear the virus present a vigorous and multi-specific response to HBV peripheral blood CD4 T cell. In contrast, the answer is weak in a patient with chronic HBV infection. (Chisari et al., 2010; Sun et al., 2018).

Moreover, cytotoxic T lymphocyte (CTL) response clears viral infections by inducing apoptosis of infected cells. Briefly, CTLs penetrate the liver and recognize viral antigens that induced two events which are the apoptosis of hepatocytes and replication in the rest of the hepatocytes. Hence, the liver disease in HBV infection is generally due to the cytopathic activity of the CTL response (Baumert et al., 2007; Chisari et al., 2010).

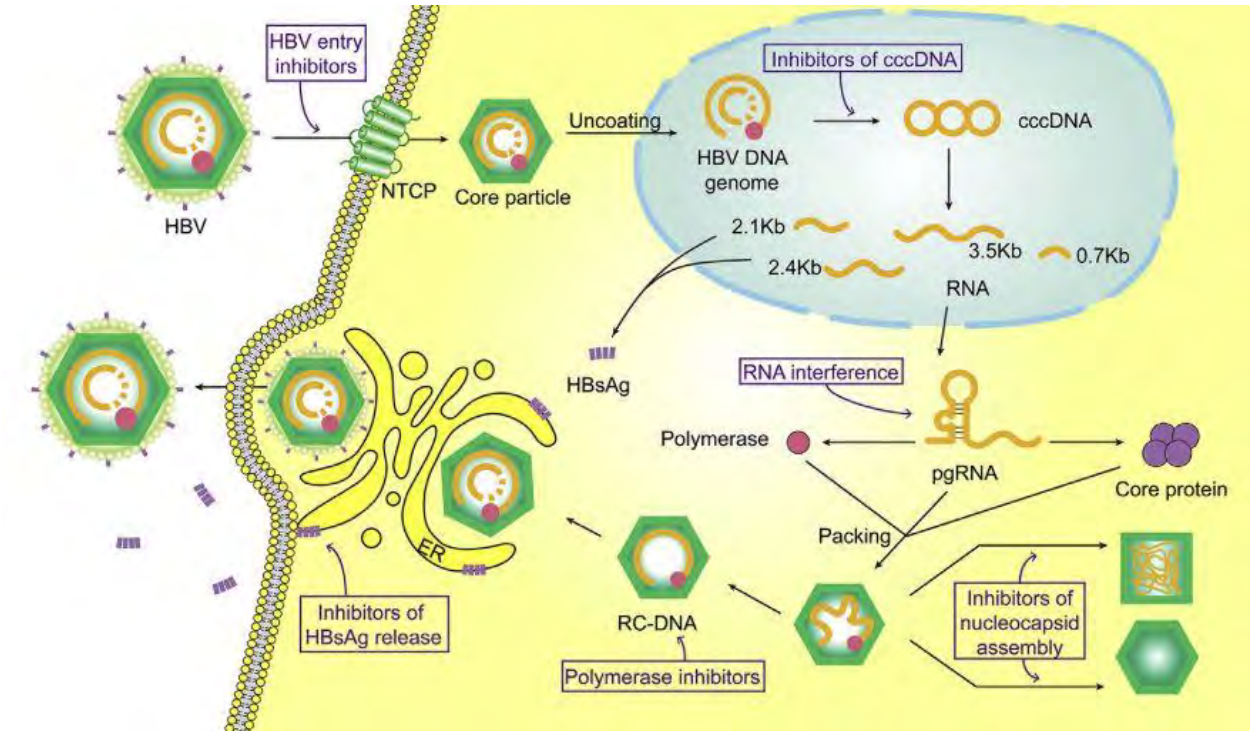

Figure 1. 3: Schematic diagram showing the major stages in the hepatitis B virus (HBV) life cycle, together with the potential therapeutic strategies targeting different levels of the cycle (Sun et al., 2018).

Legend: HBV: hepatitis B virus, NTCP: sodium taurocholate co-transporting polypeptide, cccDNA: covalently closed circular DNA, pgRNA: pregenomic RNA; RC-DNA: relaxed-circular DNA, ER: endoplasmic reticulum.

1.1.4 Diagnosis

The hepatitis B infection can be diagnosis by either serological or virological markers. The HBV viral genes contain three primary transcripts that can be translated to different viral proteins, including surface antigen (HBsAg), e antigen (HBeAg), and core antigen (HBcAg). The presence of HBV induced the production by the host immune system of corresponding antibodies against these viral proteins (anti-HBs, anti-HBe, and anti-HBc). These antibodies and antigens constitute the basis for serological diagnosis of HBV infection (Krajden et al., 2005; Song and Kim, 2016).

The surface antigen (HBsAg) is the first serological marker detected in acute HBV infections; it is considered the infection's hallmark. HBsAg is used to diagnosed acute HBV infections and its persistence for more than six months suggests a chronic disease. Moreover, the presence of HBeAg generally indicates active replication of HBV and a high probability of transmission. Serum HBV DNA is the most used virological marker in the diagnosis of HBV infection. Hence, monitoring of serum HBV DNA levels is essential for assessing liver disease activity, differentiating other causes of hepatitis activity in HBV carriers, predicting risk of HCC development or liver-related mortality, deciding to administer antiviral therapy, determination of the response to antiviral treatment, indicating the risk of developing drug resistance, and detecting the emergence of drug-resistant mutants (Kao, 2008).

1.1.5 Prevention and treatment of HBV infection

Prophylactic measures for HBV infection include avoiding high-risk behaviors (unprotected sexual intercourse, uncontrolled drug injections, etc.), avoiding exposure to infected blood and body fluids, screening pregnant women for HBV and active or passive immunization before or after exposure. Vaccines are used for active immunization, and hepatitis B immune globulin (HBIg) is used as a passive immunization (Kwon and Lee, 2011; Sarah et al., 2018).

For patients with chronic HBV infections, there are two therapy strategies: therapy with a defined duration consisting of immunomodulators like standard or pegylated interferon-α, and a long-term treatment regime with nucleoside or nucleotides analogues including lamivudine, adefovir dipivoxil, entecavir, telbivudine, or tenofovir (Tang et al., 2014).

Despite the existing preventive and therapeutic tools for HBV, the elimination of this disease is still a problem for different reasons such as the availability and affordability of both vaccine and

antihepatitic B drugs in endemic areas, the absence of national vaccination programs against HBV in many countries, and recently, the emergence of resistant HBV mutants towards existing drugs. Hence, deferent strategies need to be developed in other to tackle these problems. The emergence of antimicrobial resistance is a significant threat to world health. In the case of hepatitis B, the long medication regimen may be one reason for that emergence; thus, developing strategies to alleviate that situation can slow down that emergence. In those perspectives, we are suggesting in this thesis that the development of a long-acting formulation (one of the strategies used to fight against the AMR) of an existing antihepatitic drug (tenofovir disoproxil fumarate) could be used in the fight against HBV and other viral diseases.

1.1.6 Tenofovir disoproxil fumarate (TDF) drug profile

1.1.6.1 Physicochemical and molecular aspects

Table 1. 1: Physicochemical properties of TDF

Characteristic	**Description**
Molecular formula	$C_{23}H_{34}N_5O_{14}P$
Molecular weight	635.5 g/mole
Structure (TDF)	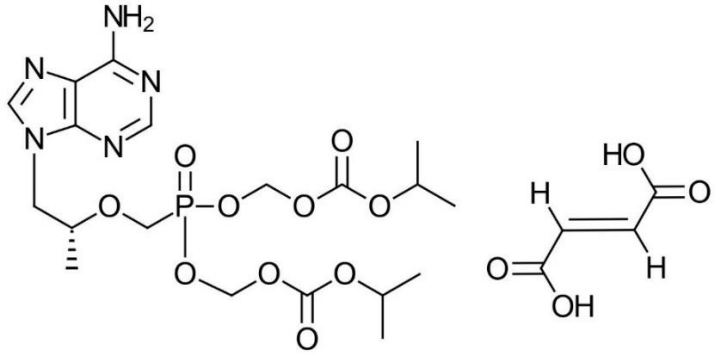
Systemic name (IUPAC)	[[(2*R*)-1-(6-aminopurin-9-yl) propan-2-yl] oxymethyl-(propan-2-yloxycarbonyloxymethoxy) phosphoryl] oxymethyl propan-2-yl carbonate; but-2-enedioic acid
Organoleptic characters	TDF is a white, fine, powder-like crystalline material
Melting point	113-115° C
Solubility	In water, 13.4 mg/mL at 25 °C

Production of tenofovir disoproxil fumarate (TDF)

TDF is a prodrug of tenofovir which was the first nucleoside reverse transcriptase inhibitors (NRTI) approved for the treatment of HIV. The prodrug was synthesized for improved oral absorption and cellular uptake of tenofovir (Piliero, 2004). TDF can be produced by many synthetic methods. Among them the synthesis of Visireddy *et al.* and the synthesis of Satyanarayana which are described at **Figure 1.4** (Mandala et al., 2016).

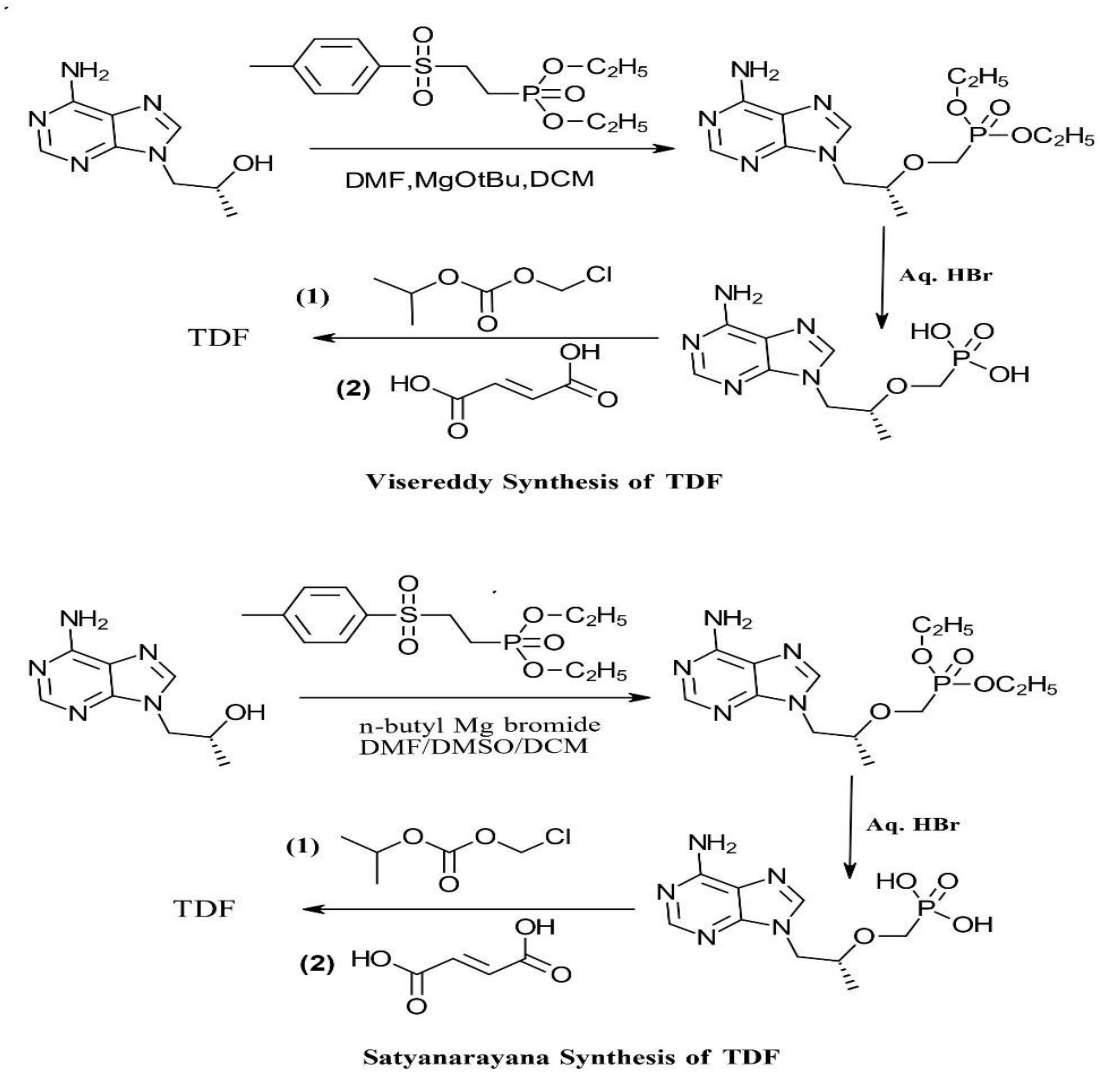

Figure 1. 4: Synthesis of TDF adapted from Mandala et al., 2016

1.1.6.2 Pharmacological aspects of tenofovir (TDF)

- ***Drug Class:*** Nucleoside reverse transcriptase inhibitors (NRTIs)

- ***Available dosage:*** Oral tablet
- ***Daily dosage:*** The recommended dosage of TDF is 300 mg administrated once a day with a meal (Chapman et al., 2003).
- ***Mechanism of action:*** TDF is a prodrug and produces the active drug, tenofovir by hydrolysis, which is then phosphorylated by the action of cellular kinase to form tenofovir diphosphate, which is a pharmacologically active metabolite. Tenofovir diphosphate inhibits the reverse transcriptase by competing with the nucleotide deoxyadenosine 5'-triphosphate for integration into viral DNA. Its incorporation into viral DNA stops DNA elongation due to the absence of the ribose ring (Chapman et al., 2003).
- ***Pharmacokinetic:*** TDF has an extended serum and intracellular half-lives (~17 h and 10-50 h, respectively); it is mainly cleared by the renal way, and a reduction of the dose is required in a patient with renal problems. The bioavailability is ~ 40%, and it is increased when administrated with a high-fat meal but is not affected with a lower-fat meal. TDF does not induce or inhibit the cytochrome p450 enzyme system (Gallant and Deresinski, 2011).
- ***Therapeutic indications:*** TDF is indicated in the treatment of HIV in combination with other antiretroviral drugs (Chapman et al., 2003) and the treatment of HBV infection (Elazar et al., 2017).
- ***Contraindications and precautions:*** TDF is contraindicated for the patient with known hypersensitivity on TDF, Previous hypersensitivity to any components, and renal insufficiency. Lactic acidosis and severe hepatomegaly with steatosis can be observed with tenofovir disoproxil fumarate and can be fatal in some cases. Obesity and prolonged nucleoside therapy may be predisposing factors (Porche, 2002).
- ***Adverse effects:*** The most observed adverse effects are Nausea, diarrhea, asthenia, headache, vomiting, flatulence, abdominal pain, and anorexia (Chapman et al., 2003).
- ***Drug interactions:*** The lack of interaction of tenofovir with CYP enzymes (it is neither a substrate nor an inhibitor) suggests a potential low clinical importance for drug-drug interactions with the drug, which are substrate or inhibitor/inducer of the CYP enzymes.

Today, tenofovir has demonstrated relevant clinical pharmacokinetics drug-drug interaction only with didanosine and atazanavir, their combination requires adjustments of the dosage of these agents (Kearney et al., 2004).

1.2 Hydrogels

The term “hydrogel” was used for the first time in 1894 by Lee, Kwon, and Park and was used to describe a colloidal gel made with inorganic salts (Chirani et al., 2015). Hydrogels, as defined today, were developed in the 1960s, primarily by Wichterle and Lim (Buwalda et al., 2017) as three-dimension polymeric networks as illustrated in **Figure 1.5**.

Hydrogels are based on hydrophilic polymers and can retain a large amount of water in their structure without dissolving (Gulrez et al., 2011; Hoare and Kohane, 2008; Mohite and Adhav, 2017; Narayanaswamy and Torchilin, 2019). Their property of taking up liquid is due to hydrophilic functional groups attached to the polymeric chains, such as amide, amino, carboxyl, and hydroxyl groups, which can ionize when in contact with water (Ferreira et al., 2018).

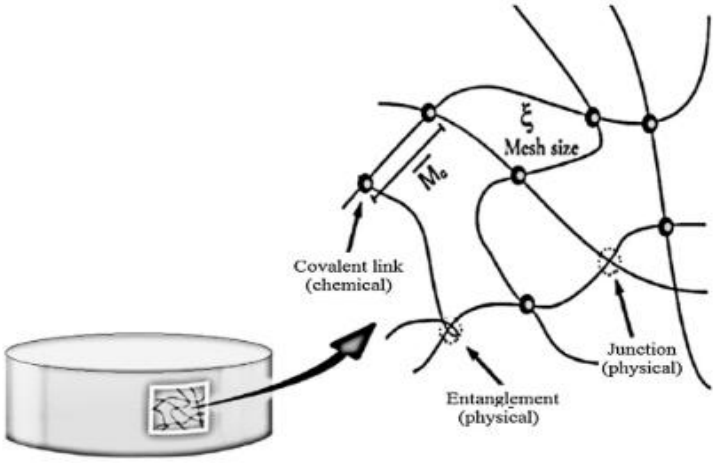

Figure 1. 5: 3D structure of hydrogels

Properties of hydrogels like softness, smartness, and their capacity to store water make hydrogels unique materials and suitable candidates for many applications (Mohite and Adhav, 2017). Most biomedical applications of hydrogels are due to their potential to simulate biological tissue when swollen. They have applications in contact lenses, wound dressing, biosensors, drug delivery, tissue engineering, and hygiene products (Caló and Khutoryanskiy, 2015). Hydrogels present many advantages as a therapeutic delivery system, including biocompatibility, biodegradability,

and non-toxicity (Gyles et al., 2017). Moreover, their physical properties, such as surface characteristics, swelling, and mechanical strength, can be modulated by physicochemical reactions to improve elasticity and mechanical resistance, which are essential features to consider when developing drug delivery systems (Ferreira et al., 2018).

1.2.1 Classification

The classification of hydrogels is mainly based on the source of polymers, ionic charge, polymeric composition, physical properties, degradability, cross-linking technique, and response to the environment (Ullah et al., 2015).

1.2.1.1 Source of polymers

Regarding the origin of polymers entering in their composition, hydrogels are subdivided into the following three groups:

Natural hydrogels are formed by natural polymers such as polysaccharides, proteins, etc. Polysaccharides are the most commonly used natural polymers to design hydrogels. They offer many advantages including, water-solubility, high swelling capacity induced by simple chemical modifications, a wide variety of chemical structures, biocompatibility, biodegradability, etc. However, natural hydrogels do have some limitations, for example they do not have strong mechanical properties and are not easily controllable due to their batch-to-batch variation. This is the reason why natural hydrogels are most of the time combine with synthetic moieties to improve these limitations (Catoira et al., 2019). Polysaccharides most often used in preparing hydrogels are alginate, chitosan, carrageenan, gellan gum, guar gum, pectin, cellulose, agarose, and xanthan gum. Proteins are the other class of natural polymers used for the design of hydrogels. Protein-based hydrogels have similar structural, mechanical, and chemical properties with the extracellular matrix, which gives them high biocompatibility and the potential to activate the precise cellular response. As well, these hydrogels can be degraded by proteolytic enzymes. For these reasons, they are one of the most used materials in tissue engineering. The silk fibroin from spider webs, collagen from skin, keratin from wool/ hair, bone and tendons, elastin from elastic tissues, fibrin from blood clots, and resilient from insect tendons are the best examples of commonly used proteins (Jonker et al., 2012; Varaprasad et al., 2017).

Synthetic polymeric hydrogels are a class of hydrogels prepared from polymers produced by chemical synthesis. Synthetic hydrogels possess many advantages, such as large water absorption abilities and good gel strength and cost. Synthetic hydrogels differ in their characteristics due to their various chemical structures, synthesis techniques, and water content or cross-linking. Raw materials used to prepare synthetic hydrogels include poly(*N*-vinyl-pyrrolidone), poly(electrolyte complexes) and poly(vinyl alcohol), poly(hydroxyalkyl methacrylate), poly(acrylate), poly(acrylamide), poly(meth-acrylamide) and its derivatives, poly(*N*-vinyl-2-pyrrolidone) and poly(vinyl alcohol) etc. (Patel and Dalwadi, 2013; Varaprasad et al., 2017). Even though synthetic hydrogels exhibit several advantages, their broader use is limited sometimes by their toxic character, poor biocompatibility and biodegradability (Shi et al., 2014). Hence, to overcome this for taking advantage of both the interesting properties of the natural and synthetic hydrogel, a class of hybrid hydrogel has been developed.

Semisynthetic hydrogels (hybrid) are hydrogels composed of natural and synthetic polymers moieties. This class is the most investigated due to many advantages over natural and synthetic ones, typically including the best of both classes of hydrogel (Buwalda et al., 2017). These hybrid hydrogels have the benefit of combining several functions such as improving physical characteristics, crosslinking capabilities, bio adhesion qualities, proteolytic degradation properties into a single hydrogel system, and balance the mechanical properties. They have also in some case limitations like cytotoxicity, low biocompatibility etc. (Bashir et al., 2017; Singhal and Gupta, 2015).

1.2.1.2 Ionic charge

Based on the presence or absence of electrical charge on the cross-linked chains of hydrogels, they are categorized into three classes. Firstly, neutral, or non-ionic hydrogels that have an overall charge of zero. Secondly, ionic hydrogels, which are further subdivided into two subclasses. Cationic hydrogels, which are hydrogels having a positive charge in their structure (hydrogels based on chitosan, poly(lysine), poly (amido-amine, etc.); and anionic hydrogels with a negative charge (e.g., hydrogels based on poly (acrylic acid) and its derivatives, etc.). Thirdly, amphoteric hydrogels contain both negative and positive charges in their cross-linked chains (Ullah et al., 2015).

1.2.1.3 Polymeric composition

According to the preparation methods, hydrogels are classified as followed:

Homopolymeric hydrogels they are polymer network systems originating from the specific class of monomer comprising the polymer network. Homopolymers may have a cross-linked backbone structure depending on the monomer and polymerization technique (Mohite and Adhav, 2017).

Copolymeric hydrogels: These are comprised of two or more different monomer species with at least one hydrophilic component. Monomers are arranged in a random, block, or alternating configuration along the chain of the polymer network (Mohite and Adhav, 2017).

Interpenetrating polymeric hydrogels (INP): INPs are defined as the combination of two polymers where the individual chains are entangled. Often at least one is synthesized or cross-linked in the presence of the other. It's done by mixing a pre-polymerized component into a solution of monomers and a polymerization initiator (Mohite and Adhav, 2017; Ullah et al., 2015).

1.2.1.4 Physical properties

Conventional hydrogels: they are hydrogels, which exhibit swelling/deswelling properties linked only to water availability in the environment (Ferreira et al., 2018).

Smart hydrogels: (see ***1.2.1.6***) also called "intelligent" or stimulus-responsive hydrogels are systems that respond immediately to a change in their environment. The stimulus that is responsible for the change in physicochemical and mechanical properties of smart hydrogel can be of different nature. Stimuli may be classified as chemical (pH, oxidant, glucose concentration, etc.), physical stimulus (temperature, pressure, light, electric, magnetic field, etc.), and biochemical stimulus (antigens, ligand, and enzymes) (Rizwan et al., 2017; Sood et al., 2016b; Ullah et al., 2015).

1.2.1.5 Cross-linking

Physically cross-linked hydrogel: In this class of hydrogel, the network structure is formed by physical interactions between the different components of the hydrogel. This hydrogel are crosslinked by weak bonds like hydrogen bonds, ionic interactions, host–guest chemistry, hydrophobic interactions, coordination bonds and π-π stacking interactions (Ding and Wang, 2017). According to the desire physical interactions different polymers can be used to achieve

specific interaction like van der Waals forces, hydrogen bonds in native starch, and ionic interactions predominantly with multivalent metal cations (e.g., alginate hydrogel formed in the presence of calcium ions) (Kulicke and Nottelmann, 2000).

Chemically cross-linked hydrogels: In these hydrogels, the networks are produced by the formation of covalent bonds. These types of networks may be created using different strategies. In some cases by using the reactive side or end groups of linear polymers and in other cases by using crosslinking agents (bi or multifunctional compounds) to create permanent networks between the polymers (e.g., *N,N,N′,N′*-tetramethylethylenediamine, *N,N′*-methylene bisacrylamide, glutaraldehyde, etc.) (Kulicke and Nottelmann, 2000).

1.2.1.6 Stimuli-responsive hydrogels

Stimuli-responsive hydrogels react to a change in their environment and experience changes in their swelling behavior, mechanical strength, network structure, and permeability, therefore called environmentally sensitive, intelligent, or smart hydrogels (Ullah et al., 2015).

Chemically responsive hydrogels: These are hydrogels that respond to a change in some chemical features in the surrounding environment of the hydrogel. In pH-sensitive hydrogels, for example, a change in pH directly affects interactions between polymers chains and solvents molecules. Such hydrogels are made with polymers containing ionizable groups that can donate or accept protons in response to a change in pH, which primarily results in solubility and structural changes and, consequently, swelling or deswelling (Ferreira et al., 2018). Most used pH-sensitive polymers to design pH-sensitive hydrogel are polyvinyl amine-containing either acidic or basic group's, e.g., poly acrylic acid (PAA; an anionic polymer) dissolves/swell more at high pH due to ionization, whereas poly(*N,N*-diethylamino ethyl methacrylate) (PDEAMA; a cationic polymer) swells more at low pH (Sood et al., 2016a). The other type of chemically responsive hydrogels is salt- or ionic strength-responsive hydrogels; these are hydrogels that undergo some structural changes in different salt concentrations in the surrounding medium(Li, 2009). Other chemically responsive hydrogels are glucose-responsive, CO_2-responsive, redox-responsive, etc. (Li and Mooney, 2016; Rizwan et al., 2017).

Physically responsive hydrogels: are hydrogels that undergo several changes in their physicochemical properties when there is a change in some physical properties of their environment (Li, 2009). Physical features most exploited to design physically responsive

hydrogels are temperature, light, pressure, magnetic fields, ultrasound, and electrical fields (Rizwan et al., 2017; Ullah et al., 2015). For example, thermo-responsive hydrogels are mostly used in the development of injectables hydrogels delivery system and as tissue engineering material due to the property of *in-situ* formation of some of these hydrogels. Light sensitive hydrogel are mostly used to design diagnostic material like biosensors (Overstreet et al., 2012; Yang et al., 2014).

Biologically responsive hydrogel: These hydrogels show responses by changing their shape or volume when exposed to biological stimuli such as enzymes, antigens, glutathione, and DNA (Rizwan et al., 2017). Bio-responsive hydrogels have gained significant interests for applications in drug delivery, tissue engineering, wound healing, and design of diagnostics materials. A great number of work on bio-responsive hydrogels for drug delivery have been done for the release of insulin in response to raise of glycemia (Ulijn et al., 2007).

1.2.2 Preparation methods

Hydrogels are prepared using various techniques. According to the type of cross-linking that is created during the preparation process, these techniques can be categorized into two main groups. Hence, there are methods to either prepare chemical or physical cross-linking hydrogel.

1.2.2.1 Physical cross-linking preparation methods

i. Heating/ cooling a polymer solution.

Some polymer solutions, when heated and cooled, formed hydrogels due to physical interactions. In some cases, the gel formation is due to the helix-formation, association of the helices, or creating junction zones. In other instances, the hydrogel can also be obtained by heating then cooling the polymer solutions that cause block copolymerization. Carrageenan and gelatin hydrogels can be prepared using this method. For carrageenan, the reaction is made in the presence of salt (NaCl, KCl, etc.) to reduce repulsion between the sulfonic groups in other to have a stable hydrogel (Gulrez et al., 2011).

ii. Ionic interaction

Physical cross-linking hydrogels are formed when ionic polymers are mixed with a di- or tri-valent ion of the opposite charge. For example, a hydrogel network can be created when sodium alginate (Na^+ $alginate^-$) is mixed with calcium chloride solution (Ca^{2+} + $2Cl^-$) (Gulrez et al., 2011).

iii. Complex coacervation

Mixing polymers of opposite charges (polyanion with polycation) leads to a complex coacervate gel formation. In this method, the construction of the hydrogel is based on the principle that polymers with opposite charges stick together and formed soluble and insoluble complexes depending on the concentration and pH of the respective solutions. For instance, a coacervate hydrogel is formed by mixing xanthan gum (polyanionic) with chitosan (polycationic) solutions (Gulrez et al., 2011; Patel and Dalwadi, 2013).

iv. Hydrogen bonding

Hydrogen bonded hydrogel can be prepared by changing the pH of an aqueous solution of polymers carrying carboxyl groups which shows pH-dependent swelling of the gels. Hydrogen bonds are formed only if the protonation of carboxylic acid groups occurs (Akhtar et al., 2016). An example of such hydrogel is a hydrogen-bond CMC (carboxymethyl cellulose) network formed by dispersing CMC into 0.1M HCl (Gulrez et al., 2011).

v. Maturation (heat-induced aggregation)

Some gums such as gum arabic, gum ghatti, and acacia kerensis are predominantly composed of saccharides but contained sections of proteins as integral parts of their structures. Heat treatment of these materials induce aggregation of the protein components, producing a hydrogel by enhancing mechanical properties and water binding. The molecular changes that result from the maturation process show that a hydrogel can be formed with precisely structured molecular dimensions. The technique is also mainly used to prepare protein and polypeptides-based hydrogels like collagen, gelatin, or albumin-based hydrogels (Jonker et al., 2012; Patel and Dalwadi, 2013). The difference with this technique with the first one is that in this one there is no need to cool the mixture in other to form the hydrogel, it is formed only by heating.

vi. Freeze-thawing

The freeze-thaw cycles can result in the formation of hydrogels by creating physical cross-linking within the polymer chains. The mechanism involves the construction of microcrystals in the structures of the polymer due to freeze-thawing. For example, the mixture of polyvinyl alcohol with xanthan formed a hydrogel after freeze-thawed treatment (Gulrez et al., 2011; Patel and Dalwadi, 2013).

1.2.2.2 Chemical cross-linking preparation methods

i. Cross-linking by radical polymerization

Chemically cross-linked hydrogels can be obtained by radical polymerization of low molecular weight monomers in the presence of crosslinking agents (Akhtar et al., 2016). The free radical that initiates the polymerization reaction is produced by several processes capable of generating radicals. Hence, radicals can be created through the application of heat (thermal), ultraviolet and visible light (photochemical), ionizing light, redox reagents, electricity (electrochemical), etc. (Charles and Carraher, 2017). This method is used to prepare a considerable number of hydrogels like poly (2-hydroxyethyl methacrylate) (pHEMA), obtained by polymerization of 2-hydroxyethyl methacrylate (HEMA) in the presence of a suitable crosslinking agent like ethylene glycol di-methacrylate (Akhtar et al., 2016; Hennink and van Nostrum, 2012). Apart from radical polymerization of vinyl-monomers mixtures, chemically cross-linked hydrogels can also be prepared by radical polymerization of water-soluble polymers containing polymerizable groups. Many hydrophilic (synthetic, semi-synthetic, and natural) polymers have been used to design hydrogels by radical polymerization (Hennink and van Nostrum, 2012).

ii. Cross-linking by chemical reaction of complementary groups

Water-soluble polymers used in preparation of hydrogels owe their hydrophile property to the presence of some hydrophilic functional groups in their structures, mainly hydroxyl (OH), carboxylic (COOH), amide ($CONH_2$), and amine (NH_2). These functional groups are involved in chemical modifications to form hydrogels. Thus covalent bonds between polymer chains can be established by reacting functional groups with complementary reactivity, such as an amine-carboxylic acid or Schiff base formation, or an isocyanate-amine (or hydroxyl) reaction (Hennink and van Nostrum, 2012; Ullah et al., 2015).

a. Crosslinking with aldehydes

Water-soluble polymers with hydroxyl functional groups (e.g., poly (vinyl alcohol)) can be cross-linked using cross-linking agents containing aldehyde function (e.g., glutaraldehyde) (**Figure 1.6**). To establish this crosslinking, extreme conditions must be applied (low pH, high temperature, methanol added as quencher). In contrast, polymers containing amine functional groups can be cross-linked with the same reagent under mild conditions whereby the so-called Schiff bases are formed. This method has primarily been used for the preparation of cross-linked proteins (e.g.,

albumin and gelatin) and amine-containing polysaccharides (e.g., partially oxidized dextran) (**Figure 1.6**) (Hennink and van Nostrum, 2012).

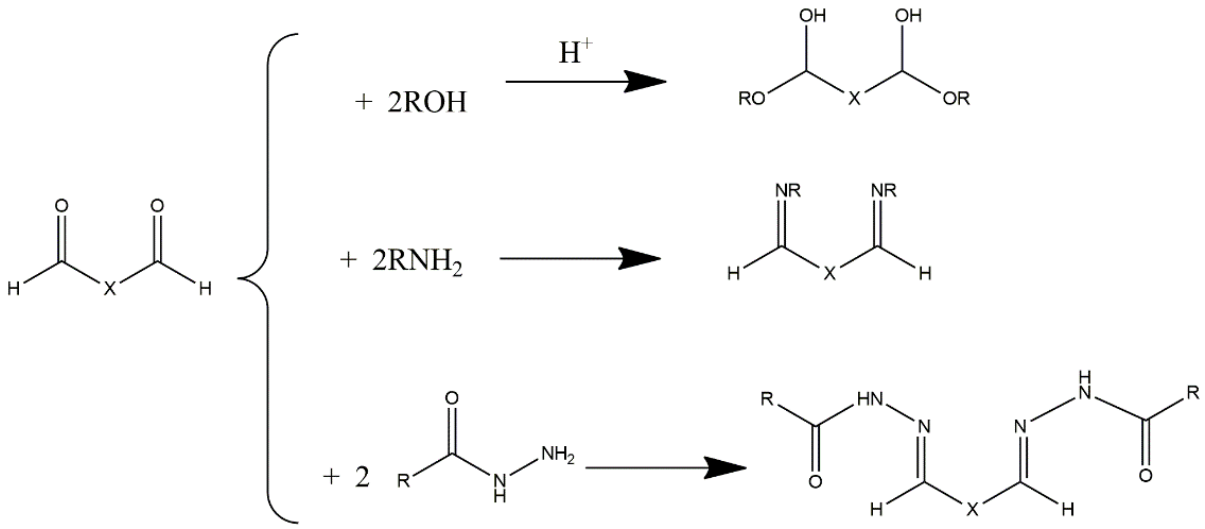

Figure 1. 6: Aldehyde-mediated crosslinking of polymers containing alcohol, amine, *or hydrazine groups (R represents the polymer chains, X is any spacer, e.g. $(CH_2)_3$ in the case of glutaraldehyde).*

b. Cross-linking by addition reaction

Water-soluble polymers can be changed into hydrogels using bi or multi-functional cross-linking agents, which react with functional groups of polymers via addition reactions (Hennink and van Nostrum, 2012). Properties of the prepared hydrogel can be optimized by the concentration of the polymer and the amount of the cross-linking agent used during the preparation. Reactions are preferably carried out in organic solvents because water can also react with the cross-linking agent. For example, polysaccharides can be cross-linked by addition reactions with 1,6-hexamethylene diisocyanate, divinyl sulfone (**Figure 1.7**), 1,6-hexane dibromide, and many other reagents (Coviello et al., 1999; Hennink and van Nostrum, 2012).

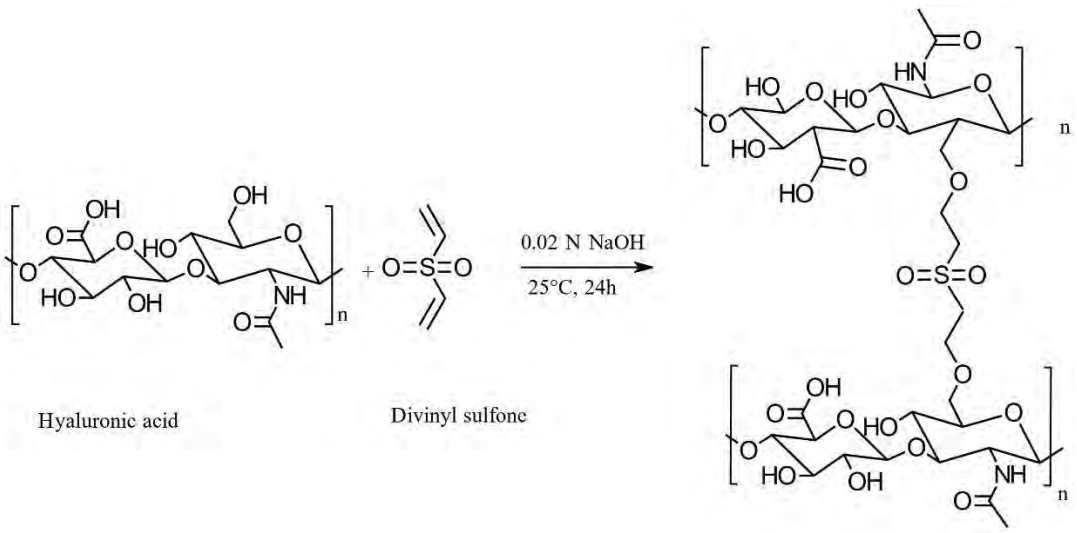

Figure 1. 7: Cross-linking reaction scheme of hyaluronic acid with divinyl sulfone (Lai, 2014).

c. Cross-linking by condensation reactions

Condensation reactions between hydroxyl groups or amines with carboxylic acids or derivatives hereof are frequently applied to synthesize polymers to yield polyesters and polyamides, respectively. These types of reactions are also used for the preparation of hydrogels. (Hennink and van Nostrum, 2012). Many hydrogels based on carboxylated polysaccharides are obtained by using this method. The Passerini and Ugi multicomponent condensation reactions are the most used for that purpose. In the Passerini condensation, carboxylic acid and a carbonyl (aldehyde or ketone) are condensed with an isocyanide derivative, which after acyl rearrangement and tautomerization, yields an α-(acyloxy) amide (**Figure 1.8**). While in the Ugi condensation, an amine is added to the mixture of the Passerini condensation (carboxylic acid, carbonyl, and isocyanide) to form an α-(acylamino) amide (**Figure 1.9**). The reaction is carried out in aqueous conditions with a slightly acidic pH and at room temperature. Since the Passerini condensation generates hydrogels with ester bonds in their crosslinks, these gels degrade at ambient temperature and pH 9.5. The degradation time varied, depending on their composition, from 1 to 8 days, but hydrogels prepared by the Ugi condensation contain amide bonds in their crosslinks; they are stable under these conditions.

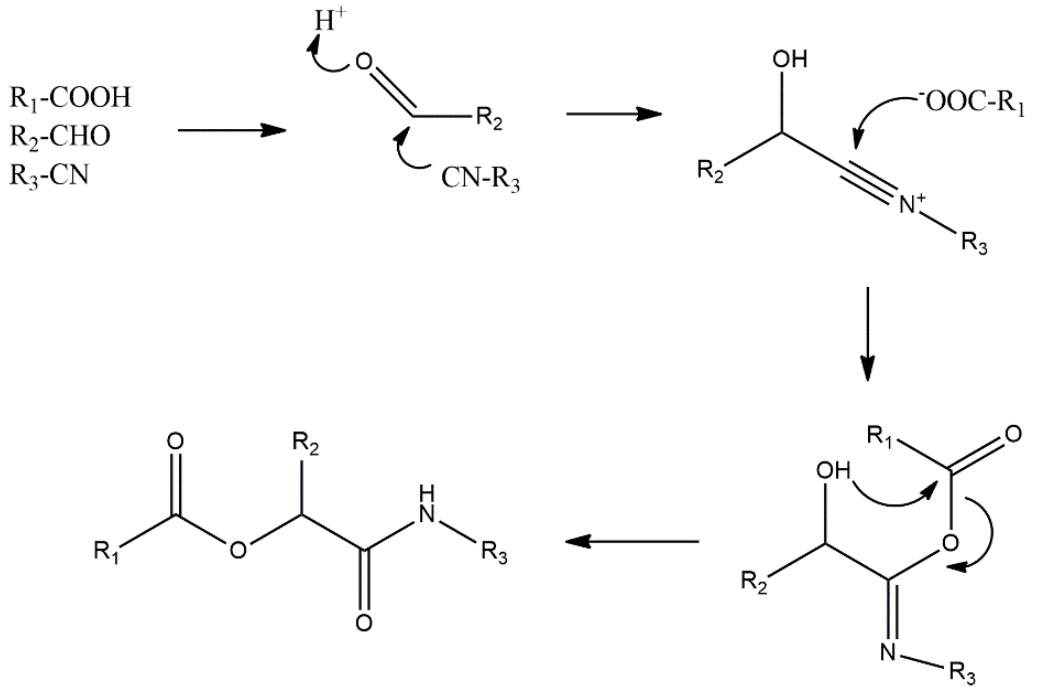

Figure 1. 8: Passerini condensation reaction

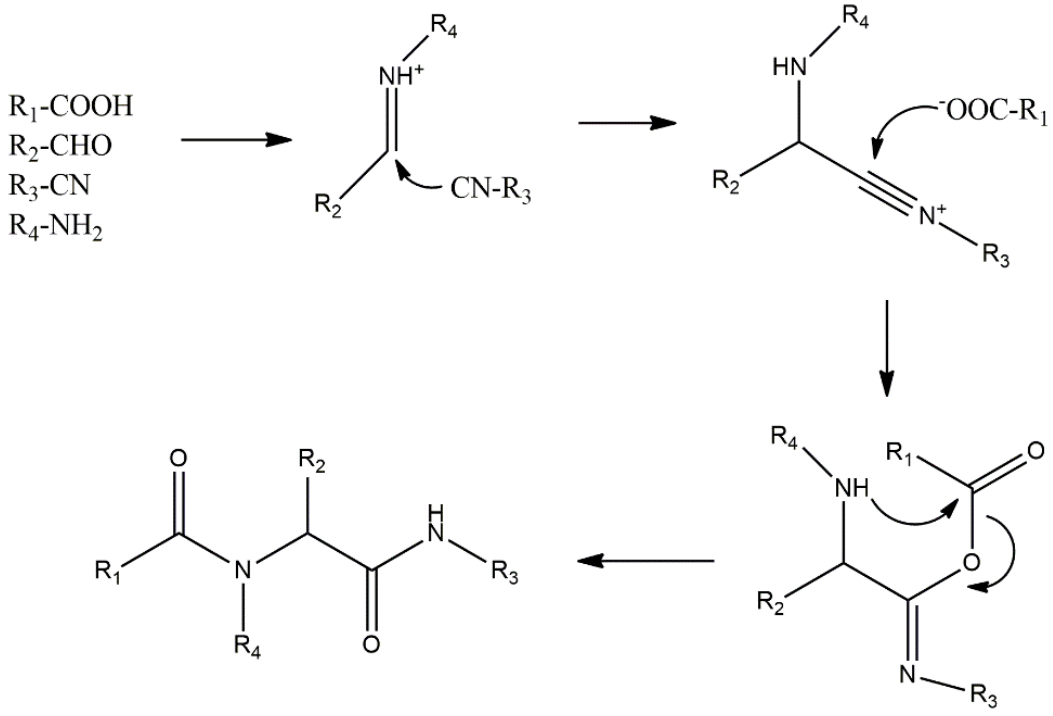

Figure 1. 9: Ugi condensation reaction

iii. Cross-linking by high energy radiation

Polymeric networks can be generated by irradiating some polymers or monomers using high-energy ionizing radiation, like electron beams, gamma, or x-rays. Gamma irradiation is the most commonly used for different advantages. Firstly, it is the most economical, used at lower doses (~80 kGy and below) and offers large, high-density parts (Maitra and Shukla, 2014). Unsaturated compounds can be polymerized by using high-energy radiation, in particular gamma and electron beams. Therefore, water-soluble polymers derivatized with vinyl groups can be converted into hydrogels using this high-energy irradiation. Hydrogels can be produced by irradiation of a mixture of a monofunctional acrylate (e.g., acryloyl-l-proline methyl esther) and a suitable crosslinker. In addition, water-soluble polymers can be converted into hydrogels by high-energy irradiation without adding vinyl groups. During irradiation of polymers in an aqueous solution, radicals can be formed on the polymer chains by, e.g., the homolytic scission of C-H bonds. Furthermore, the radiolysis of water molecules generates hydroxyl radicals that can attack polymer chains to form macroradicals. Recombination of the formed macroradicals results in the formation of covalent bonds and finally in a cross-linked structure. As the generated macroradicals can react with the oxygen, the reaction is performed in an inert atmosphere (under nitrogen or argon gas) (Devasani et al., 2016; Hennink and van Nostrum, 2012).

iv. Enzymatic cross-linking.

Enzymes are proteins that catalyse biochemical and chemical reactions, and a high specificity characterizes them in the reaction they catalyse and their choice of substrates (Park et al., 1993). Enzymes can be used to initiate the cross-linking of polymers and thus form hydrogels. Recently, increasing interest has been devoted to enzymatically cross-linked hydrogels. This is mainly due to, on the one hand, the fact that hydrogels produced by this process offer good biocompatibility, fast gelation processes, and tuneable mechanical properties, and on the other hand, enzymatic biocatalysts are environment friendly and work under mild conditions. The majority of the enzymes involved in the crosslinking are common to the enzymes catalysing reactions occurring in the human body, and this also offers the advantage of preparing enzyme responsive hydrogels, which is gaining interest, especially in the field of drug delivery (Federsel et al., 2021; Moreira et al., 2012). Horseradish peroxidase (HRP) is the most widely used enzyme for preparing hydrogels because of its high stability and good biocompatibility. Horseradish peroxidase is a hemoprotein that catalyzes the coupling of aniline or phenol derivatives via a carbon-carbon bond or a carbon-

nitrogen/oxygen bond with the presence of hydrogen peroxide (Ren et al., 2012). **Figure 1.10** demonstrate the use of HRP in preparing hyaluronic acid-tyramine hydrogel.

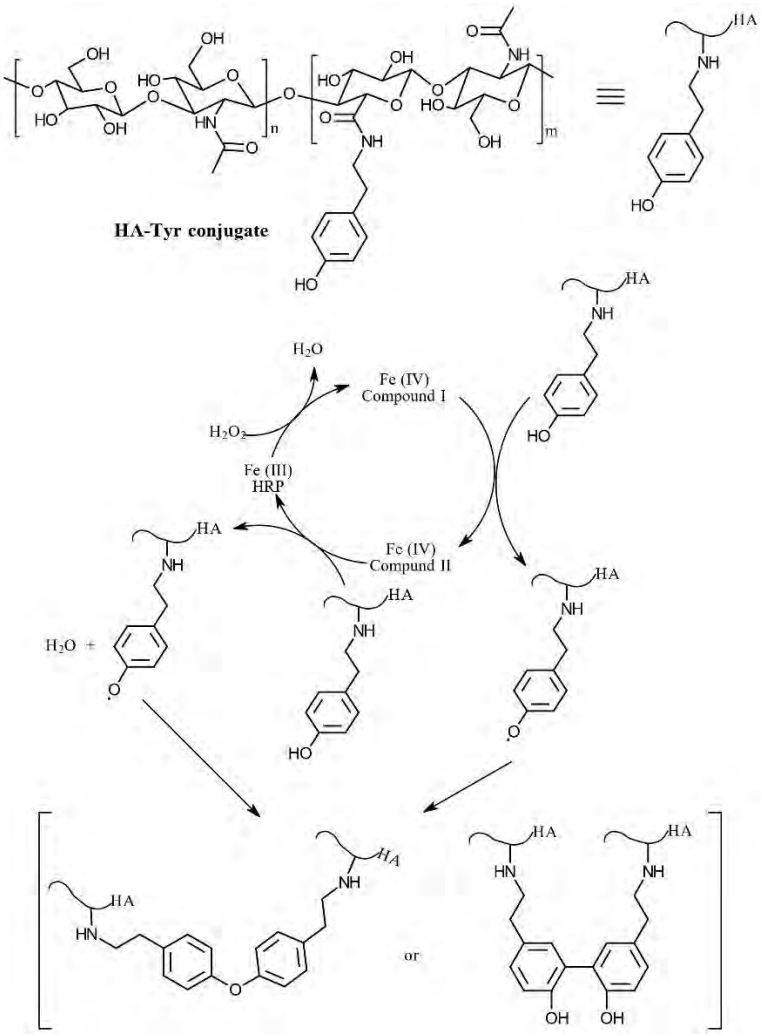

Figure 1. 10: Crosslinking mechanism of hyaluronic acid-tyramine (HA-Tyr) conjugates by the HRP-mediated crosslinking reaction (Kurisawa et al., 2010; Lee et al., 2015)

v. Grafting

Grafting is the attachment of monomers onto the backbone of a pre-formed polymer (natural or synthetic). The polymer chains are activated by the action of chemical reagents or by the treatment with high-energy radiation. The growth of functional monomers on activated macroradicals leads to branching and further to cross-linking. Once again, based on the technique used to generate radicals, grafting can be classified into two types: Chemical grafting in which the action of a chemical reagent activates the macromolecular backbones, the chemical is referred to as the initiator (e.g., ammonium or potassium persulfate), and radiation grafting, where the reaction is

initiated by high-energy radiations such as gamma and electron beam radiation (Gulrez et al., 2011).

1.2.3 Characterization

Table 1. 2: Some of the important characterisation techniques of hydrogels

N°	Characterization	Techniques / Methods
1	Water content	Swelling studies (teabag, filtration, and sieves methods)
2	Thermal analysis	Differential Scanning Calorimetry (DSC)
		Thermogravimetric Analysis (TGA)
3	Structure and composition	Fourier Transform Infrared Spectroscopy (FTIR)
		Powder X-ray diffraction spectroscopy XRD
		Nuclear magnetic resonance spectroscopy (solution NMR and ssNMR)
		Energy-dispersive X-ray spectroscopy (EDS)
4	Surface morphology	Scanning electron microscopy (SEM)
		Environmental SEM
5	Mechanical properties	Dynamic Mechanical Analysis (DMA)
6	Drug encapsulation and release (hydrogel for drug delivery)	High-performance liquid chromatography (HPLC)
		Ultraviolet-visible spectroscopy UV-Vis

1.2.3.1 Swelling studies

Since by definition, hydrogels are polymeric networks that swell in water and hold a significant fraction of water in their structure without dissolving in water; this is the most exceptional property of hydrogels and justified most of their applications. A xerogel is a polymeric network devoid of water, also known as dry hydrogel. When put in contact with an aqueous media, water starts penetrating the hydrogel networks, and hence the hydrogel swell. Therefore, determining the amount of water imbibed within the hydrogel is one of the most critical features to study when working on the hydrogel. This property is known as the hydrogels' swelling rate or swelling capacity, which is defined as the number of grams of water contained in one gram of xerogel. It is often represented in terms of swelling ratio (g/g) or percentage of swelling ratio (% SR) (Pal et al., 2012). Experimentally, the swelling ratio of the hydrogel can be determined by the tea-bag method, the sieve method, or the filtration method.

a) Tea-bag method

In this method, the initial weight of the dry hydrogel (W_0) is usually between 0.01 g and 0.05 g. The dry hydrogel is placed into a tea bag (acrylic/polyester gauze with fine meshes ranging from 40 to 60 meshes). The bag is dipped in an excessive amount of water or aqueous solution (buffer, salt solution, etc.) for a prescribed period. Then the teabag is placed on a dry cloth and gently wiped with another dry cloth to remove excess fluid and weakly bound liquid. The tea bag containing the swollen hydrogel is then weighed as W_2. The same procedure is also carried out for an empty teabag, and the weight of the bag saturated with water is measured and recorded as W_1. The swelling ratio at time t (the time of contact of the hydrogel and the aqueous media) is calculated using the equation (1) (Zhang et al., 2019).

$$S_t = \frac{W_2 - W_1 - W_0}{W_0}, \quad (1)$$

b) Filtration method

For the filtration method, the initial weight of the powdered hydrogel (W_0) is typically between 0.01 g and 0.05 g. A Buchner flask is connected to a vacuum pump, and then a funnel is firmly inserted into the flask. The weighed hydrogel powder is put into a glass beaker, and an excessive amount of water or aqueous solution is then added. The dry hydrogel is placed in contact with the media. A filter paper is pre-saturated with water, and its mass is recorded as W_1; the water pre-saturated filter paper is then placed into the funnel. After a prescribed period, the swollen sample is poured onto the centre of the filter paper, and the vacuum pump is turned on. After the excess fluid is removed from the gel, the filter paper (with the gel on it) is taken out and weighed, and its mass is recorded as W_2. Again, the swelling capacity at time t is calculated using equation (1) (Zhang et al., 2019).

c) Sieve method

The sieve method is also called the rubbing method, which is used to measure the swelling capacity of larger amounts of samples. The initial weight of the dry hydrogel W_0 is usually between 1.0 g and 2.0 g. The sample is then poured into excessive water or aqueous solution and dispersed with a stirring rod to ensure complete contact with the liquid. After a prescribed time, t, the water-absorbed gel is filtered through a 300-mesh wire gauze. The surface water is dried carefully by repeatedly rubbing the underside of the gauze using a piece of a soft open-cell polyurethane foam until the gel no longer slips from the sieve when held vertically. The mass is measured and recorded

as W_1. The swollen hydrogel and the sieves are weighed and their mass recorded as W_2, and equation (1) is used to calculate the swelling capacity of the hydrogel (Zhang et al., 2019).

1.2.3.2 Fourier Transform Infrared Spectroscopy (FTIR)

Infrared spectroscopy (IR) is one of the common spectroscopic techniques which helps identify the chemical structure in both organic and inorganic chemistry. The main function of IR spectroscopic analysis is to determine the different chemical functional groups present in the structure of the sample. Functional groups and bonds (OH, CO, NH_2, C=C, COOH, CONH, etc.) absorb radiation at characteristic frequencies. Infrared spectrometers can accept a wide range of sample types such as gases, liquids, and solids. Fourier Transform Infrared Spectroscopy (FTIR) is a specific infrared spectrometer that converts the detector output to an interpretable spectrum and generates spectra with patterns that provide structural insights (Abdul Rahman et al., 2019). This technique is widely used to confirm the formation of the cross-linked network in the hydrogel structures. This is by investigating the construction of new bonds and the structural arrangement in hydrogel by comparing the spectra of the starting materials and the one of the prepared hydrogel (Gulrez et al., 2011).

1.2.3.3 Powder X-ray diffraction spectroscopy (XRD)

X-ray is electromagnetic radiation with a wavelength range from 0.1 to 100A˚. For the characterization of materials, the X-rays with wavelength ranged from 0.7 to 2.0A˚ are used extensively. Powder X-ray diffraction (XRD) is a spectroscopy method that analyses the scattering of the X-rays by the crystal lattices of the material and is often regarded as wide-angle X-ray scattering (WAXS). It helps then in understanding the crystal profile of a compound (Pal et al., 2013).

Powder XRD spectroscopy is used for the characterization of hydrogels. The XRD profile of hydrogel may reveal information about their crystallinity. Polymers (hydrogels) are usually semi-crystalline, meaning that they have both unorganized organizations of the polymer chains (amorphous region) and several sites of organized polymer chains of crystallites (crystalline region). The amorphous regions of the polymer architecture cause scattered diffraction, whereas the defined XRD peaks are associated with the crystalline regions within the polymer matrices

(Pal et al., 2013). This technique is extensively used in the characterization of hydrogel mainly to determine its interaction with other materials.

1.2.3.4 Thermal analysis

Hydrogel, as for most polymeric materials, can be studied using several thermal techniques. Under some conditions they are used to predict potential applications of the hydrogel. The investigation of these properties is generally made by the two following techniques: Differential Scanning Calorimetry (DSC) and Thermogravimetric Analysis (TGA).

Differential scanning calorimetry (DSC) is defined as the measurement of the change in the heat flow rate to the sample and a reference sample. At the same time, they are subjected to a controlled temperature program. This technique is used to assess hydrogels' stability and determine the glass transition, the enthalpy of degradation, and the melting region. It also gives relevant information about the degree of crystallinity of the hydrogels, which are completed by the XRD data (Hahne et al., 2003).

Thermogravimetric analysis (TGA) or thermogravimetry (TG) is a technique in which the mass of a compound is measured as a function of temperature or time while the sample is subjected to a controlled temperature program in a controlled atmosphere. The atmosphere can be inert (under nitrogen or argon), oxidizing (under air or oxygen) or reducing (8-10% hydrogen in nitrogen). This technique is used to investigate the degradation of polymers (hydrogel) by the action of heat. Polymers (hydrogel) generally exhibit mass loss when heated, but mass gain may be observed before degrading at slow heating rates in an oxidizing atmosphere. This technique evaluates hydrogels' thermal and oxidative stability in completing supplements to DSC (Menwzel and Prime, 2009).

1.2.3.5 Scanning Electron Microscopy (SEM)

The surface morphology of hydrogel is one of the most relevant features to investigate, leading to the choice of the application. Microscopic techniques (SEM and environmental SEM) are utilized to examine the microstructure of the surface of hydrogels. These microscopic techniques use electron beams as the analysing radiation. The scanning electron microscopic (SEM) technique involves imaging the samples by capturing the backscattered electrons; the image's resolution is

about 10 nm. The analysis of the samples is carried out under a high vacuum. The major limitation of SEM is that wet samples cannot be studied using this technique. This limitation can be overcome by using "environmental SEM", which allows the use of wet samples. (Pal et al., 2013). Environmental SEM (ESEM) is low-vacuum scanning electron microscopy technique which can be used to observed hydrated samples. The main difference between the environmental SEM and SEM is the presence of a gas in the sample chamber. The gases include nitrous oxide, helium, argon and other, but water vapour is the most efficient amplifying gas found and the most common gas used. ESEM offers some advantages like minimal processing of samples, shorter time scales and lower costs. ESEM provides spatial resolutions of 10 nm or less. Compared to SEM, ESEM produces different complementary information for biological specimens for examples cell structures are visible with SEM, but external polymers around cells are more apparent in ESEM (Echlin, 2009; El et al., 2012)

1.2.3.6 Nuclear magnetic resonance spectroscopy

Nuclear magnetic resonance (NMR) spectroscopy exploit transitions in nuclear spin states. When put inside an external magnetic field, nuclei with a spin quantum number of one-half, such as ^{1}H and ^{13}C, have two potential nuclear spin energy states. The magnetic moment of the spinning nucleus aligned with the external magnetic field belongs to the lower energy state, while the magnetic moment opposite to the field corresponds to the higher energy level. The energy difference between the two states is proportional to the intensity of the external magnetic field (Math and Scranton, 1996).

Both solution NMR and solid-state NMR are used in the characterization of hydrogels, hence these techniques are applied in resolving the structure, degree of grafting, molecular organization, water-biopolymer interactions and internal dynamical behavior of hydrogels (El Hariri El Nokab and van der Wel, 2020; Karoyo and Wilson, 2017).

1.2.3.7 Mechanical properties of hydrogel

Mechanical properties of hydrogels, including storage and loss moduli, young modulus, and Poisson modulus, are significant features to be investigated when hydrogels are being manufactured. The change in mechanical properties is linked to various variables (crosslinking density, preparation methods, type of polymers, etc.). All these variables must be analysed

according to the material, the expected application, and the aim of the study. For example, the hydrogel is expected to be used for ligament and tendon repair wound dressing material, matrix for drug delivery and tissue engineering require hydrogel with different mechanical properties. The mechanical properties can be evaluated by a Dynamic Mechanical Analysis (DMA) device or a rheometer according to various techniques available on the market (Beckett et al., 2020; Chirani et al., 2015; Pal et al., 2012).

1.2.4 Biomedical applications

Hydrogels are becoming more and more popular for biomedical applications due to the remarkable properties they offer, such as flexibility, high water content, biodegradability, biocompatibility, softness, non-toxicity, etc. (Camara and Ferreire, 2012). Initially, hydrogels were developed and used as soft contact lenses and tissue scaffolds (Ferreira et al., 2018). In addition to the above-mentioned biomedical applications, hydrogels are used in wound healing, tissue engineering, production of hygiene products, the culture of organs on chips, bone regeneration, and drug and gene delivery (Caló and Khutoryanskiy, 2015; Chirani et al., 2015).

1.2.4.1 Application of hydrogel in drug delivery

Drug delivery refers to a whole ensemble of approaches, devices, manufacturing techniques, storages systems, and technologies implicated in transporting a drug to its target site to achieve a desired therapeutic effect. The drug delivery systems are designed to avoid the problems of the conventional drug dosage forms, which include burst release and quick decay of the effects of the drug over time, especially for pharmaceuticals with a short half-life (Bruschi, 2015; Lavik et al., 2012).

Hydrogels, particularly smart hydrogels, are intensively investigated as drug delivery systems. They offer exciting solutions in reaching a sustained and targeted release of several drugs, which increase the drug's therapeutic effect and reduce its side effects at the same time (Chirani et al., 2015). Once loaded into the hydrogel, the drug can be released by different mechanisms: diffusion-controlled, swelling controlled, chemically controlled, and environmentally-responsive release (Narayanaswamy and Torchilin, 2019).

Therefore, apart from a considerable number of scientific publications demonstrating the potential of hydrogels as excellent drug delivery systems. Some hydrogel drug delivery systems are already approved by the Food and Drug Administration (FDA) (Patel and Dalwadi, 2013).

Table 1. 3: Hydrogel-based products approved by FDA

Product	**Drug**	**Application**
Atridox	8.5% Doxycycline	Periodontal treatment product with sub-gingival delivery
Eligard	Leuprolide acetate	For treatment of prostate cancer
Lupron depot	Leuprolide acetate	Fort treatment of advanced prostate cancer
Sandostatin	Octreotide acetate	Acromegaly
Cervidil	Dinoprostone	Continuation of cervical ripening or near term
Timoptic-XE	Timolol malate	Glaucoma

1.2.5 Chitosan-based hydrogels

Chitosan is a linear polysaccharide of randomly distributed N-acetylglucosamine, and glucosamine units produced by deacetylation of chitin a natural polysaccharide, which can be isolated from exoskeletons of crustacean. It is a pH- sensitive biodegradable, biocompatible, and non-toxic polymer, having potential applications in biomedical field. Chitosan and chitosan derivatives-based hydrogels are extensively studied for biomedical applications, and they have demonstrated several advantages such as good biocompatibility, biodegradability by human enzymes, non-toxicity, pH sensitivity, mucoadhesive etc. (Bhattarai et al., 2010; Racine et al., 2017; Yao et al., 2012).

1.3 Controlled drug delivery

The concept of controlled drug delivery was introduced in the early 1950s and it was referring to a system capable to sustain the release of drugs where the drugs' concentrations remain within the therapeutic range for a long time. The first reported controlled drug delivery systems were the oral and transdermal sustained release systems (Sanjay et al., 2018).

In general, drug administration has caused uncomplicated, fast-acting reactions (traditional forms) via oral or injectable delivery methods for most of the pharmaceutical industry's history. Reduced potencies owing to partial breakdown (first pass metabolism), hazardous levels of administration (in situations of excess dosage), increased expenses associated with excess dosing, and compliance concerns due to administration discomfort have all been reported as issues with this technique. The continuous oral distribution of medications at predictable and repeatable kinetics for a defined delivery throughout the course of gastrointestinal (GI) transit is provided by the oral controlled drug delivery system (Bassyouni et al., 2015; Park, 2014).

A sustained release drug delivery system is a continuous release method that releases the medication for a long time along the whole length of the GI tract while the dose form travels normally. The following are the numerous systems that fall within this category (Hoffman, 2008; Sanjay et al., 2018) :

- Dissolution-controlled release system.
- Diffusion-controlled release system.
- Diffusion- and dissolution-controlled release system.
- Ion exchange resin drug complexes.
- pH-independent formulations.
- Osmotic pressure-controlled systems.
- Hydrodynamic pressure-controlled systems.
- Slow dissolving salt and complexes.

Delayed transit and continuous release systems are intended to extend the time they spend in the GI tract while also allowing them to be released. The medicine should be stable to gastric pH since the dose form is frequently created to be detained in the stomach. Mucoadhesive systems and size-based systems are included in this category (Bassyouni et al., 2015).

1.4 Problem statement

Hepatitis B virus infection is an important threat to global public health. In the recent statistics, the World Health Organization (WHO) estimates that almost 247 million people are affected by chronic HBV infection, and more than 887 000 deaths are attributed annually to HBV-related complications (hepatocellular carcinoma (HCC), cirrhosis, liver cancer, etc.) in the world (Howell et al., 2021).

In general, there are two different available strategies used in the treatment of HBV infection, the short-term therapy based on immune-modulators (such as standard or PEGylated interferon-α); and the long-term regime based on the nucleosides and nucleotides analogues, such as tenofovir, lamivudine, entecavir, telbivudine, etc.(Ghany, 2017; Tang et al., 2014). The main goal of these therapeutic approaches is to ensure that a cure without a relapse can be achieved to prevent death, the development of hepatocellular carcinoma, transmission, and the emergence of drug resistance. Therefore, the therapeutic actions of antihepatitic B drugs commonly employed are expected to lower the viral load to undetectable levels, decrease the disease rate, and reduce the rate of evolution of HBV resistant variants (Latavia et al., 2018).

However, the lengthy medication period of HBV infection leads to poor patient compliance to the treatment that causes lower concentrations of the drug in the patient's system. This under dosage resulting from poor patient compliance can promote the development of drug resistance. Moreover, HBV resistant variants against some antiviral drugs used in the treatment of HBV infection (lamivudine, entecavir, adefovir, and telbivudine) have been recently reported in some regions of the world (Asia and Africa), and documented in the literature (Sun et al., 2018; Zhou and Terrault, 2017). This significantly affects the cure rates of existing drugs that are also used to treat other viral infections, such as the human immunodeficiency virus (HIV). The situation mentioned above underlines the need for long-acting formulations that control and sustain the release for improving the management of HBV infection that can enhance patient compliance. In addition, patient compliance is a crucial parameter of the efficacy of any antimicrobial therapy, and in contrast, low patient compliance can be responsible for the emergence of antimicrobial resistance (Tong et al., 2018).

In recent decades, intelligent or smart drug delivery systems (SDDSs) capable of controlling the location, the rate, and the time of drug release by the action of external stimuli, have captured many researchers' attention. This results from several advantages offered by the SDDSs to achieve expected therapeutic results, such as their potential to increase drug efficiency, reduce toxic side effects, enhance drug absorption, promote access to the target site, and control the drug input within the required time (Bazban-Shotorbani et al., 2017).

In a particular way, polymers play a significant role as starting material in the design of SDDSs. Natural and synthetic polymers are widely used to develop various types of drug delivery systems, among which we have micelles, dendrimers, particulate systems (beads, micro-and nanoparticles), and hydrogels (James et al., 2014; Parhi, 2020). The last type used mostly in the preparation of controlled drug delivery systems is the one focused on in the present study.

Hydrogels are three-dimension polymeric networks based on crosslinked hydrophilic polymers capable of retaining a considerable amount of water or biological fluid without dissolving while maintaining their 3D structure. Hydrogels are one of the most study polymeric materials for controlled drug delivery (Anwar et al., 2021; Narayanaswamy and Torchilin, 2019). According to the types of interactions resulting from the crosslinked structure, hydrogels can be classified as physically crosslinked when non-covalent interactions form them; chemically crosslinked when formed by covalent bonds, or both interactions can also crosslink them. Depending on the origin of the constituting polymers, hydrogels can be grouped as synthetic, natural, or hybrid. (Buwalda et al., 2017).

In general, hydrogels exhibit good biocompatibility, biodegradability, low toxicity, and tunable physical properties, such as surface characteristics, swelling potential (stimuli-responsive), and mechanical strength, making them a promising material for controlled control drug delivery (Ferreira et al., 2018). To achieve these properties, naturally occurring polymers like chitosan and its derivatives hydrogels have been extensively studied and have proven to be a potential vehicle for delivering various drugs at a different site and using different administration ways (Bashir et al., 2017; Bhattarai et al., 2010; Cheng et al., 2018).

Chitosan is a polysaccharide chemically formed by glucosamine and *N*-acetylglucosamine linked through a β (1-4) bond. It is produced by the deacetylation of chitin, the main component of the

exoskeleton of crustaceans and insects (Delmar and Bianco-Peled, 2016). Chitosan and its derivatives hydrogels have been studied and proven to be a potential vehicle for delivering various drugs (Bashir et al., 2017; Cheng et al., 2018). The biocompatibility, biodegradability, pH-sensitive, non-toxicity of chitosan (Bhattarai et al., 2010), and the low cost motivated our choice of this polymer. Hence based on these properties, in this work, we prepared a pH-sensitive chitosan-based hydrogel to be used for a controlled release of antihepatitic B drugs and tenofovir disoproxil fumarate (a nucleotide analogue reverse-transcriptase inhibitor) was used as a model drug for this study.

1.5 Aim and objectives of the research.

This study aimed to design and develop a chitosan-based pH-sensitive hydrogel using acrylamide and acrylic acid as modifying monomers and *N,N*-methylene bisacrylamide as the crosslinking agent, and assess the drug delivery potential of the developed hydrogel using antihepatitic B drug (TDF) as a model drug.

The specific objectives of the study were:

1) To synthesize, optimize and characterize chitosan-based hydrogel by radical polymerization method,
2) To study the pH and ionic strength-sensitivity properties and assess the biocompatibility of the hydrogel,
3) To encapsulate of tenofovir disoproxil fumarate in the hydrogel and study it the release profile.

Chapter Two

Material and Methods

2 MATERIALS AND METHODS

2.1 Materials

2.1.1 Chemicals

Chitosan, low molecular weight (CS), acrylic acid (AA), *N,N*-methylene bisacrylamide (MBA), triethylamine, monobasic potassium phosphate (KH_2PO_4), and dibasic sodium phosphate (Na_2HPO_4) were purchased from Sigma Aldrich (Germany). Tenofovir disoproxil fumarate (TDF) was donated by Aspen Pharmacare (South Africa). Acrylamide (AAm), hydrogen chloride (HCl), and HPLC grade acetonitrile were purchased from Merck (Germany). Ammonium persulfate and orthophosphoric acid were purchased from Saarchem (South Africa). Glacial acetic acid, sodium hydroxide (NaOH), Magnesium chloride ($MgCl_2$), sodium chloride (NaCl), potassium chloride (KCl), methanol, and acetone were purchased from Minema (South Africa). Aluminum chloride was purchased from Fluka Chemika (Switzerland). Ultra-pure water was HPLC grade 18 mega Ohm water, prepared using a Milli-Q academic A10 water purification system (Millipore® Bedford, MA, USA).

2.1.2 Equipment

A hot plate equipped with a magnetic stirrer, a pH meter (Hanna, Italy), and an oven were used for the hydrogel's preparation process. A PerkinElmer Spectrum 100 FT-IR Spectrometer (PerkinElmer, USA) was used for recording FTIR spectra, in ATR mode. A PerkinElmer DSC-6000 and PerkinElmer TGA 4000 instrument (PerkinElmer, USA) were used for thermal analysis. An XRD D8 Discover instrument (Bruker, USA) was used for the assessment of the crystallinity of the materials. An INCA PENTA FET coupled to VAGA TESCAM (Germany) was used for energy-dispersive X-ray spectroscopy and scanning electron microscopy to assess the structure of the materials. An Agilent 1100 Liquid Chromatography equipped with a quaternary pump (G1311A), a degasser (G1322A), a diode array detector (G1315B), and a manual injector (G1328B), (Agilent, USA) was used for HPLC analysis with a Luna® LC column (5 µm C18, 100 Å, 250 x 4.6 mm i.d.). A Lyo Lab 3000 Lyophilizer Apollo Scientific CC (South Africa) was used to freeze-dry the samples before the SEM analysis. A bath sonicator (Digital Ultrasonic Cleaner PS-10A, China) was used for degassing HPLC mobile phase and sonicating TDF solution.

2.2 Methods

2.2.1 Preparation and optimization of chitosan-based hydrogel

The optimization of different parameters involved in the hydrogel synthesis was done and evaluated based on the swelling capacity. The ratio of monomers (acrylamide/acrylic acid), the concentration of the cross-linker, and the initiator were the considered parameters that could affect the outputs (swelling ratio) and were studied at three levels each for the optimization. Minitab software was used for the full factorial design of experiments to generate 27 possible combinations corresponding to a hydrogel formulation that was run in duplicate. **Table 2.1** presents the different factors and their level.

Table 2. 1: Design of experiment of the preparation of hydrogel

Parameters	**Levels**		
	1	2	3
Ratio of monomer (Acrylamide: Acrylic acid)	3:1	1:1	1:3
Crosslinking agent, *N, N*-methylene bisacrylamide (MBA) in mg	100	150	200
Initiator, Ammonium persulfate (APS) in mg	50	100	150

The free-radical polymerization method was used to graft acrylamide and acrylic acid into chitosan using *N, N*-methylene bisacrylamide (MBA) as a cross-linking agent and ammonium persulfate (APS) as the initiator of the reaction. The procedure described by Mahdavinia *et al*. (2004) was followed with slight modifications regarding the amounts of reagents and condition of the reaction (Mahdavinia et al., 2004a).

Briefly, 500 mg of chitosan (CS) was dissolved in 50 ml of 1% acetic acid solution in a two necks reactor on a hot plate equipped with a magnetic stirrer. The reactor was placed in an oil bath pre-set at 60°C and allowed to stir (600 rpm) for 15 minutes under nitrogen to remove the air in the solution. Then variable amounts of ammonium persulfate (APS) (50-150 mg) were added to the chitosan solution and allowed to stir for 10 minutes at 60°C. After that, different amounts of acrylic acid, AA (500-1500 mg), acrylamide, AAm (500-1500 mg) and *N, N* methylene bisacrylamide, MBA (100-200 mg) were added directly, and the reaction mixture was continuously stirred for 60

minutes at 60°C. Hence, the ratio of chitosan/synthetic monomer was 0.25. The reaction's product was cooled at room temperature then the pH was adjusted to pH = 8 by adding a solution of sodium hydroxide (NaOH 1N). Then methanol (250 ml) was added to the gelled product while stirring and dewatered for twenty-four hours. After total dewatering, the mixture was filtered, and the gel particles were washed with fresh methanol (2 x 50 ml) and dried at 50°C in an oven.

The chitosan grafted poly (acrylamide-*co*-acrylic acid) prepared was then saponified in 50 ml of an aqueous solution of NaOH 1N in a loose stopper 100-ml flask at 100°C for 60 minutes. The reaction product was cooled at ambient temperature, and the pH was adjusted to pH eight by adding a solution of acetic acid (10%). While stirring, methanol was added to the gelled product. After complete dewatering (24 h), the product was filtered, washed with fresh methanol (2 x 50 ml), and dried at 50°C in the oven. The prepared hydrogel was stored at room temperature for further characterization.

2.2.2 Characterization of chitosan-based hydrogel

2.2.2.1 Swelling studies

The capacity of the synthesized hydrogel to swell in an aqueous medium was assessed using the filtration method. The swelling ratio (SR) is defined as the mass (in gram) of solvent (water) absorbed per gram of dried hydrogel. The swelling ratio of the hydrogel in water was considered as the response for the optimization studies.

Furthermore, the swelling ratio of the optimized formulations was assessed in buffer solutions at different pH values to establish the pH sensitivity profile of the hydrogel. Hence, the swelling ratio was measured at pH 1.2, I=0.1 (HCl/KCl), pH 4, 0.1M (acetate buffer), pH 5.8, 0.1M (phosphate buffer), pH 7.4, 0.1M (phosphate buffer), and pH 9.8, I=0.1M (carbonate buffer).

In addition, the swelling-deswelling-reswelling assay was performed to assess the reversibility of the pH-sensitive potential of the hydrogel. The experiment was done by first putting the dried hydrogel in contact with the buffer solution at pH 7.4 for two hours, the swelling ratio was measured, and then the same hydrogel was put in a buffer solution at pH 1.2 for another two hours for deswelling, and the swelling ratio was again measured. Finally, the same sample was put back in the buffer solution at pH 7.4 to reswell, and the final swelling ratio was calculated.

Finally, ionic strength sensitivity studies were done out by measuring the swelling ratio of the optimized hydrogel in various salts solutions (NaCl, $MgCl_2$, and $AlCl_3$) at different concentrations (0.05, 0.1, and 0.15 M).

Typically, a mass between 0.01 g to 0.05 g of the dried hydrogel was weighted, recorded as W_0, and placed in a beaker, then an excessive amount of water or aqueous solution (50-100 ml) was poured in, and the hydrogel was left in contact with the swelling medium for two hours. A Buchner flask equipped with a funnel and connected to a vacuum pump was set up. Afterward, a filter paper pre-saturated with water was weighed, its mass was recorded as W_1, the filter paper was then placed in the funnel. After two hours of contact between the dried hydrogel and the swelling medium, the swollen sample was filtered to remove the excess fluid from the hydrogel. The filter paper (with the swollen hydrogel on it) was taken out weighted its mass was recorded as W_2. The swelling ratio or capacity was calculated using equation (2) (Zhang et al., 2019).

$$SR = \frac{W2 - W1 - W0}{W0} \quad (2)$$

2.2.2.2 Fourier Transform Infra-red spectroscopy (FTIR)

The FT-IR analysis was performed using a PerkinElmer Spectrum 100 FT-IR Spectrometer. The IR spectra were obtained by the attenuated total reflection (ATR) method. For each experiment, 16 scans at the rate of 4 cm^{-1} were done in the frequency range from 650 to 4000 cm^{-1}, and the software FTIR Spectrum and Origin Pro 9 were used for the processing of data. The signals from the functional groups of chitosan grafted poly (acrylamide-*co*-acrylic acid) (CS-P(AAm-AA)) loaded TDF were compared to those of empty hydrogel chitosan and TDF.

2.2.2.3 X-ray Diffraction spectroscopy (XRD)

X-ray powder diffraction (XRD) was used to compare the crystalline nature of chitosan, chitosan-based-hydrogel, and the hydrogel-drug loaded. It was also used to assess the crystallinity of the model drug used. Analyses were performed using a nickel filter and Cu-Ka radiation at 1.5404 Angstrom, and the scans were run at a 2-θ range from 10 to 100° with a slit width of 6.0 mm at a scanning speed of 1° min^{-1}.

2.2.2.4 Thermal gravimetric analysis (TGA)

The thermal gravimetric analyzer studied the thermal stability of chitosan and dried hydrogel. TGA data were also used to confirm the modification of chitosan into the chitosan-based hydrogel. Briefly, a sample of the studied material, with a mass between 2 to 5 mg, was heated with a heating rate of 10°C per minute from 30 to 900°C in an inert atmosphere of nitrogen (20 ml/min).

2.2.2.5 Differential Scanning Calorimetry (DSC)

Differential scanning calorimetry (DSC) was used to assess the change in the material's thermal stability after different modifications to complete TGA studies. DSC analysis was also used for pre-formulation studies to evaluate the model drug's compatibility and carrier. A material sample with a mass between 3 and 5 mg was placed into an aluminum pan and heated from 30°C to 350°C at a heating rate of 10°C/min. An empty aluminum pan was used as a reference. The analysis was carried under a nitrogen gas atmosphere at a flow of 20 ml/min. The changes in the heating flow of the samples were recorded and date processed with DSC Pyris and Origin Pro 9 software.

2.2.2.6 Scanning Electron Microscopy (SEM) and Energy-dispersive X-ray spectroscopy (EDS)

Scanning electron microscopy (SEM) was carried out to observe the surface morphology of the synthesized hydrogel, and energy-dispersive X-ray spectroscopy was used for the elemental analysis of the hydrogel. The hydrogel was swelled to equilibrium in water for 24 hours, and at room temperature, the swollen hydrogel was lyophilized on a freeze-dryer. The lyophilized hydrogel was fixed on sellotape with aluminum stubs, then coated with gold for 30 minutes (sputter-coating). The prepared sample was then observed on SEM, and the same sample was used to do the elemental analysis on the hydrogel’s surface using EDS.

2.2.2.7 Cytotoxicity studies

Cytotoxicity of the prepared hydrogel was assessed to have an idea of its cytocompatibility. To evaluate the cytotoxicity of the hydrogel [CS-P(AAm-AA)], the hydrogels were incubated at a fixed concentration (50 µg/ml) in 96-well plates containing HeLa cells for 24 hours. The number of cells surviving hydrogel exposure was determined by using the resazurin-based reagent and reading resorufin fluorescence in a multi-well plate reader. Results were expressed as a percentage

of cell viability, based on fluorescence reading is treated wells vs. untreated control well. Emetine (which induces cell apoptosis) was used as a positive control drug standard.

2.2.3 *In vitro* release studies of Tenofovir disoproxil fumarate

2.2.3.1 Drug-excipient compatibility

Physicochemical compatibility between the active pharmaceutical ingredient (API) and the carrier (excipients) is an important feature to be considered when designing a drug delivery system; that is why differential scanning calorimetry (DSC) was conducted as a preliminary compatibility study. Thus, Tenofovir disoproxil fumarate (TDF) was physically mixed with chitosan-based hydrogels in a 1:1 masse ratio. The phase behavior of the physical mixture was studied in comparison with pure Tenofovir disoproxil fumarate by (DSC) following the procedure described in section ***2.2.2.5***. The experiment was conducted from 25 to 250°C.

2.2.3.2 Validation of High-Performance Liquid Chromatography (HPLC) method for analysis of Tenofovir disoproxil fumarate

The RP-HPLC method developed by Agrahari and Youan (2012) for quantification of Tenofovir with slight modifications was validated following the International Council for Harmonization guidelines (ICH 2005) (Agrahari and Youan, 2012; EMA, 2006). The method was validated in its linearity, range, accuracy, and precision (intra- and inter-day precision).

An Agilent 1100 Liquid Chromatography series equipped with a quaternary pump (G1311A), degasser (G1322A), diode array detector (G1315B), and manual injector (G1328B) was used for HPLC analysis with a Luna® LC column (5 µm C18, 100 Å, 250 x 4.6 mm i.d.) column was used for the analysis. The HPLC was performed in isocratic elution at ambient temperature for 3.5 minutes, with the flow rate being 1 ml/min.

The mobile phase consisted of a mixture of acetonitrile and water with adjusted pH in the ratio of 65:35. The aqueous phase (pH 5.1) was prepared by adding 1 ml of triethylamine to 1000 ml of Millipore water, and the pH was adjusted with orthophosphoric acid (85%) at the value of 5.1. The injection volume was 20 µL, and for TDF detection, the wavelength was set at 259 nm.

The stock solution was prepared by weighing 10 mg of Tenofovir disoproxil fumarate in a 10 ml clean and dry volumetric flask. About 8 ml of ultra-pure water was added, and the solution was

sonicated for 5 minutes; after the total dissolution of TDF, the volume was made up to volume with the same solvent.

i. Linearity and range, and accuracy

Six solutions (0.5, 1, 2.5, 5, 7.5, and 10 µg/ml) were prepared by serial dilution of the stock solution using ultra-pure water. Each solution was injected three times into the HPLC system. Using Microsoft Excel, the means of the peak's areas were plotted against the concentration to generate the calibration curve. The regression equation and correlation coefficient (R^2) were determined to assess the linearity. At the concentrations of 5, 7.5, and 10 µg/ml, the percent recovery of TDF was calculated to assess the accuracy of the method.

ii. Precision

Precision was assessed in triplicate using three concentration levels (5, 7.5, and 10 µg/mL) and was reported as the percentage of relative standard deviation (RSD). Similarly, the intra-day precision was determined, and the inter-day precision was based on analysis of these concentrations over three days.

2.2.3.3 Optimization of the encapsulation of Tenofovir disoproxil fumarate

Tenofovir disoproxil fumarate (TDF) was chosen as an antihepatitic B drug model to investigate the loading and release properties of the synthesized hydrogel. The encapsulation was done using the swelling equilibrium method (Qi et al., 2017), where a defined amount of dried hydrogel (100 mg) was soaked in a fixed volume (50 ml) of a solution of TDF for 24h at room temperature. After 24h, the swollen hydrogel was removed from the solution, washed with ultra-pure water to remove residual TDF, and then dried in the oven at 40°C. The concentration of TDF was determined before and after soaking using the validated HPLC method. The encapsulation efficiency (EE) and the drug loading (DL) were calculated using the formula (3) and (4), respectively. The optimization of the EE and DL was done using four different concentrations of TDF, which are 100, 150, 200, and 250 µg/ml.

$$EE(wt,\%) = \frac{\mathrm{W0} - Wf}{\mathrm{W0}}\ x\ 100 \quad (3)$$

$$DL\ (wt,\%) = \frac{\mathrm{W0} - Wf}{\mathrm{WdH}} x100 \quad (4)$$

Where W_0 and W_f are the total weight of TDF in the solution before and after soaking the dried in the solution, respectively, and W_{dH} is the weight of the dried hydrogel. All the encapsulations' assays were performed in triplicate.

2.2.3.4 Drug release profile

The concentration with optimum EE and DL of TDF (200 µg/ml) was considered for *in-vitro* release studies. *In-vitro* drug release studies of TDF were done using the following procedure. Dried TDF-loaded hydrogel was immersed in 25 mL of buffer solutions (pH=1.2 and 7.4, I=0.1M) in a dialysis bag. The hydrogel samples were submerged at 37°C for 96 h while maintaining a constant shaking (100 rpm). At selected time intervals (0.5, 1, 1.5, 2, 4, 8, 12, 24, 48, 72, and 96h), an aliquot (5 mL) of the release milieu was withdrawn and immediately substituted with 5 mL of fresh buffer solution. The amount of TDF released was quantified by HPLC for each aliquot, and the cumulative percentage of TDF release was calculated using equation (5).

$$\text{Cumulative drug release } = \frac{\text{Ve}\sum_{i}^{n-1}\text{Ci} + \text{VoCn}}{\text{m}}\text{x}100 \quad (5)$$

Where m represents the amount of TDF in the hydrogel, V_0 is the volume of the release medium (V_0=25 mL), Ve is the volume of the media remove any time (5 mL), Ci is the concentration of the drug in the release media and C_n is the concentration of TDF in the n^{th} sample. All TDF drug releases were performed in triplicate.

Chapter Three

Results and Discussion

Safari, J.B.; Bapolisi, A.M.; Krause, R.W.M. Development of pH-Sensitive Chitosan-g- poly (acrylamide-co-acrylic acid) Hydrogel for Controlled Drug Delivery of Tenofovir Disoproxil Fumarate. Polymers 2021, 13, 3571. https://doi.org/10.3390/ polym13203571

A paper with the above title based largely on the results from this Chapter have been published in Polymers

3 RESULTS AND DISCUSSION

3.1 Synthesis and optimization of chitosan grafted poly (acrylamide-co-acrylic acid)

3.1.1 Synthesis chitosan grafted poly (acrylamide-co-acrylic acid)

Ammonium persulfate used as initiator generates the ion persulfate once in solution. Persulfate ions are well known for producing sulfate radicals under elevated temperatures, which are potent oxidants (Zrinyi and Pham, 2017). These free radicals reacted with the alcohol functional groups of the polysaccharide (chitosan) and created numerous free radical sites on the backbone of chitosan, which constitute an active site to initiate polymerization of chitosan with acrylamide and acrylic acid. The addition of acrylamide (AAm), acrylic acid (AA), and *N,N*-methylene bisacrylamide (MBA), chemicals having carbon-carbon double bonds, resulted in a simultaneous polymerization and MBA creating crosslinking between the different chains (Bashir et al., 2017). The last stage of the synthesis, which consisted of treating the hydrogel with sodium hydroxide, resulted in the transformation of the amide function into carboxylate, followed by the saponification of the carboxylic group, which has the potential to be highly hydrated (Mahdavinia et al., 2004a). The proposed reaction scheme of the synthesis of chitosan grafted poly (acrylamide co acrylic acid) hydrogel is shown in **Figure 3.1**.

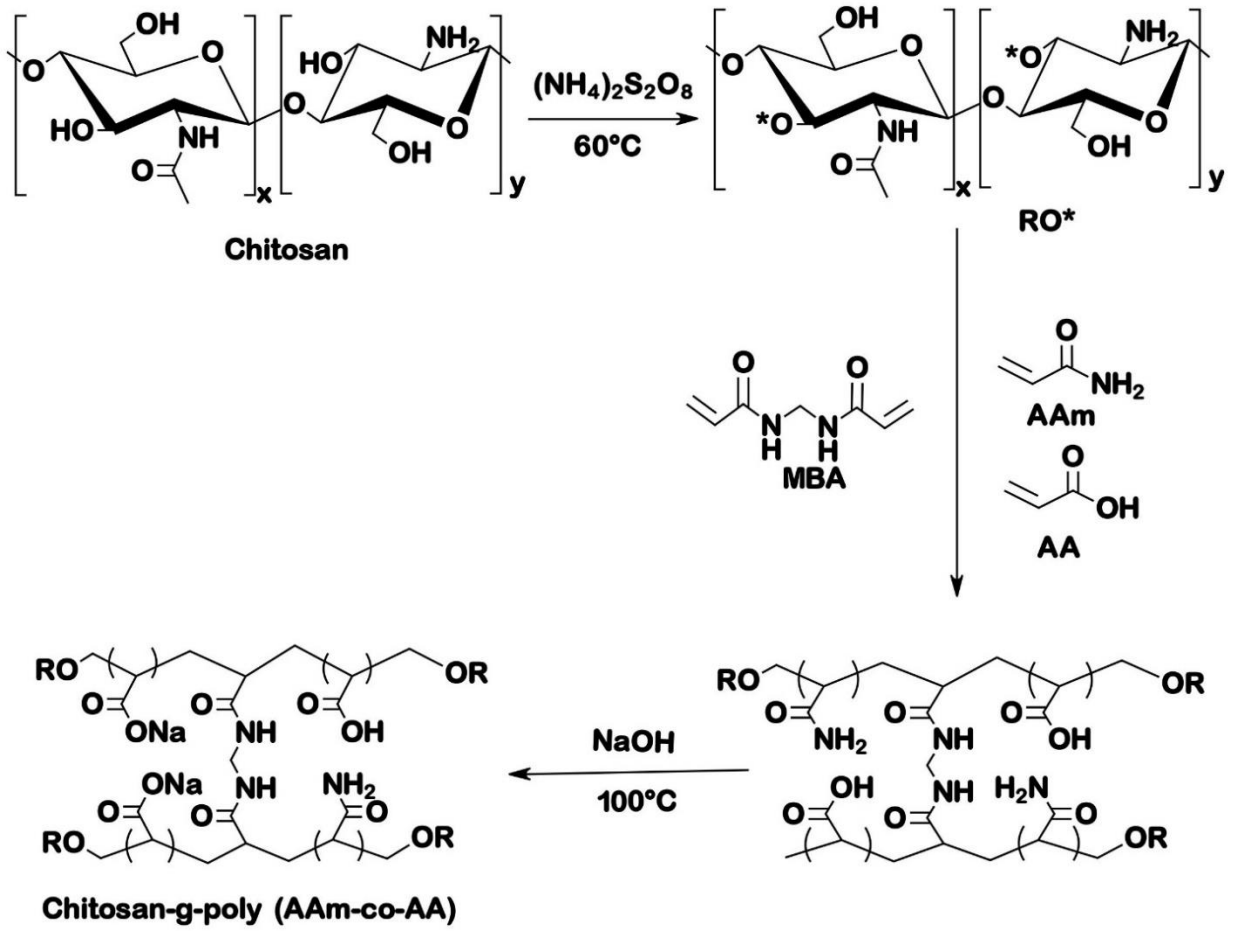

Figure 3.1: Reaction scheme *of the synthesis CS-P(AAm-AA) hydrogel*

3.1.2 Optimization of the synthesis of chitosan grafted poly (acrylamide-co-acrylic acid)

Minitab 17 software was used to generate 27 formulations with different constituent compositions, the different hydrogels were synthesized in triplicate, and their swelling capacity was assessed in ultra-pure water. **Table 3.1** presents the values of the various factors of the optimization and the swelling ratio, which is the response of the optimization of each formulation.

Table 3.1: Swelling ratio of different formulations at different values of monomers ratio, a crosslinking agent (MBA), and initiator (APS)

Formulation	***Ratio of monomers (AAm:AA)***	***MBA (mg)***	***APS (mg)***	***Swelling ratio ± SD (g/g)***
1	3:1	100	50	221.83 ± 30.37
2	**3:1**	**100**	**100**	**319.48 ± 23.21**
3	3:1	100	150	256.68 ± 41.29
4	3:1	150	50	99.57 ± 14.05
5	**3:1**	**150**	**100**	**167.98 ± 8.41**
6	3:1	150	150	54.74 ± 11.08
7	3:1	200	50	58.62 ± 9.39
8	**3:1**	**200**	**100**	**95.42 ± 15.62**
9	3:1	200	150	69.84 ± 4.77
10	1:1	100	50	235.57 ± 11.52
11	1:1	100	100	185.89 ± 15.63
12	1:1	100	150	115.2 ± 18
13	1:1	150	50	130.09 ± 12.49
14	1:1	150	100	161.36 ± 9.31
15	1:1	150	150	97.57 ± 26.88
16	1:1	200	50	96.44 ± 18.5
17	1:1	200	100	100.7 ± 8.28
18	1:1	200	150	81.47 ± 6.11
19	1:3	100	50	225.9 ± 21.61
20	1:3	100	100	143.12 ± 17.02
21	1:3	100	150	92.09 ± 26.25
22	1:3	150	50	97.26 ± 14.49
23	1:3	150	100	125.04 ± 5.43
24	1:3	150	150	61.43 ± 6.13
25	1:3	200	50	61.42 ± 6.24
26	1:3	200	100	94.53 ± 13.63
27	1:3	200	150	59.38 ± 5.99

Three formulations were picked randomly for each parameter to illustrate how the parameter affects the swelling capacity of the hydrogel. For each parameter, the other two parameters studied were kept unchanged while the considered parameter was changed.

Firstly, Figure 3.2 A presents how the monomers (AAm/AA) ratio affected the swelling. Formulations 3, 12, and 21 (**Table 3.1**) with 3:1, 1:1, and 1:3 monomer ratio, respectively and with 100 mg of MBA and 150 mg of APS was selected for illustration. The result shows that the swelling ratio of the hydrogel is affected by the ratio of the monomer. As depicted in **Figure 3.2A**, the higher the acrylamide is, the higher the swelling ratio is; this may be because, after the treatment with NaOH, a considerable part of the amide function ($-CONH_2$) is directly transformed into carboxylate after the liberation of ammonia (NH_3), the carboxylate functional group have the ability to be strongly solvated in aqueous media than non-ionic group for example (Mahdavinia et al., 2004b).

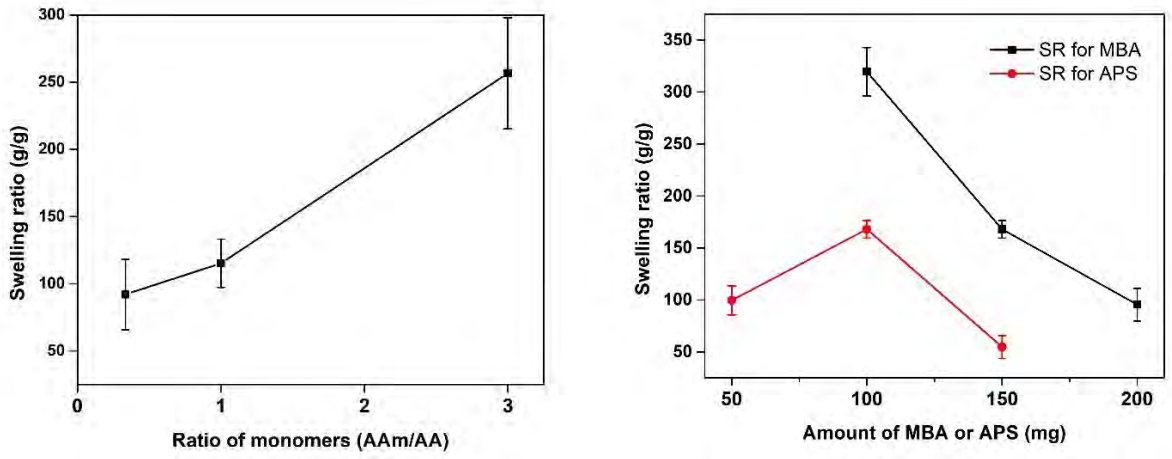

Figure 3. 2: Influence of studied parameters on swelling ratio (A) monomer ratio, (B) Amount of crosslinking agent and initiator

Secondly, the swelling capacity face to the change in the amount of the crosslinking agent was assessed, and formulations 2, 5, and 8 (**Table 3.1**) with 100, 150, and 200 mg of MBA respectively and with 3:1 as monomer ratio and 100 mg of APS was chosen to demonstrate the effect. The graph in **Figure 3.2 B** shows that the swelling capacity of the hydrogel decrease with the augmentation of the crosslinking agent. When the crosslinking agent is high, the crosslinking

density is also high, meaning there is the formation of a system with many networks that reduce the penetration of water into the system and, consequently, the swelling capacity (Pourjavadi et al., 2004). (See also later SEM and other studies that confirm this.)

Finally, formulations 4, 5, and 6 (**Table 3.1**) with 50, 100, and 150 mg of initiator and with 3:1 as monomer ratio and 15 mg of MBA (**Figure 3.2 B**) illustrate the influence of the initiator on the profile of the swelling capacity. The graph exhibits two events in the swelling behavior of the hydrogel, where firstly, an increase in swelling with increase of the initiator and secondly, a decrease of the swelling ratio with a further increase of the initiator. The first increase of the swelling can be due to creating a considerable amount of free radical site on the chitosan backbone, which results in the building of good polymeric networks capable of holding an enormous amount of water. Still, the decrease of the swelling ratio in the second stage may be due to an increase of the terminating stage of the reaction, consequently increasing the crosslinking density, which decreases the penetration of water in the networks (Pourjavadi et al., 2005).

Formulations 2, 5, and 8 were selected for father characterizations and encapsulation and release studies. According to their best swelling capacity, these formulations were chosen in terms of the optimized monomer ratio (3:1) and initiator concentration (10 mg) data. The following text will be labeled as F1, F2, and F3 with 100, 150, and 200 mg of MBA, respectively. The three formulations have different concentrations of the crosslinking agent because we will also have to observe how this factor influences the hydrogels' other properties like pH sensitivity, ionic strength-sensitivity, encapsulation efficiency, drug loading, and release profile.

Further characterization of hydrogel (TGA, DSC, SEM, FTIR, XRD, etc.) was performed on the formulation F2.

3.2 Characterization of chitosan grafted poly (acrylamide-co-acrylic acid)

3.2.1 Thermal gravimetric analysis (TGA)

Thermal gravimetric analysis (TGA) was performed to assess the change that occurred after the grafting of acrylamide and acrylic acid into chitosan and creating a crosslinked structures by the crosslinking agent. The TGA thermogram of CS (**Figure 3.3 A**) showed that its decomposition could be split into three successive zones of weight loss. The first one goes from 30-230°C representing a loss of 11,1% that can be attributed to the moisture loss of the sample. The second zone exhibits a sharp decomposition from 230-385°C (42,9%); this sudden fall in weight can be

due to the fragmentation of the backbone of chitosan. The last zone goes from 385-600°C (20,5%); this last gradual decomposition can be attributed to the complete degradation of the polymer. However, the TGA thermogram of CS-P(AAm-AA) (**Figure 3.3A**) showed a weight loss in four zones, the first one 30-190°C (7,1% weight loss) can be attributed to the loss of moisture, the second 190-321°C (20,7%) and the third 321-500 (29,4%) are attributed to the grafting chains degradation and the fragmentation of the backbones, respectively. The fourth zone (500-600°C) represents the complete degradation of the material (Pal et al., 2018). In addition, at 600°C, 33.38% of CS-P(AAm-AA) remained, but for CS at the same temperature, there is only 25,4%. The difference between the TGA thermogram of CS and CS-P(AAm-AA), which is well depicted in the graph of the first-order derivatives of the weight (**Figure 3.3 B**), confirms the crosslinking of CS and the grafting of AAm and AA.

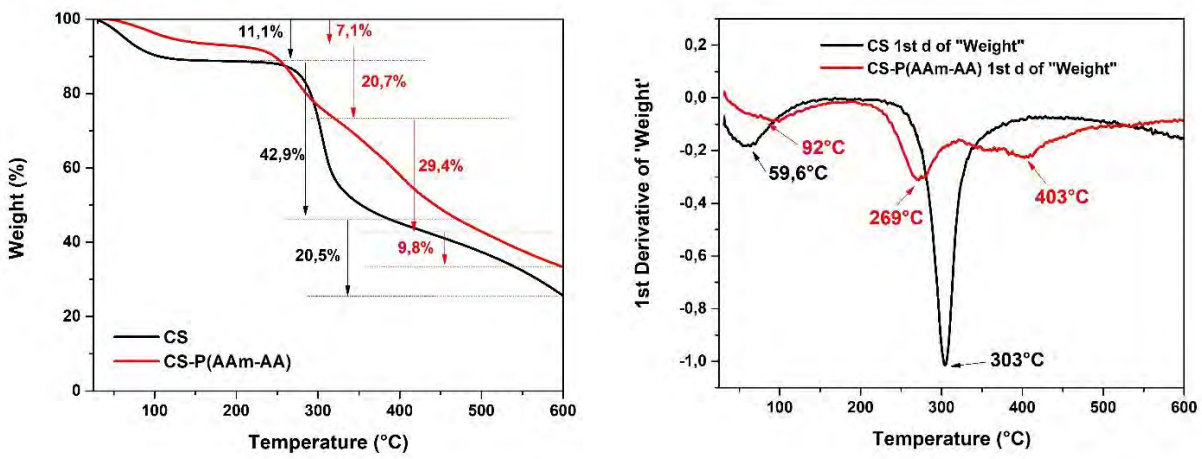

Figure 3. 3: TGA thermogram of CS and dry CS-P(AAm-AA) (A) graph of the first-order derivatives of the weight loss of CS and CS-P(AAm-AA) (B)

3.2.2 Differential Scanning Calorimetry (DSC)

Differential scanning calorimetry (DSC) thermograms of Chitosan and dry CS-P(AAm-AA) are presented in **Figure 3.4**. DSC thermogram of chitosan shows two thermodynamics events, one large endothermic peak between 25°C and 119°C giving a glass transition temperature (Tg) at 57°C and with an enthalpy (ΔH) of 156 J/g and a second exothermic peak ranged between 280 and 333°C with a Tg of 305°C and an ΔH of -128 J/g. The first thermodynamic event might be

associated with the loss of bound water and the transition from hard material to a soft and rubbery state. In contrast, the second event corresponds to the degradation of chitosan (Bashir et al., 2017). These results confirm the TGA data where a weight loss of 42,9% was observed in the temperature range of 230-385°C (range in which the exothermic peak is observed) and that was attributed to the degradation of the chitosan.

CS-P(AAm-AA) hydrogel thermogram shows two curves; an endothermic one ranged between 25°C and 132°C with a Tg at 65°C and with ΔH of 211 J/g and an exothermic peak between 273°C and 305°C with a Tg at 290°C and with ΔH of -12J/g. In addition to the TGA data, the shifts in both glass transition temperatures and enthalpies between the starting polymer and the prepared hydrogel can be due to the change in the stability of the gel network after crosslinking, which confirm the modification of chitosan and formation of the hydrogel (Saboktakin et al., 2011).

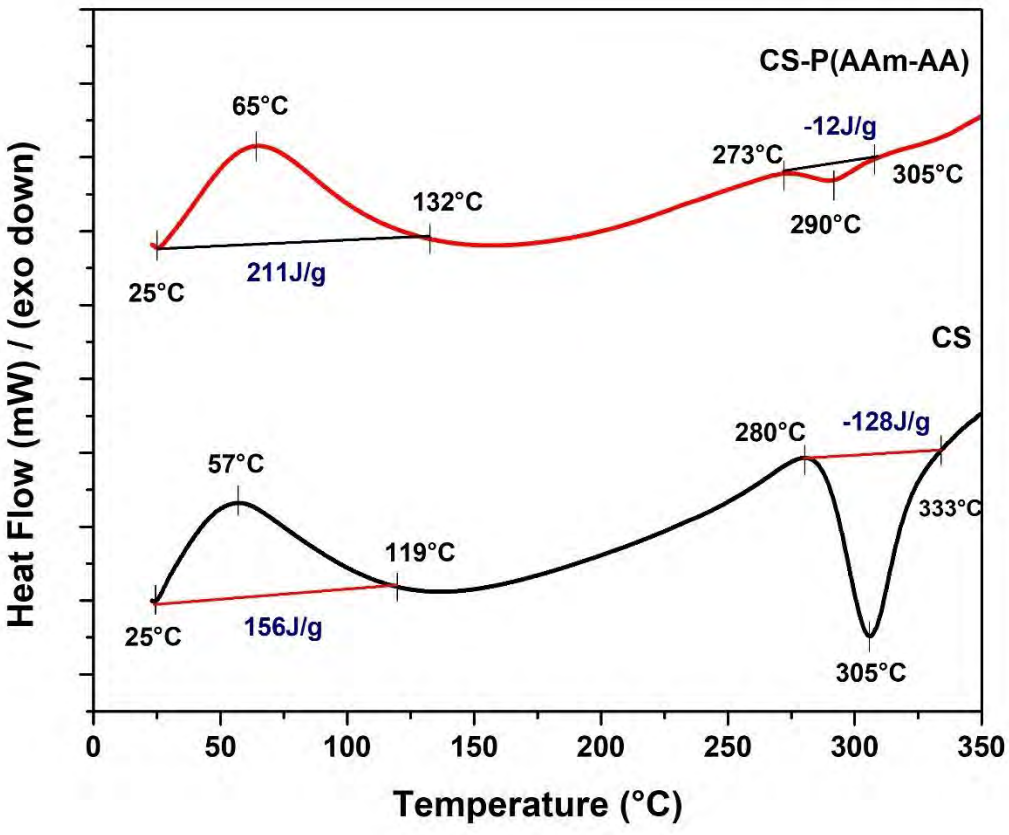

Figure 3.4: DSC thermogram of CS and CS-P(AAm-AA)

3.2.3 Scanning Electron Microscopy (SEM) and Energy-dispersive X-ray spectroscopy (EDS)

Freeze-dried samples of CS-g-P(AAm-AA) hydrogels were analyzed to study their surface morphology by scanning electron microscopy (SEM). The surface morphology of hydrogel is a critical parameter in the design of hydrogels for drug delivery application since it affects the swelling characteristics, drug encapsulation, and release behavior (Chen et al., 2009). As shown in the microphotographs (**Figures 3.5 A and B**), the surface of freeze-dried CS-P(AAm-AA) hydrogel is rough and fibrous, with numerous pores, which are ideal properties for drug delivery application of hydrogel. Elemental analysis was carried out by energy-dispersive X-ray spectroscopy (EDS) to confirm the hydrogel structure presented in the suggested scheme of hydrogel synthesis (**Figure 3.1**). The result given in (**Figure 3.5 C**) confirms the presence of carbon, oxygen, nitrogen, and sodium in the structure of the prepared material. The company of sodium maybe consider as a confirmation of the saponification of both the carboxylic and amide functional groups, as reported by other authors in the literature (Kulicke and Nottelmann, 2000; Savoji and Pourjavadi, 2006).

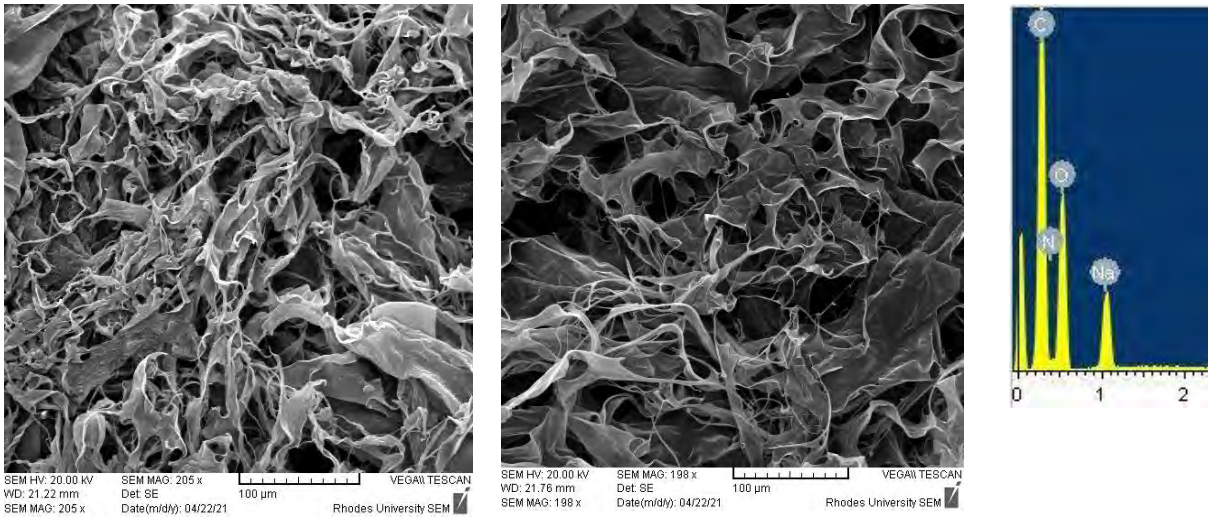

A B C

Figure 3.5: SEM microphotographs of freeze-dried CS-g-P(AAm-AA) (A) and (B), EDS spectrum of CS-g-P(AAm-AA) (C)

3.2.4 Evaluation of cytotoxicity of CS-P(AAm-AA)

Biocompatibility is a relevant factor to consider when choosing a material for drug delivery application, there are several techniques used to assess the biocompatibility of material, and the

evaluation of the cytotoxicity of the material against normal cell or HeLa cell lines are one of the techniques used for that purpose (Hu et al., 2015).

Chitosan is a deacetylated version a chitin which is a natural polymer with a good biocompatibility (Parhi, 2020). And although multiple studies have demonstrated the non-cytotoxicity, biodegradability, and biocompatibility of chitosan, its derivatives must be carefully assessed for biocompatibility before further biomedical application (Li et al., 2012). Hence, a study on the cytocompatibility of the synthesized chitosan grafted poly (acrylamide-*co*-acrylic acid) hydrogel was performed by studying the cell viability of HeLa cells in the presence of the hydrogel using resazurin based reagent. As depicted in **Figure 3.6**, all the hydrogel formulations were found to be non-cytotoxic at 50µg/ml. This result suggests that the prepared hydrogel has good cytocompatibility, making it suitable for biomedical applications.

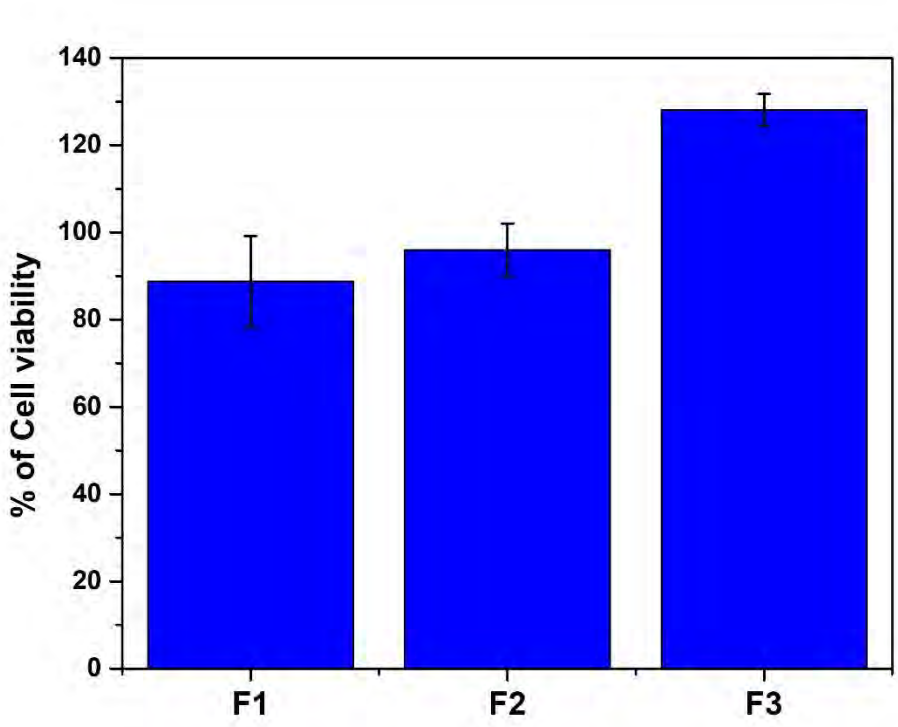

Figure 3.6: The cell viability % of HeLa cells tested with CS-P(AAm-AA) hydrogel at 50µg/ml after 24-h incubation. Each point was the mean ± SD (standard deviation) of three independent experiments performed in triplicate (with F1, F2 and F3 prepared with 100 mg, 150 mg, and 200 mg of N, N methylene bisacrylamide, respectively)

3.3 Swelling studies

The swelling capacity is a very relevant feature in the studies of hydrogels. In this section, we will discuss the swelling capacity of chitosan grafted poly (acrylamide-*co*-acrylic acid) in terms of its pH and salt sensitivity and its potential to swell and de-swell when the pH is being changed.

3.3.1 pH-sensitivity of chitosan grafted poly (acrylamide-*co*-acrylic acid)

The swelling capacity of CS-P(AAm-AA) hydrogel was studied in different buffer solutions at different pH values to assess its pH sensitivity. The result is summarized in **Figure 3.7.**

The swelling capacity of CS-P(AAm-AA) hydrogel was measured at pH 1.2 (HCl/KCl), pH 4 (acetate buffer), pH 5.8 (phosphate buffer), pH 7.4 (phosphate buffer), and pH 9.8 (carbonate buffer). At lower pH (1.2 and 4), the swelling ratio (SR) was very low, but at pH 5.8 it increased significantly, also, at pH 7.4, a further increase in SR was observed. At pH 9.8 the swelling ratio was slightly lower than the maximum observed around neutral pH, but the value was still relatively high when compared to those at pH 1.2 and pH 4. At low pH (1.2 and 4), the low swelling capacity may be because the pH value is below the pKa (4.75) of the carboxylic acid (-COOH); hence the functional groups were protonated. However, at high pH (5.8, 7.4, and 9.8), the swelling capacity increase because the pH is above the pKa of carboxylic acid, and in that condition, a huge number of –COOH function is deprotonated, and the electrostatic repulsion between the carboxylates group ($–COO^-$) increase the swelling capacity. In addition, the $–COO^-$ group being changed has the ability to be more hydrated than the –COOH group (Pourjavadi et al., 2005).

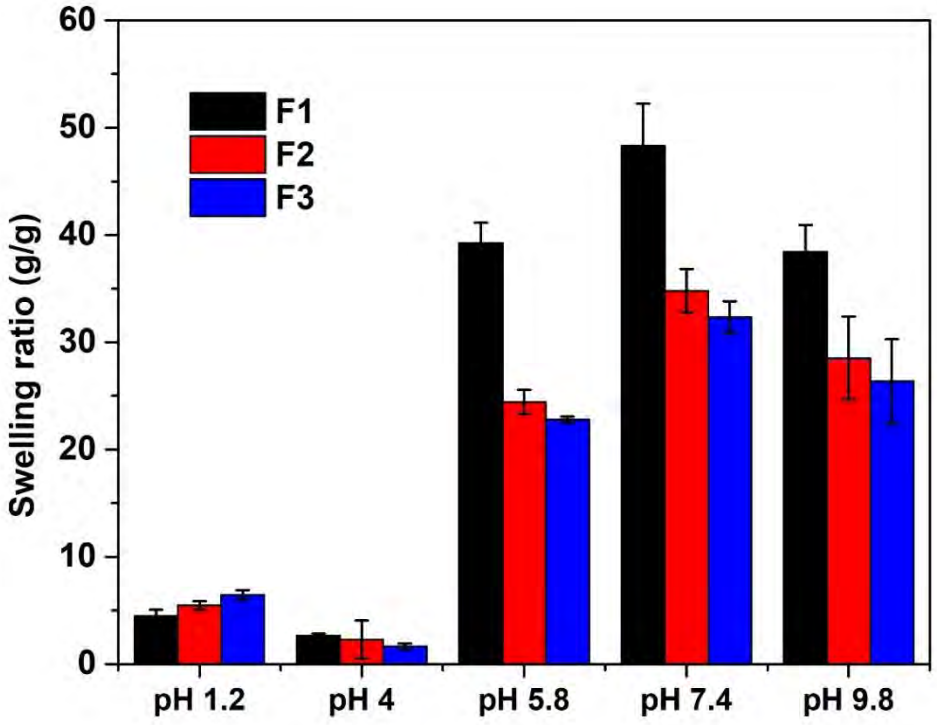

Figure 3.7: Effect of pH on the swelling capacity of CS-AAm-AA (with F1, F2 and F3 prepared with 100 mg, 150 mg, and 200 mg of N, N methylene bisacrylamide, respectively)

3.3.2 Swelling-deswelling-reswelling of chitosan grafted poly (acrylamide-co-acrylic acid)

The pH-dependent swelling-deswelling-reswelling of CS-P(AAm-AA) hydrogel was studied at pH 7.4 and 1.2. As presented in **Figure 3.8**, the results show that the hydrogel has a high swelling ratio at pH 7.4, but when put at pH 1.2, they shrink. Finally, when put back at pH 7.4, they re-swell again, which confirms the reversible pH-sensitivity property of the hydrogel. In fact, the swelling was generally found to be even better after the second exposure to pH 7.4, this may be due to the time of contact which was long in the second exposure as it was a continuing process.

At high pH values, carboxyl groups from the monomers become negatively charged. A high electrostatic repulsion occurs between neighboring polymers chains, which increases the hydrogel's swelling ratio. While at low pH condition, carboxyl groups from monomers structure become protonated which reduce the electrostatic repulsion. In the absence of repulsive forces,

hydrogen bonds form between polymer chains, which lower water penetration (Cinay et al., 2017; Mahon et al., 2020).

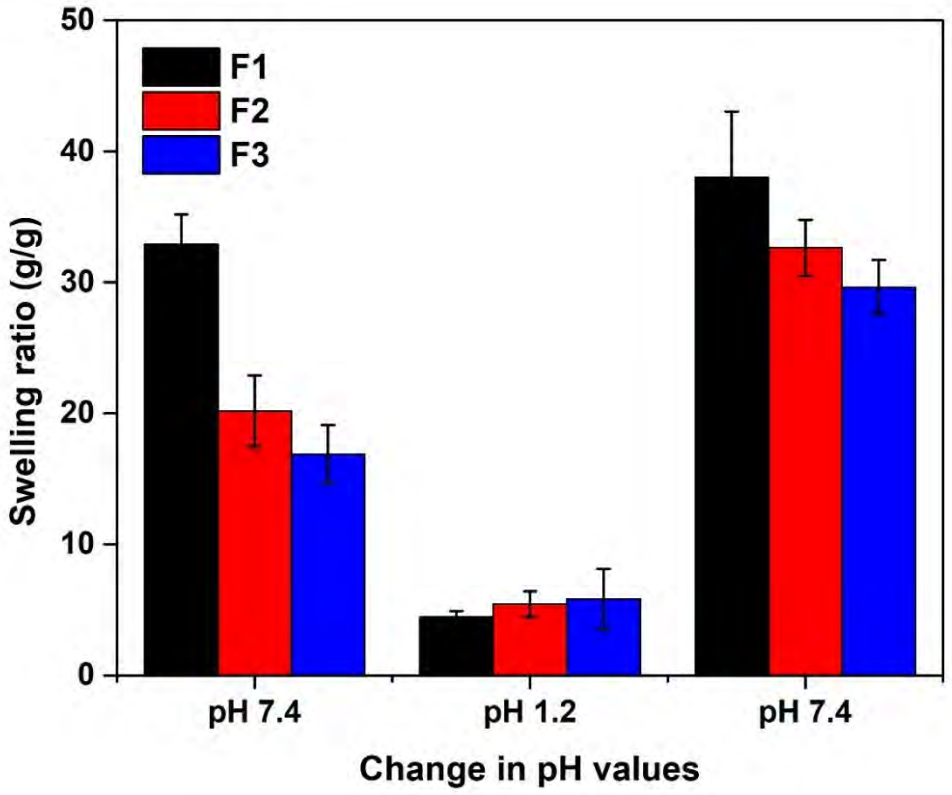

Figure 3. 8: Reversible swelling behavior of CS-P (AAm-AA) in buffer solutions (with F1, F2 and F3 prepared with 100 mg, 150 mg, and 200 mg of N, N methylene bisacrylamide, respectively)

3.3.3 Ionic strength-sensitivity of chitosan grafted poly (acrylamide-co-acrylic acid)

For the evaluation of the salt or ionic strength-sensitivity of CS-P(AAm-AA) hydrogel, the swelling behavior of the hydrogels was studied in solutions of different salts sodium chloride (NaCl), magnesium chloride ($MgCl_2$), and aluminum chloride ($AlCl_3$) and at various molar concentrations (0.05, 0.1 and 0.15 Mol/L).

The result presented in **Figure 3.9** revealed that on the one hand, the swelling capacity of the CS-P(AAm-AA) hydrogel decreases when the concentration of the salt increases **(Figure 3.9 A, B, and C**), this mean that the change in ionic strength of the solution also affects the swelling behavior of the hydrogel. On the other hand, it shows that when the metal's valence in the salt is high, the

swelling capacity is low (**Figure 3.9D**). The swelling capacity decrease may be explained by the shielding effect created by the presence of a cation in the solution. The negatively charged groups ($-COO^-$) present in the chain of the hydrogel is surrounded by the cations, which decreases the hydration (Bashir et al., 2017).

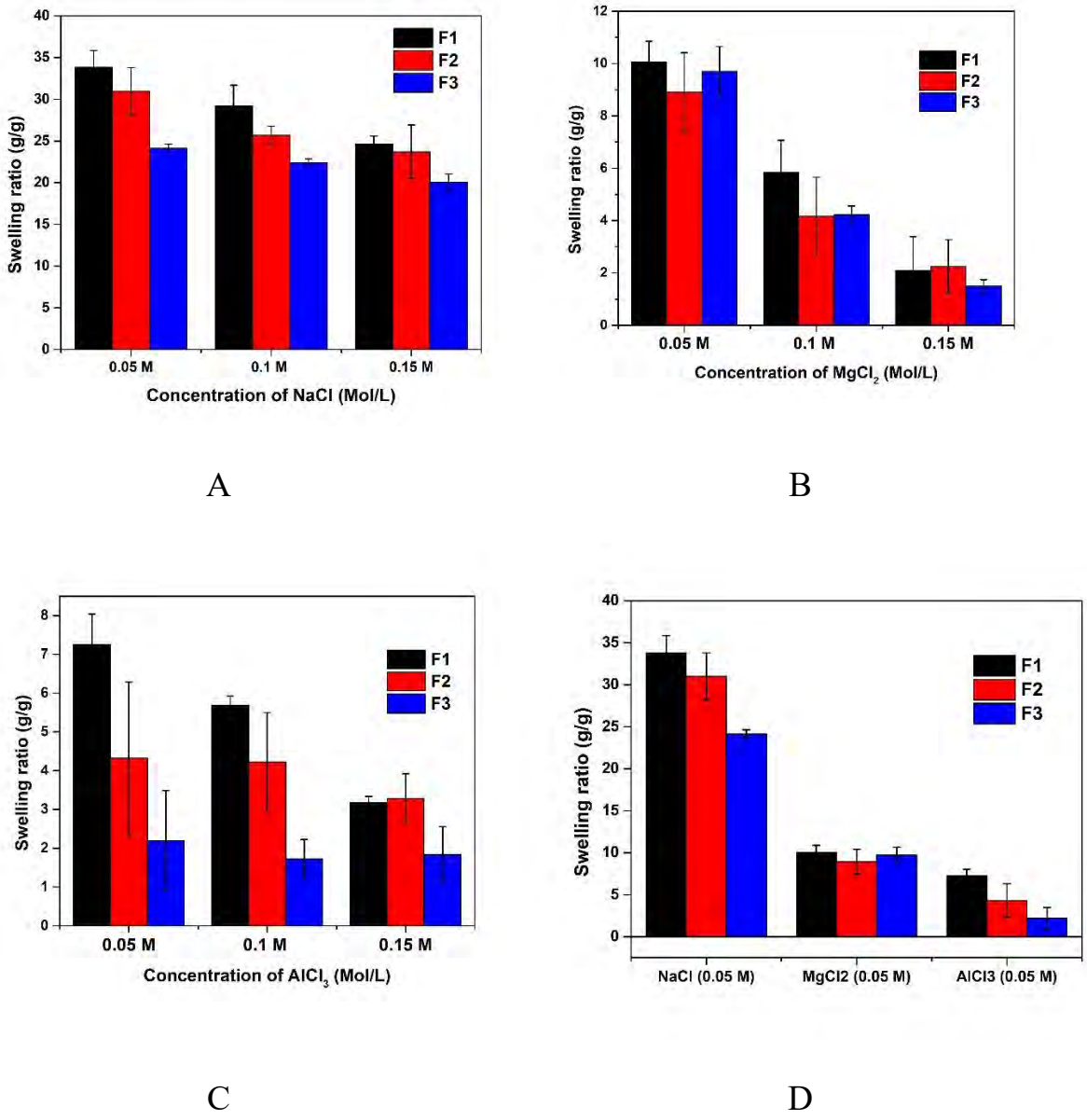

Figure 3.9: Effects of salts on the swelling capacity of CS-AAm-AA hydrogel: (A) NaCl, (B) $MgCl_2$, (C) $AlCl_3$, and (D) comparison of NaCl, $MgCl_2$ and $AlCl_3$ (with F1, F2 and F3 prepared with 100 mg, 150 mg and 200 mg of N, N methylene bisacrylamide, respectively)

Overall, the synthesized chitosan grafted poly (acrylamide-*co*-acrylic acid) hydrogels may be ideal for pH-controlled drug delivery applications because of their shown cytocompatibility, thermal stability, excellent surface morphology with well-defined pores, and optimal swelling capacity under physiological circumstances.

3.4 Drug encapsulation and *in vitro* release

3.4.1 Drug-excipient compatibility

Tenofovir disoproxil fumarate (TDF) was chosen as the antihepatitic B model drug for encapsulation. Hence physicochemical compatibility between the drug and the carrier was studied by differential scanning calorimetry (DSC) as a pre-formulation essay. **Figure 3.10** presents the DSC thermogram of TDF and a physical mixture on a 1:1 ratio with the hydrogel.

The thermogram of TDF has characterized endothermic peaks (Tg =117°C), which approximatively corresponding to the melting point of TDF (Elionai et al., 2015; Silva et al., 2017). In the physical mixtures, despite a slight decrease in the intensity of the peak, there was no shift in the melting point of TDF, and no new peak appeared. The DSC data confirmed no significant physicochemical incompatibilities between the TDF, our active pharmaceutical ingredient, and the carriers (hydrogel).

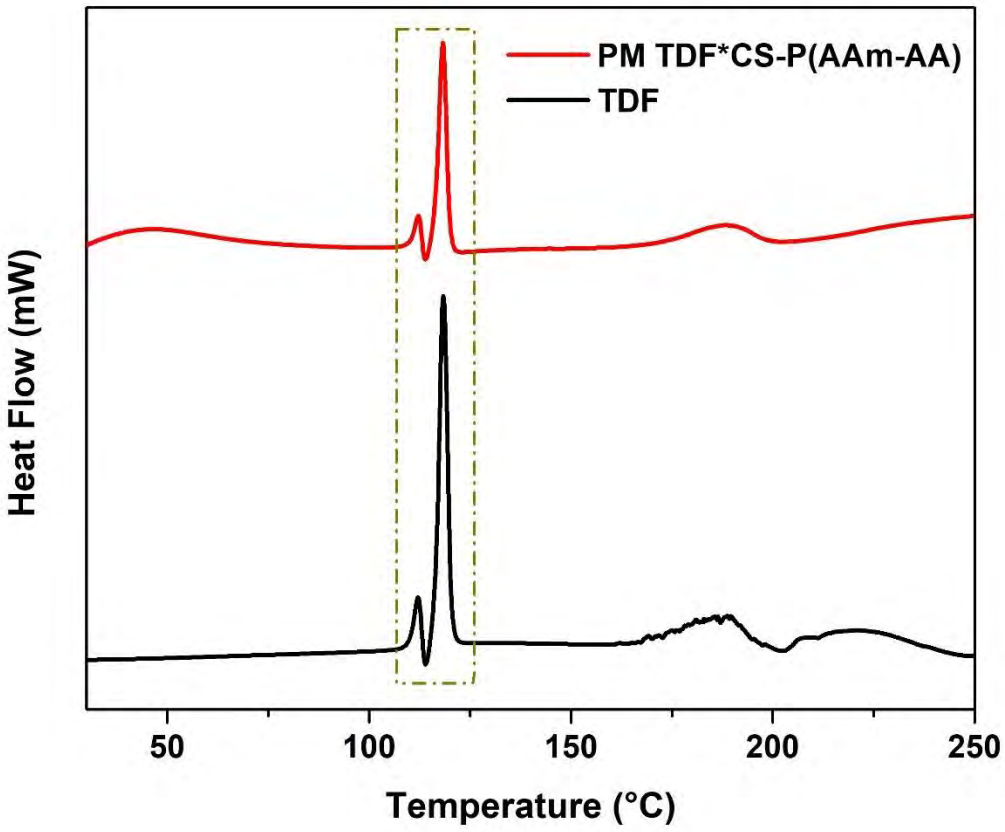

Figure 3.10: DSC thermogram of TDF compared to the physical mixtures (1:1) with the hydrogel CS-P(Aam-AA)

3.4.2 Validation of the HPLC method for analysis of tenofovir disoproxil fumarate

The high-performance liquid chromatography (HPLC) technique was used to quantify TDF in the encapsulation and release studies. Hence, an HPLC method for quantification of TDF was validated as per International Council for Harmonization (ICH) guidelines.

As depicted in the representative chromatogram of TDF (**Figure 3.11**), the retention time of TDF was approximately 3.03 ± 0.2 (n=6) at the detection wavelength of 259 nm. The quantification of TDF was based on the calibration curve constructed between the peak areas of the TDF chromatogram (y-axis) and concentration (x-axis). The regression equation of the calibration curve (y=23.519x+136.6) was linear in the range of 10-0.5 µg/ml, and the correlation coefficient (R^2) was 0.9993 (**Figure 3.12**). The HPLC method was accurate, as shown in (**Table 3.2**) where the percent recovered was in the acceptable limits (90-110%). As shown in (**Table 3.3**), the HPLC

method was precise both for intra- and inter-days precision since the percentage of relative standard deviation (%RSD) was less than 2% (EMA, 2006).

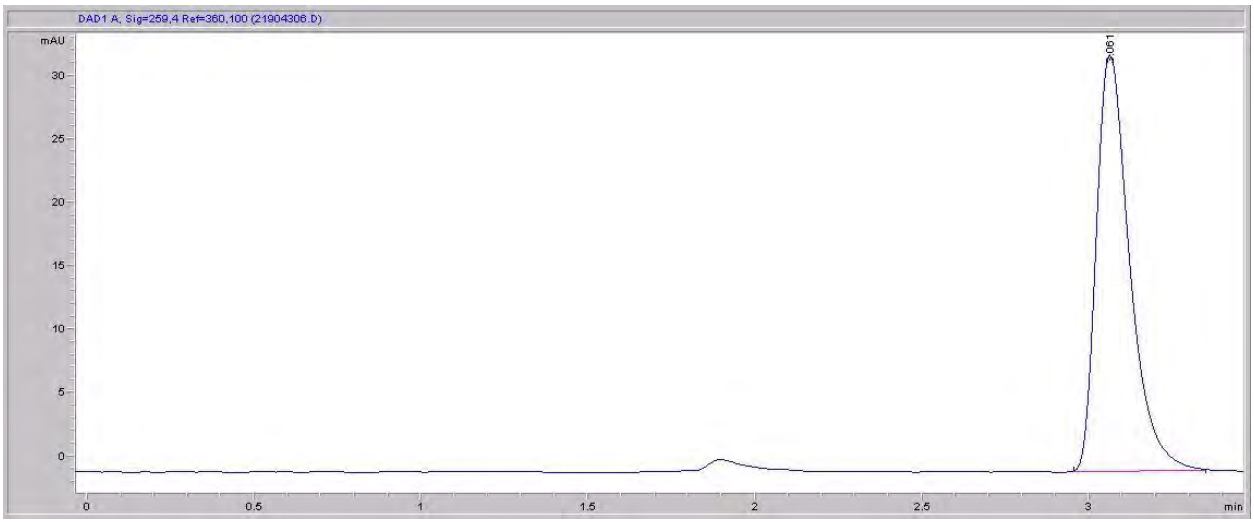

Figure 3.11: Typical HPLC chromatogram for a standard solution of TDF (5 µg/ml)

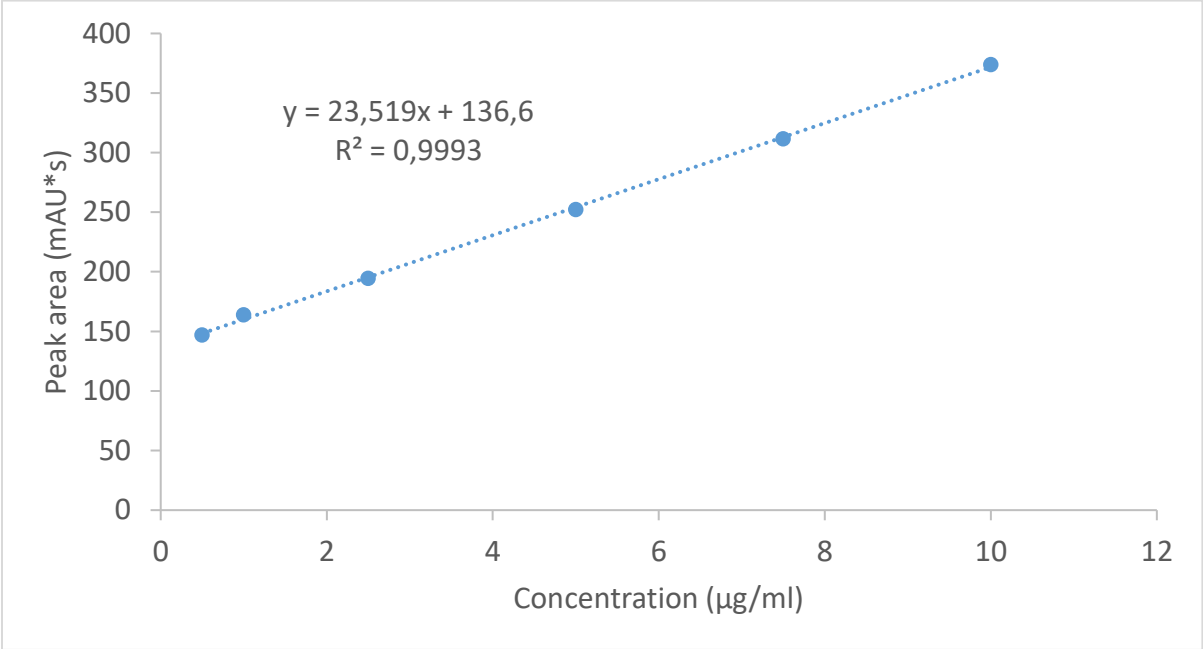

Figure 3.12: Standard calibration curve for TDF over the concentration range 0.5-10 µg/ml

Table 3.1: Result of accuracy for TDF analysis

Level of Standard solution (µg/ml)	Amount recovered (µg/ml)	Amount recovered (%)	RSD (%)
5	4.7225		
	5.0499	98.39	1.62
	4.9874		
7.5	7.2813		
	7.4867	99.12	1.015
	7.5343		
10	10.0068		
	10.2619	100.8731	0.952
	9.9931		

Table 3.2: Result of the precision (intra-day and Inter-day)

Precision

	Intra-day		Inter-day					
	Within day		Day 1		Day 2		Day 3	
Concentration (µg/ml)	Peak area (mAU.S)	RSD (%)	Peak area (mAU.S)	RSD (%)	Peak area (mAU.S)	RSD (%)	Peak area (mAU.S)	RSD (%)
5	229.13	0.625	250.73	1.084	272.98	0.379	264.88	1.519
	230.33		248.9		274.91		259.98	
	232		254.26		274.62		357.04	
7.5	279.35	0.657	316.6	1.944	338.65	1.103	334.54	0.901
	277.06		304.72		331.58		336.07	
	280.69		308.87		333.28		330.27	
10	315.42	0.508	361.24	0.974	384	0.707	362	0.343
	313.02		368.24		379.33		363.96	
	312.4		365.52		379.33		361.65	

3.4.3 Optimization of TDF encapsulation

Tenofovir disoproxil fumarate (TDF) is used as a first-line drug to treat HBV chronic infection and it is also used in combination with other antivirals drugs in the treatment of human immunodeficiency virus, acquired immunodeficiency syndrome (HIV/AIDS) (Gallant and Deresinski, 2011).

In this section, we investigated the effect of TDF concentration on the percentage of drug loading (DL) and the encapsulation efficiency (EE) to know the suitable concentration of the drug that must be used for further release studies. Encapsulation was done by the swelling equilibrium method, and four concentrations of TDF (100, 150, 200, and 250 µg/ml) were selected for optimization. As shown in **Figure 3.13**, on the one hand, the EE was the highest at 100 µg/ml with a gradual decrease as the drug concentration increases; on the other hand, the DL increases with the increase in drug concentration.

This result contradicts the result of Hanna and Saad (2019), who found that the DL and EE increased with the increasing concentrations of the drug, however their system was used to encapsulate ciprofloxacin in xanthan gum-chitosan based hydrogel (Hanna and Saad, 2019). This may be because ciprofloxacin is more highly soluble in water (42 mg/ml) than TDF (13.4 mg/ml), which is its high drug-loading in hydrogels. In addition, the concentration of the crosslinking agent affects both the EE and DL.

Samples F1, F2, and F3 containing 100, 150, and 200 mg of the crosslinking agent (MBA), respectively. As presented in **Figure 3.13** the encapsulation efficiency (EE) decreases with the increase in the concentration of TDF while the drug loading (DL) first increase with an increase in the concentration of TDF but after the concentration of 200 µg/ml the DL decreases was not significant in same samples. While the higher concentration (250 µg/ml) gave slightly better DL in some cases, this was to the detriment of the EE. Hence at the concentration of 200 µg/ml, concentration both the values of EE and DL were highest in all formulations as compared to other concentrations. It was observed that the DL of F1, F2, and F3 are 10.3±0.1, 9.7±0.1, and 8,6±0.1%, respectively, while the EE are 96.4±0.3, 91.8±0.9, and 81.2±1.3, respectively. Therefore, the hydrogels formulations loaded with 200 µg/ml solution of TDF were selected for further characterization and release studies.

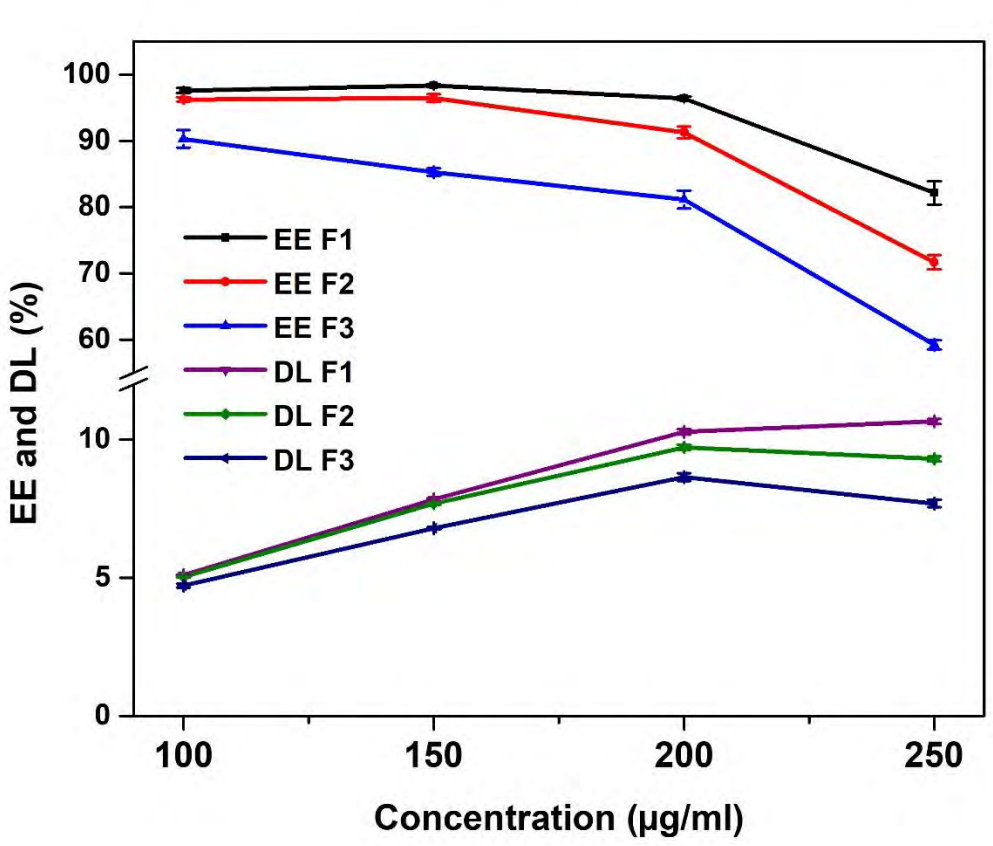

Figure 3.13: Optimization of encapsulation efficiency and drug loading (with F1, F2 and F3 prepared with 100 mg, 150 mg, and 200 mg of N, N methylene bisacrylamide, respectively)

3.4.4 FTIR spectroscopy

FTIR spectroscopy was used to assess different functional groups present in the chitosan and the hydrogels and see how they were affected following various modifications.

The spectral analysis (**Figure 3.14**) of pure chitosan indicates the presence of its characteristic vibration peaks, consistent with literature. Of interest are the broad band in the region of 3355-3286 cm^{-1} corresponds to -NH_2 and -OH stretching vibrations, as well as the absorptions bands at around 2869, 1641, and 1020 cm^{-1} (attributed to C-H, C=O, and C-O-C stretches, respectively). In addition, the vibration bands at 1584 cm^{-1} is due to the -NH- bend, and this can be quite sensitive to substitution (Queiroz et al., 2014). The spectrum for the CS-P(AAm-AA) hydrogels show the bands for carboxylic acid and amide bonds from AA and AAm, but these cannot be distinguished because they overlap with the characteristic bands of pure CS. Hence the successful grafting of AAm and AA into the backbone

of CS can be confirmed by the shift C=O to the higher frequency at 1657 cm^{-1} which suggests a high predominance of C=O groups in CS-P(AAm-AA) compared to pure CS. The saponification of CS-P(AAm-AA) resulted in the formation of -COONa groups whose presence is confirmed by the peak at 1541 cm^{-1} in the spectrum of CS-P(AAm-AA). The absence of noticeable changes in the spectrum of the TDF-loaded hydrogel (CS-P(AAm-AA)-TDF), when compared with CS-P(AAm-AA), confirms the entrapment of the drug without significant interaction (Hanna and Saad, 2019).

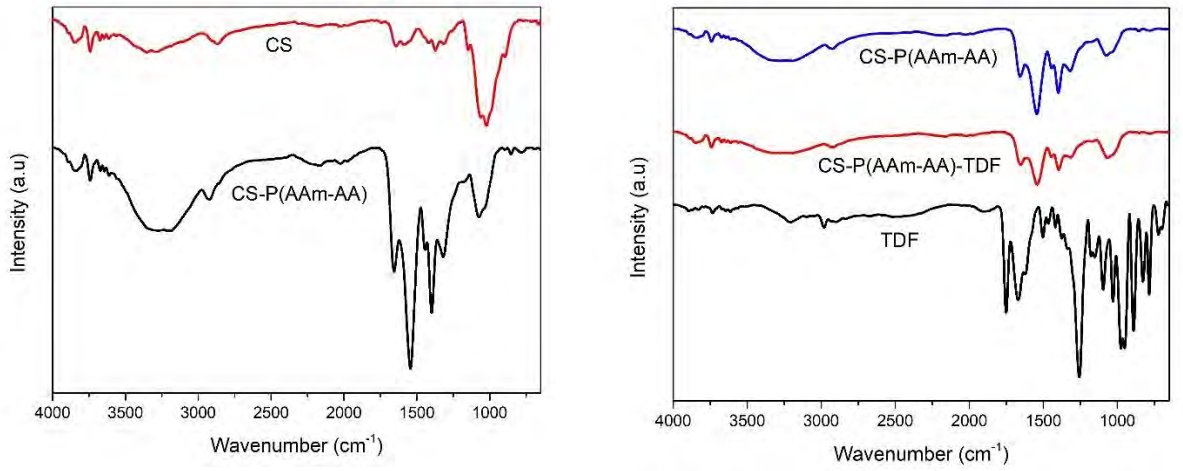

Figure 3.14: FTIR spectrum of (A) CS and CS-P(AAm-AA), (B) CS-P(AAm-AA), CS-P(AAm-AA)-TDF and TDF

3.4.5 Powder X-Ray Diffraction Spectroscopy

Powder X-ray diffraction was run to assess the change in the structure of chitosan after the chemical modification with AAm and AA and to see how encapsulation of TDF affects the crystalline structure of the material. Figure 3.15 presents the XRD pattern of CS, CS-P(AAm-AA), CS-P(AAm-AA)-TDF, and TDF hydrogel.

For chitosan, the spectrum shows one broad and weak peak at $2\theta = 20°$ indicating its semi-crystalline nature. That may be because chitosan has regular monomers (saccharides) in its structure and due to the formation of intramolecular and intermolecular hydrogen bonds between the amide and hydroxyl groups of chitosan (Bashir et al., 2017). However, in the spectrum of CS-

P(AAm-AA), the peak at 2θ = 20° is still present but which is broader than the one of chitosan. That change suggests a modification in the structure of chitosan and the reduction of its ability to form hydrogen bonds, hence the hydrogel is more amorphous (Julkapli et al., 2012; Wang et al., 2017). Tenofovir disoproxil fumarate (TDF) pattern presents many peaks where can be identified two prominent sharp and intense peaks at 2θ = 20° and 25° and other peaks at 2θ = 10.3°, 18.5°, 22°, 28°, and 30°, which confirm the crystalline nature of TDF (Elionai et al., 2015). However, after encapsulation of TDF in the hydrogel, the material presents no peaks but has a broad band around 20°, which suggests the amorphous profile of CS-P(AAm-AA)-TDF.

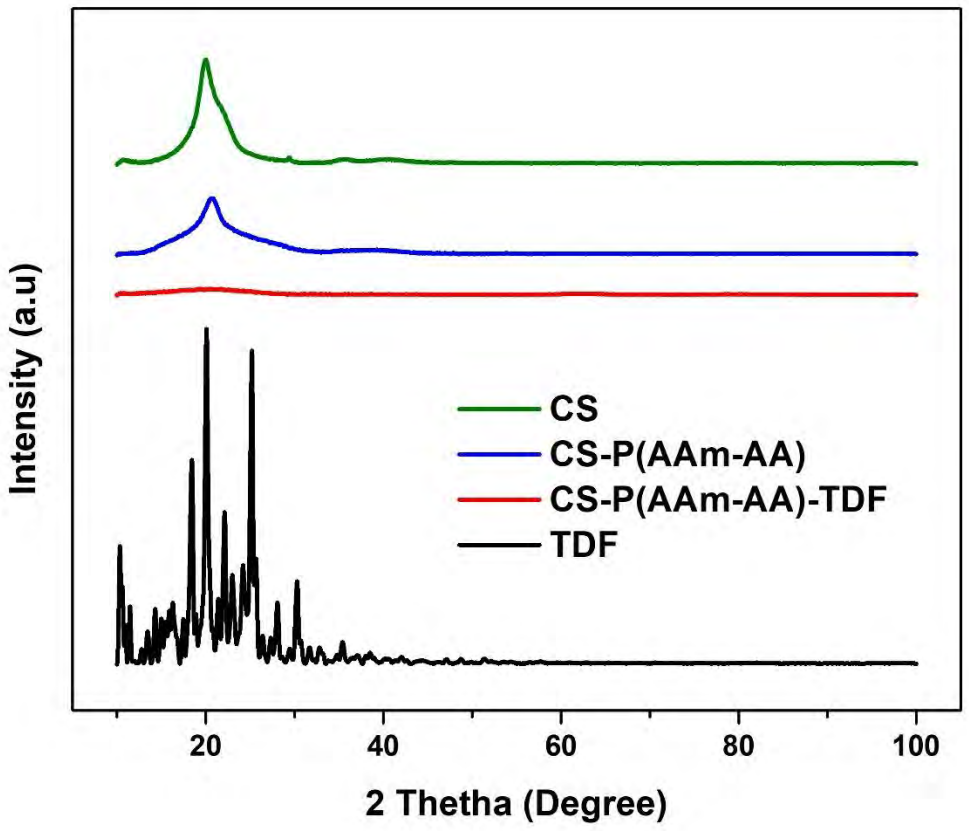

Figure 3.15: XRD spectrum of CS, CS-P(AAm-AA), CS-P(AAm-AA)-TDF and TDF

3.4.6 In vitro release profile of TDF

In the design of a drug delivery system, choosing a drug model is a critical stage; at this stage, the stability of the drug after encapsulation in the carrier is relevant. Interaction of drug encapsulated

with the carrier and the solvent may cause denaturation of the drug, affecting its structural stability and biological activity (Bashir et al., 2017). UV-Visible spectroscopy was used to assess the chemical activity of TDF before encapsulation and after release. As depicted in **Figure 3.16,** there is no change in λ_{max} (259 nm) of TDF before encapsulation and after release from the hydrogel; this result can be correlated with those of FTIR, which confirm a non-significant interaction between the carrier and the drug. Hence, TDF was chosen as a drug model.

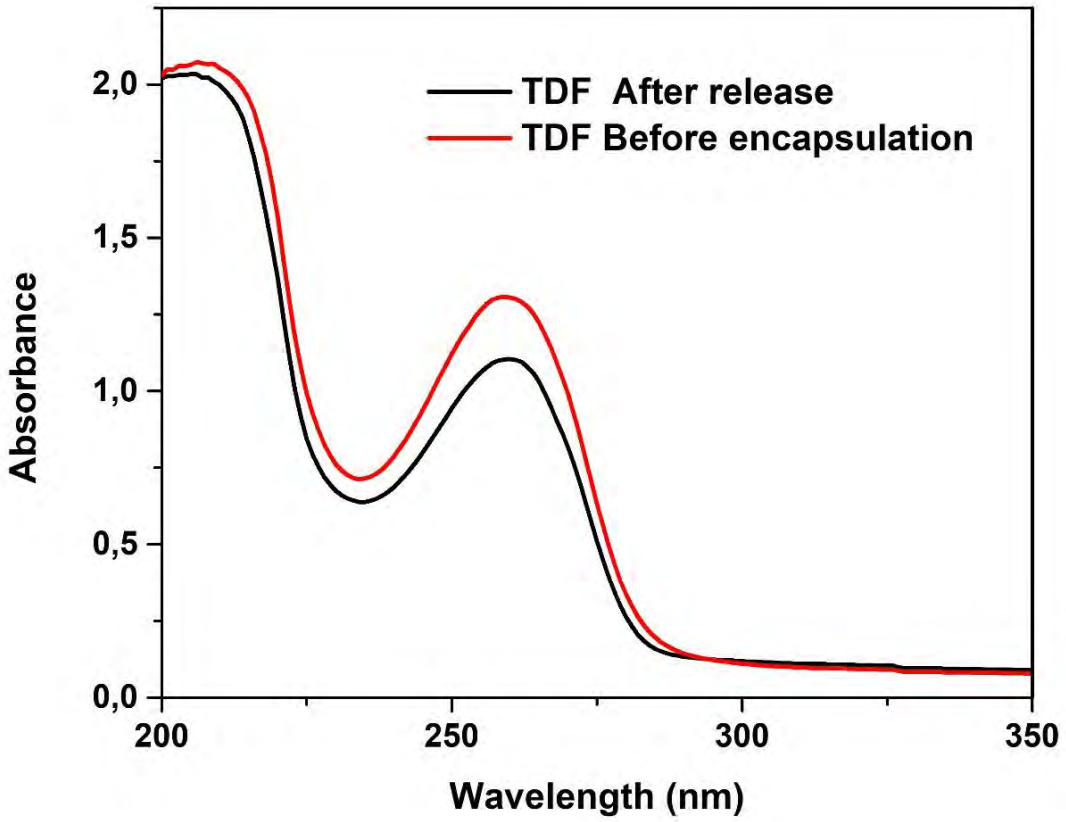

Figure 3.16: Chemical activity of pure TDF and TDF from in vitro release

Many variables influence *in vitro* drug release from hydrogels; these include its composition, swelling behavior, drug affinity for the polymer gel matrix (amount of drug content), and the release medium (Bashir et al., 2018). In this study, the release experiments of Tenofovir disoproxil fumarate from TDF-loaded hydrogels were carried out in buffer solution at pH 1.2 and 7.4 (I=0.1M), which are physiological pHs of stomach and intestine, respectively. **Figures 3.17 A** and

B show cumulative release curves at pH 1.2 and 7.4, respectively. At both pHs, all the formulations present a burst release in the (first 12h) followed by a controlled release. At pH 1.2, formulations F1, F2, and F3 released only 5.4±0.3, 6.1±0.9, and 10.3±1.6, respectively, while 38.8±2.3, 39.4±1, and 53.4±3.5, respectively was released at pH 7.4 after 96 h. It is depicted that the rate of release is high in neutral pH than in acid pH, which is consistent with the hydrogel swelling more in neutral and basic media than in acid media. Even though, TDF if more soluble in acidic conditions (Bazzo et al., 2019), at the lower pH can result in formation of hydrogen bonds between COOH and OH groups, which retard the release of the drug. This type of hydrogel was reported in the literature, Sokker et al reported a chitosan and gelatin grafted with poly acrylamide and poly (vinyl alcohol) which exhibited high release of oxytetracycline at high pH (9). In addition, Yue Wang et al, developed a poly (Maleic anhydride-β-cyclodextrin-*co*-*N*-isopropylacrylamide) hydrogels which demonstrated a pH dependent release profile of naproxen sodium which was high at pH 7.35 but lower at pH 1.5 (Sokker et al., 2009; Wang et al., 2018). Moreover, we observe that a not significant quantity of the drug was released in acidic media; this feature might be beneficial for long-term oral administration that makes use of the pH differential between the stomach and the intestine, as it has been reported for other drug delivery systems, Woraphatphadung et al reported a chitosan-based pH-sensitive polymeric micelles which was able to target the delivery of curcumin in the intestine and colon, only a slight amount of the drug was released in the stomach (Davaran et al., 1999; Woraphatphadung et al., 2018).

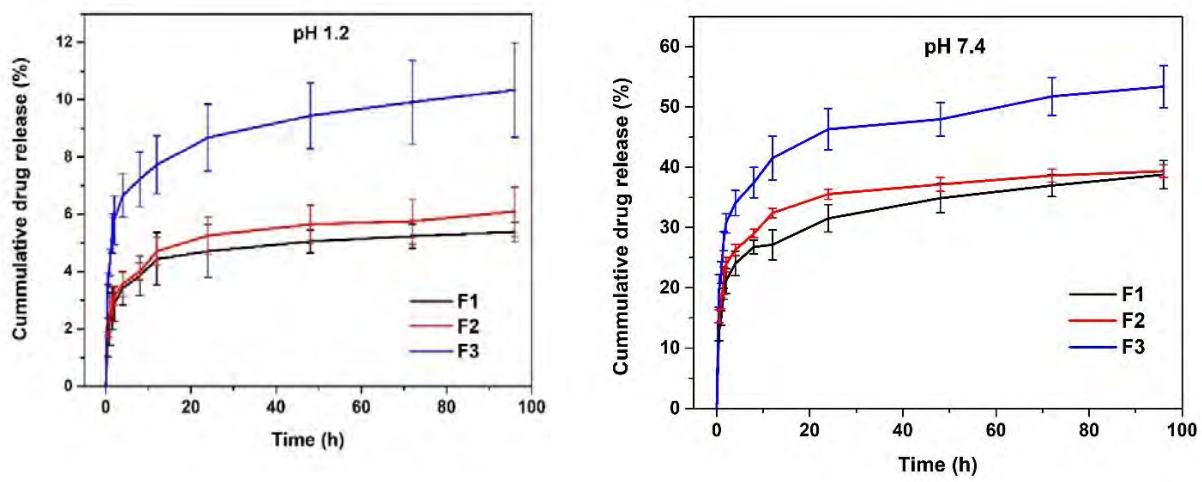

A B

Figure 3.17: In vitro release of TDF at pH 1.2 (A) and pH 7.4 (B)

Chapter Four

Conclusion

4 CONCLUSION

The main aim of this research was to develop a pH-sensitive drug delivery system in other to achieve a controlled drug delivery. In the course of this work, chitosan-based hydrogels were designed, optimized, synthesized, characterized, and evaluated as pH-sensitive drug delivery system of tenofovir disoproxil fumarate (TDF), an antihepatitic B drug. The HPLC method for quantification of TDF was validated for its suitability under actual analytical conditions.

Therefore, in this study, free radical polymerization reaction was used to prepare pH-sensitive chitosan grafted poly (acrylamide-co-acrylic acid) hydrogels. The preparation was optimized by looking at how parameters like the monomer's ratio (Aam/AA), the concentration of the crosslinking agent and the rection initiators affected the swelling ration of the synthesized materials. It was found that all the three parameters were able to impact the swelling ration of the hydrogels.

Further characterization of the optimized hydrogels was then undertaken to understand the structure, the composition and morphology of the hydrogels by the mean of the following analytical techniques FTIR, DSC, TGA, XRD, EDS, and SEM. The optimized hydrogels were also investigated for their cytotoxicity against Hela, it was demonstrated that they were not toxic to HeLa cell at 50 µg/ml.

Furthermore, smartness (pH and ionic strength responsive) of the hydrogels was investigated, for that purpose the swelling capacity of the hydrogels was investigated in buffer solutions with different values of pH and in solution with different salt composition. The outcomes indicated that the swelling ratio of all the investigated hydrogels was dependent of both the pH and ionic strength. It was observed that the maximum swelling at neutral or basic conditions and lower salt concentrations (low ionic strength).

Moreover, encapsulation of tenofovir disoproxil fumarate (TDF) was done by swelling equilibrium method and optimization of the encapsulation efficiency and the drug loading were investigated. Optimum values of encapsulation efficiency and drug loading were found when the concentration of TDF in the encapsulation solution was 200 µg/ml. In addition, it was observed that the amount of the crosslinking agent affected the encapsulation efficiency (EE) and drug loading (DL) of the

hydrogel. The EE was high in hydrogel with low amount of crosslinking agent while the DL was high when in hydrogel with high amount of the crosslinking agent.

Lastly, release of TDF was investigated at pH 1.2 and 7.4 simulating gastric and intestinal medium respectively. The release rate of TDF as a function of pH and hydrogel composition, with the maximum release at pH 7.4 being five times higher than at pH 1.2 after 96 hours for the formulation made with the highest amount of crosslinker (200 mg of *N, N* methylene bisacrylamide). Thus, the findings suggest that the developed drug delivery system can be applied for controlled delivery of TDF, potentially for oral routes.

However, further *in and ex vivo* studies are needed to provide additional insights on the pharmacological activity of the drug after release as well as the pharmacokinetic profile of the developed drug delivery system. Also, the synthesized and characterized material can be used to investigate the release profile of other drugs.

REFERENCES

Abdul Rahman, N., Katon, M.K., Zulkifli, N.A.Z., 2019. Analysis of Automatic Transmission Using Fourier Transform Infrared (Ftir) Spectrocopy. e-Academia J. 7, 58–66. https://doi.org/10.24191/e-aj.v7isi-temic18.5378

Agrahari, V., Youan, B.C., 2012. Sensitive and Rapid HPLC Quantification of Tenofovir from Hyaluronic Acid-Based Nanomedicine. AAPS PharmSciTech 13, 202–210. https://doi.org/10.1208/s12249-011-9735-6

Akhtar, M.F., Hanif, M., Ranjha, N.M., 2016. Methods of synthesis of hydrogels: A review. Saudi Pharm. J. 24, 554–559. https://doi.org/10.1016/j.jsps.2015.03.022

Anwar, M., Pervaiz, F., Shoukat, H., Noreen, S., Shabbir, K., Majeed, A., Ijaz, S., 2021. Formulation and evaluation of interpenetrating network of xanthan gum and polyvinylpyrrolidone as a hydrophilic matrix for controlled drug delivery system. Polym. Bull. 78, 59–80. https://doi.org/10.1007/s00289-019-03092-4

Bashir, S., Teo, Y.Y., Ramesh, S., Ramesh, K., 2018. Synthesis and characterization of karaya gum-g- poly (acrylic acid) hydrogels and in vitro release of hydrophobic quercetin. Polymer (Guildf). 147, 108–120. https://doi.org/10.1016/j.polymer.2018.05.071

Bashir, S., Teo, Y.Y., Ramesh, S., Ramesh, K., 2017. Physico-chemical characterization of pH-sensitive N-Succinyl chitosan-g-poly (acrylamide-co-acrylic acid) hydrogels and in vitro drug release studies. Polym. Degrad. Stab. 139, 38–54. https://doi.org/10.1016/j.polymdegradstab.2017.03.014

Bassyouni, F., Elhalwany, N., Abdel Rehim, M., Neyfeh, M., 2015. Advances and new technologies applied in controlled drug delivery system. Res. Chem. Intermed. 41, 2165–2200. https://doi.org/10.1007/s11164-013-1338-2

Baumert, T.F., Thimme, R., von Weizsäcker, F., 2007. Pathogenesis of hepatitis B virus infection. World J. Gastroenterol. 13, 82–90. https://doi.org/10.3748/wjg.v13.i1.82

Bazban-Shotorbani, S., Hasani-Sadrabadi, M.M., Karkhaneh, A., Serpooshan, V., Jacob, K.I., Moshaverinia, A., Mahmoudi, M., 2017. Revisiting structure-property relationship of pH-

responsive polymers for drug delivery applications. J. Control. Release 253, 46–63. https://doi.org/10.1016/j.jconrel.2017.02.021

Bazzo, G.C., Mostafa, D., França, M.T., Pezzini, B.R., Stulzer, H.K., 2019. How tenofovir disoproxil fumarate can impact on solubility and dissolution rate of efavirenz? Int. J. Pharm. 570, 118597. https://doi.org/10.1016/j.ijpharm.2019.118597

Beckett, L.E., Lewis, J.T., Tonge, T.K., Korley, L.S.T.J., 2020. Enhancement of the Mechanical Properties of Hydrogels with Continuous Fibrous Reinforcement. ACS Biomater. Sci. Eng. 6, 5453–5473. https://doi.org/10.1021/acsbiomaterials.0c00911

Bhattarai, N., Gunn, J., Zhang, M., 2010. Chitosan-based hydrogels for controlled , localized drug delivery. Adv. Drug Deliv. Rev. 62, 83–99. https://doi.org/10.1016/j.addr.2009.07.019

Bruschi, M.L., 2015. Drug delivery systems, in: Strategies to Modify the Drug Release from Pharmaceutical Systems. pp. 87–194. https://doi.org/10.1016/B978-0-08-100092-2.00006-0

Buwalda, S.J., Vermonden, T., Hennink, W.E., 2017. Hydrogels for Therapeutic Delivery : Current Developments and Future Directions. Biomacromolecules 18, 316–330. https://doi.org/10.1021/acs.biomac.6b01604

Caló, E., Khutoryanskiy, V. V, 2015. Biomedical applications of hydrogels : A review of patents and commercial products. Eur. Polym. J. 65, 252–267. https://doi.org/10.1016/j.eurpolymj.2014.11.024

Camara, F.V., Ferreire, L.J., 2012. Hydrogels: Synthesis, Characterization and Applications. Biochemistry Research Trends.

Catoira, M.C., Fusaro, L., Di Francesco, D., Ramella, M., Boccafoschi, F., 2019. Overview of natural hydrogels for regenerative medicine applications. J. Mater. Sci. Mater. Med. 30, 1–10. https://doi.org/10.1007/s10856-019-6318-7

Chapman, T.M., McGavin, J.K., Noble, S., 2003. Tenofovir disoproxil fumarate. Drugs 63, 1597–1608. https://doi.org/10.2165/00003495-200363150-00006

Charles, E., Carraher, J., 2017. Introduction to Polymer Chemistry, Fouth Edit. ed. Taylor & Francis Group, New York.

Chen, J., Liu, M., Liu, H., Ma, L., 2009. Synthesis, swelling and drug release behavior of poly(N,N-diethylacrylamide-co-N-hydroxymethyl acrylamide) hydrogel. Mater. Sci. Eng. C 29, 2116–2123. https://doi.org/10.1016/j.msec.2009.04.008

Cheng, Y., Ko, Y., Chang, Y., Huang, S., Liu, C.J., 2018. Thermosensitive chitosan-gelatin-based hydrogel containing curcumin-loaded nanoparticles and latanoprost as a dual-drug delivery system for glaucoma treatment. Exp. Eye Res. https://doi.org/10.1016/j.exer.2018.11.017

Chirani, N., Yahia, L., Gritsch, L., Motta, F.L., Chirani, S., Faré, S., 2015. History and Applications of Hydrogels. J. Biomed. Sci. 4, 1–23.

Chisari, F. V., Isogawa, M., Wieland, S.F., 2010. Pathogenesis of hepatitis B virus infection. Pathol. Biol. 58, 258–266. https://doi.org/10.1016/j.patbio.2009.11.001

Cinay, G.E., Erkoc, P., Alipour, M., Hashimoto, Y., Sasaki, Y., Akiyoshi, K., Kizilel, S., 2017. Nanogel-Integrated pH-Responsive Composite Hydrogels for Controlled Drug Delivery. ACS Biomater. Sci. Eng. 3, 370–380. https://doi.org/10.1021/acsbiomaterials.6b00670

Coviello, T., Grassi, M., Rambone, G., Santucci, E., Carafa, M., Murtas, E., Riccieri, F.M., Alhaique, F., 1999. Novel hydrogel system from scleroglucan : synthesis and characterization. J. Control. Release 60, 367–378.

Davaran, S., Hanaee, J., Khosravi, A., 1999. Release of 5-amino salicylic acid from acrylic type polymeric prodrugs designed for colon-specific drug delivery. J. Control. Release 58, 279–287. https://doi.org/10.1016/S0168-3659(98)00167-9

Delmar, K., Bianco-Peled, H., 2016. Composite chitosan hydrogels for extended release of hydrophobic drugs. Carbohydr. Polym. 136, 570–580. https://doi.org/10.1016/j.carbpol.2015.09.072

Devasani, S.R., Dev, A., Rathod, S., Deshmukh, G., 2016. An overview of in situ gelling systems. Pharm. Biol. Eval. 3, 60–69.

Ding, X., Wang, Y., 2017. Weak bond-based injectable and stimuli responsive hydrogels for biomedical applications. J. Mater. Chem. B 5, 887–906. https://doi.org/10.1039/c6tb03052a

Echlin, P., 2009. Handbook of Sample Preparation for Scanning Electron Microscopy and X-Ray Microanalysis. Springer, New York.

El Hariri El Nokab, M., van der Wel, P.C.A., 2020. Use of solid-state NMR spectroscopy for investigating polysaccharide-based hydrogels: A review. Carbohydr. Polym. 240, 116276. https://doi.org/10.1016/j.carbpol.2020.116276

El, S., Koraichi, S., Latrache, H., Hamadi, F., 2012. Scanning Electron Microscopy (SEM) and Environmental SEM: Suitable Tools for Study of Adhesion Stage and Biofilm Formation, Scanning Electron Microscopy. InTech. https://doi.org/10.5772/34990

Elazar, M., Koh, C., Glenn, J.S., 2017. Hepatitis delta infection – Current and new treatment options. Best Pract. Res. Clin. Gastroenterol. 31, 321–327. https://doi.org/10.1016/j.bpg.2017.05.001

Elionai, E.C., Mussel, W.N., Resende, J.M., Fialho, S.L., Barbosa, J., Carignani, E., Geppi, M., Yoshida, M.I., 2015. Characterization of tenofovir disoproxil fumarate and its behavior under heating. Cryst. Growth Des. 15, 1915–1922. https://doi.org/10.1021/acs.cgd.5b00089

EMA, E.M.A., 2006. Validation of Analytical Procedures, Text and Methodology. Eur. Med. Agency.

Federsel, H., Moody, T.S., Taylor, S.J.C., 2021. Recent Trends in Enzyme Immobilization — Concepts for Expanding the Biocatalysis Toolbox. Molecules 26, 2822.

Ferreira, N.N., Ferreira, L.M.B., Cardoso, V.M.O., Boni, F.I., Souza, A.L.R., Gremião, M.P.D., 2018. Recent advances in smart hydrogels for biomedical applications : From self- assembly to functional approaches. Eur. Polym. J. 99, 117–133. https://doi.org/10.1016/j.eurpolymj.2017.12.004

Gallant, J.E., Deresinski, S., 2011. Tenofovir disoproxil fumarate. Rev. Anti-infective Agents 37, 944–950. https://doi.org/10.2165/00128415-201113680-00136

Ghany, M.G., 2017. Current treatment guidelines of chronic hepatitis B: The role of nucleos(t)ide analogues and peginterferon. Best Pract. Res. Clin. Gastroenterol. 31, 299–309. https://doi.org/10.1016/j.bpg.2017.04.012

Gulrez, S., Al-assaf, S., Phillips, G.O., 2011. Hydrogels : Methods of Preparation , Characterisation and Applications, in: Progress in Molecular and Environmental Bioengineering - From Analysis and Modeling to Technology Applications. pp. 117–150.

Gyles, D.A., Castro, L.D., Silva, J.O.C., Ribeiro-Costa, R.M., 2017. A review of the designs and prominent biomedical advances of natural and synthetic hydrogel formulations. Eur. Polym. J. 88, 373–392. https://doi.org/10.1016/j.eurpolymj.2017.01.027

Hahne, G.W.H., Hemminger, W.F., Flammersheim, H.J., 2003. Differential Scanning Calorimetry, 2nd Editio. ed. New York. https://doi.org/10.1007/978-3-662-06710-9

Hanna, D.H., Saad, G.R., 2019. Encapsulation of ciprofloxacin within modified xanthan gum-chitosan based hydrogel for drug delivery. Bioorg. Chem. 84, 115–124. https://doi.org/10.1016/j.bioorg.2018.11.036

Hennink, W.E., van Nostrum, C.F., 2012. Novel crosslinking methods to design hydrogels. Adv. Drug Deliv. Rev. 64, 223–236. https://doi.org/10.1016/j.addr.2012.09.009

Hoare, T.R., Kohane, D.S., 2008. Hydrogels in drug delivery : Progress and challenges. Polymer (Guildf). 49, 1993–2007. https://doi.org/10.1016/j.polymer.2008.01.027

Hoffman, A.S., 2008. The origins and evolution of "controlled" drug delivery systems. J. Control. Release 132, 153–163. https://doi.org/10.1016/j.jconrel.2008.08.012

Howell, J., Pedrana, A., Schroeder, S.E., Scott, N., Aufegger, L., Atun, R., Baptista-Leite, R., Hirnschall, G., 't Hoen, E., Hutchinson, S.J., Lazarus, J. V., Olufunmilayo, L., Peck, R., Sharma, M., Sohn, A.H., Thompson, A., Thursz, M., Wilson, D., Hellard, M., 2021. A global investment framework for the elimination of hepatitis B. J. Hepatol. 74, 535–549. https://doi.org/10.1016/j.jhep.2020.09.013

Hu, X., Wei, W., Qi, X., Yu, H., Feng, L., Li, J., Wang, S., Zhang, J., Dong, W., 2015. Preparation and characterization of a novel pH-sensitive Salecan-g-poly(acrylic acid) hydrogel for controlled release of doxorubicin. J. Mater. Chem. B 3, 2685–2697. https://doi.org/10.1039/c5tb00264h

James, H.P., John, R., Alex, A., Anoop, K.R., 2014. Smart polymers for the controlled delivery

of drugs – a concise overview. Acta Pharm. Sin. B 4, 120–127. https://doi.org/10.1016/j.apsb.2014.02.005

Jonker, A.M., Lo, D.W.P.M., Hest, J.C.M. Van, 2012. Peptide- and Protein-Based Hydrogels. Chem. Mater. 24, 758–773.

Julkapli, N.M., Ahmad, Z., Akil, H., Julkapli, N.M., Ahmad, Z., 2012. XRay Diffraction Studies of Cross Linked Chitosan With Different Cross Linking Agents For Waste Water Treatment Application. AIP Conf. Proc. 106, 106–111. https://doi.org/10.1063/1.3295578

Kao, J.H., 2008. Diagnosis of hepatitis B virus infection through serological and virological markers. Expert Rev. Gastroenterol. Hepatol. 2, 553–562. https://doi.org/10.1586/17474124.2.4.553

Karoyo, A.H., Wilson, L.D., 2017. Physicochemical Properties and the Gelation Process of Supramolecular Hydrogels : A Review. Gels 3, 1–18. https://doi.org/10.3390/gels3010001

Kearney, B.P., Flaherty, J.F., Shah, J., 2004. Tenofovir disoproxil fumarate: Clinical pharmacology and pharmacokinetics. Clin. Pharmacokinet. 43, 595–612. https://doi.org/10.2165/00003088-200443090-00003

Krajden, M., McNabb, G., Petric, M., 2005. The laboratory diagnosis of hepatitis B virus. Can. J. Infect. Dis. Med. Microbiol. 16, 65–72. https://doi.org/10.1155/2005/450574

Kulicke, W.-M., Nottelmann, H., 2000. Structure and Swelling of Some Synthetic, Semisyjthetic, and Biopolymer Hydrogels, in: Polymer in Aqueous Media. American Chemical Society, Washington, pp. 15–44.

Kurisawa, M., Lee, F., Wang, L.S., Chung, J.E., 2010. Injectable enzymatically crosslinked hydrogel system with independent tuning of mechanical strength and gelation rate for drug delivery and tissue engineering. J. Mater. Chem. 20, 5371–5375. https://doi.org/10.1039/b926456f

Kwon, S.Y., Lee, C.H., 2011. Epidemiology and prevention of hepatitis B virus infection. Korean J. Hepatol. 17, 87–95. https://doi.org/10.3350/kjhep.2011.17.2.87

Lai, J.Y., 2014. Relationship between structure and cytocompatibility of divinyl sulfone cross-

linked hyaluronic acid. Carbohydr. Polym. 101, 203–212. https://doi.org/10.1016/j.carbpol.2013.09.060

Latavia, S., Sunaina, I., Mershen, G., Pradeep, K.I., Lisa, du T., Yahya E., C., Viness, P., 2018. Drug Delivery Strategies for Antivirals against Hepatitis B Virus. Viruses 10, 1–20. https://doi.org/10.3390/v10050267

Lavik, E.B., Kuppermann, B.D., Humayun, M.S., 2012. Drug Delivery, Fifth Edit. ed, Retina Fifth Edition. Elsevier Inc. https://doi.org/10.1016/B978-1-4557-0737-9.00038-2

Lee, F., Bae, K.H., Kurisawa, M., 2015. Injectable hydrogel systems crosslinked by horseradish peroxidase. Biomed. Mater. 11, 14101. https://doi.org/10.1088/1748-6041/11/1/014101

Lemoine, M., Thursz, M.R., 2017. Battlefield against hepatitis B infection and HCC in Africa. J. Hepatol. 66, 645–654. https://doi.org/10.1016/j.jhep.2016.10.013

Li, H., 2009. Smart Hydrogel Modeling. Springer-Verlag Berlin Heidelberg. https://doi.org/10.1007/978-3-642-02368-2

Li, J., Mooney, D.J., 2016. Designing hydrogels for controlled drug delivery. Nat. Publ. Gr. 1, 1–18. https://doi.org/10.1038/natrevmats.2016.71

Li, X., Kong, X., Zhang, Z., Nan, K., Li, L.L., Wang, X.H., Chen, H., 2012. Cytotoxicity and biocompatibility evaluation of N,O-carboxymethyl chitosan/oxidized alginate hydrogel for drug delivery application. Int. J. Biol. Macromol. 50, 1299–1305. https://doi.org/10.1016/j.ijbiomac.2012.03.008

Mahdavinia, G.R., Pourjavadi, A., Hosseinzadeh, H., Zohuriaan, M.J., 2004a. Modified chitosan 4. Superabsorbent hydrogels from poly(acrylic acid-co-acrylamide) grafted chitosan with salt- and pH-responsiveness properties. Eur. Polym. J. 40, 1399–1407. https://doi.org/10.1016/j.eurpolymj.2004.01.039

Mahdavinia, G.R., Zohuriaan-Mehr, M.J., Pourjavadi, A., 2004b. Modified chitosan III, superabsorbency, salt- and pH-sensitivity of smart ampholytic hydrogels from chitosan-g-PAN. Polym. Adv. Technol. 15, 173–180. https://doi.org/10.1002/pat.408

Mahon, R., Balogun, Y., Oluyemi, G., Njuguna, J., 2020. Swelling performance of sodium

polyacrylate and poly(acrylamide-co-acrylic acid) potassium salt. SN Appl. Sci. 2. https://doi.org/10.1007/s42452-019-1874-5

Maitra, J., Shukla, V.K., 2014. Cross-linking in Hydrogels - A Review. Am. J. Polym. Sci. 4, 25–31. https://doi.org/10.5923/j.ajps.20140402.01

Mandala, D., Thompson, W.A., Watts, P., 2016. Synthesis routes to anti-HIV drugs. Tetrahedron 72, 3389–3420. https://doi.org/10.1016/j.tet.2016.04.075

Math, A.M., Scranton, A.B., 1996. Characterization of hydrogels using nuclear magnetic resonance spectroscopy. Biomaterials 17, 547–557.

Mckenzie, S., Logan, J., 2019. Hepatitis B structure: Capsid Flexibility and Function [WWW Document]. News-medical.net.

Menwzel, J.D., Prime, R.B., 2009. Thermal Analysis of Polymers: Fundamentals and Applications. Wiley, New Jersey.

Mohite, P.B., Adhav, S.S., 2017. A hydrogels : Methods of preparation and applications. Int. J. Adv. Pharm. 06, 79–85.

Moreira, L.S., Feijen, J., Blitterswijk, C.A. Van, Dijkstra, P.J., Karperien, M., 2012. Biomaterials Enzyme-catalyzed crosslinkable hydrogels : Emerging strategies for tissue engineering. Biomaterials 33, 1281–1290. https://doi.org/10.1016/j.biomaterials.2011.10.067

Narayanaswamy, R., Torchilin, V.P., 2019. Hydrogels and Their Applications in Targeted Drug Delivery. Molecules 24, 1–18. https://doi.org/10.3390/molecules24030603

Overstreet, D.J., Dutta, D., Stabenfeldt, S.E., Vernon, B.L., 2012. Injectable hydrogels. J. Polym. Sci. Part B Polym. Phys. 50, 881–903. https://doi.org/10.1002/polb.23081

Pal, K., Banthia, A.K., Majumdar, D.K., 2012. Polymeric Hydrogels : Characterization and Biomedical Applications. Des. Monomers Polym. 12, 197–220. https://doi.org/10.1163/156855509X436030

Pal, K., Singh, V.K., Anis, A., Thakur, G., Bhattacharya, M.K., 2013. Hydrogel-Based Controlled Release Formulations : Designing Considerations , Characterization Techniques

and Applications. Polym. Plast. Technol. Eng. 52, 1391–1422. https://doi.org/10.1080/03602559.2013.823996

Pal, P., Pandey, J.P., Sen, G., 2018. Sesbania gum based hydrogel as platform for sustained drug delivery: An 'in vitro' study of 5-Fu release. Int. J. Biol. Macromol. 113, 1116–1124. https://doi.org/10.1016/j.ijbiomac.2018.02.143

Parhi, R., 2020. Drug delivery applications of chitin and chitosan: a review. Environ. Chem. Lett. 18, 577–594. https://doi.org/10.1007/s10311-020-00963-5

Park, K., 2014. Controlled drug delivery systems: Past forward and future back. J. Control. Release 190, 3–8. https://doi.org/10.1016/j.jconrel.2014.03.054

Park, K., Shalaby, W.S.W., Park, H., 1993. Biodegradable Hydrogels for Drug Delivery. Taylor & Francis Group, New York.

Pastergiou, V., Lombardi, R., MacDonald, D., Tsochatzis, E.A., 2015. Global epidemiology of hepatitis B virus (HBV) infection. Curr. Hepat. Rep. 14, 171–178. https://doi.org/10.1007/s11901-015-0269-3

Patel, G.C., Dalwadi, C.A., 2013. Recent Patents on Stimuli Responsive Hydrogel Drug Delivery System. Recent Patents Drug Deliv. Formul. 2013, 7, 206–215.

Peppa, D., Maini, M.K., 2012. Pathogenesis of hepatitis B virus infection and potential for new therapies. Br. J. Hosp. Med. 73, 581–584. https://doi.org/10.12968/hmed.2012.73.10.581

Piliero, P.J., 2004. Pharmacokinetic properties of nucleoside/nucleotide reverse transcriptase inhibitors. J. Acquir. Immune Defic. Syndr. 37, 2–12. https://doi.org/10.1097/01.qai.0000137001.40505.56

Porche, D.J., 2002. Tenofovir Disoproxil Fumarate (Viead). J. Assoc. Nurses AISS Care 13, 100–102.

Pourjavadi, A., Hosseinzadeh, H., Mazidi, R., 2005. Modified Carrageenan . 4 . Synthesis and Swelling Behavior of Crosslinked kappaC- g -AMPS Superabsorbent Hydrogel with Antisalt and pH-Responsiveness Properties. J. Appl. Polym. Sci. 98, 255–263. https://doi.org/10.1002/app.22162

Pourjavadi, A., Sadeghi, M., Hosseinzadeh, H., 2004. Modified carrageenan. 5. Preparation, swelling behaviour, salt- and pH-sensitivity of partially hydrolyzed crosslinked carrageenan-graft-polymethacrylamide superabsorbent hydrogel. Polym. Adv. Tecnol. 15, 645–653. https://doi.org/10.1002/pat.524

Qi, X., Wei, W., Li, J., Zuo, G., Pan, X., Su, T., Zhang, J., Dong, W., 2017. Salecan-Based pH-Sensitive Hydrogels for Insulin Delivery. Mol. Pharm. 14, 431–440. https://doi.org/10.1021/acs.molpharmaceut.6b00875

Queiroz, M.F., Rachel, K., Melo, T., Sabry, D.A., Sassaki, G.L., Alexandre, H., Rocha, O., 2014. Does the Use of Chitosan Contribute to Oxalate Kidney Stone Formation. Mar. Drugs 13, 141–158. https://doi.org/10.3390/md13010141

Racine, L., Texier, I., Auzély-Velty, R., 2017. Chitosan-based hydrogels: recent design concepts to tailor properties and functions. Polym. Int. 66, 981–998. https://doi.org/10.1002/pi.5331

Razavi-Shearer, D., Gamkrelidze, I., Nguyen, M.H., Chen, D.S., Van Damme, P., Abbas, Z., Abdulla, M., Abou Rached, A., Adda, D., Aho, I., Akarca, U., Al Ali, F.H., Lawati, F.A.L., Naamani, K.A.L., Alashgar, H.I., Alavian, S.M., Alawadhi, S., Albillos, A., Al-Busafi, S.A., Aleman, S., Alfaleh, F.Z., Aljumah, A.A., Anand, A.C., Anh, N.T., Arends, J.E., Arkkila, P., Athanasakis, K., Bane, A., Ben-Ari, Z., Berg, T., Bizri, A.R., Blach, S., Brandão Mello, C.E., Brandon, S.M., Bright, B., Bruggmann, P., Brunetto, M., Buti, M., Chan, H.L.Y., Chaudhry, A., Chien, R.N., Choi, M.S., Christensen, P.B., Chuang, W.L., Chulanov, V., Clausen, M.R., Colombo, M., Cornberg, M., Cowie, B., Craxi, A., Croes, E.A., Cuellar, D.A., Cunningham, C., Desalegn, H., Drazilova, S., Duberg, A.S., Egeonu, S.S., El-Sayed, M.H., Estes, C., Falconer, K., Ferraz, M.L.G., Ferreira, P.R., Flisiak, R., Frankova, S., Gaeta, G.B., García-Samaniego, J., Genov, J., Gerstoft, J., Goldis, A., Gountas, I., Gray, R., Guimarães Pessôa, M., Hajarizadeh, B., Hatzakis, A., Hézode, C., Himatt, S.M., Hoepelman, A., Hrstic, I., Hui, Y.T.T., Husa, P., Jahis, R., Janjua, N.Z., Jarcuš ka, P., Jaroszewicz, J., Kaymakoglu, S., Kershenobich, D., Kondili, L.A., Konysbekova, A., Krajden, M., Kristian, P., Laleman, W., Lao, W.C.C., Layden, J., Lazarus, J. V., Lee, M.H., Liakina, V., Lim, Y.S.S., Loo, C.K.K., Lukš ic, B., Malekzadeh, R., Malu, A.O., Mamatkulov, A., Manns, M., Marinho, R.T., Maticic, M., Mauss, S.,

Memon, M.S., Mendes Correa, M.C., Mendez-Sanchez, N., Merat, S., Metwally, A.M., Mohamed, R., Mokhbat, J.E., Moreno, C., Mossong, J., Mourad, F.H., Müllhaupt, B., Murphy, K., Musabaev, E., Nawaz, A., Nde, H.M., Negro, F., Nersesov, A., Nguyen, V.T.T., Njouom, R., Ntagirabiri, R., Nurmatov, Z., Obekpa, S., Ocama, P., Oguche, S., Omede, O., Omuemu, C., Opare-Sem, O., Opio, C.K., Örmeci, N., Papatheodoridis, G., Pasini, K., Pimenov, N., Poustchi, H., Quang, T.D., Qureshi, H., Ramji, A., Razavi-Shearer, K., Redae, B., Reesink, H.W., Rios, C.Y., Rjaskova, G., Robbins, S., Roberts, L.R., Roberts, S.K., Ryder, S.D., Safadi, R., Sagalova, O., Salupere, R., Sanai, F.M., Sanchez-Avila, J.F., Saraswat, V., Sarrazin, C., Schmelzer, J.D., Schréter, I., Scott, J., Seguin-Devaux, C., Shah, S.R., Sharara, A.I., Sharma, M., Shiha, G.E., Shin, T., Sievert, W., Sperl, J., Stärkel, P., Stedman, C., Sypsa, V., Tacke, F., Tan, S.S., Tanaka, J., Tomasiewicz, K., Urbanek, P., van der Meer, A.J., Van Vlierberghe, H., Vella, S., Vince, A., Waheed, Y., Waked, I., Walsh, N., Weis, N., Wong, V.W., Woodring, J., Yaghi, C., Yang, H.I., Yang, C.L., Yesmembetov, K., Yosry, A., Yuen, M.F., Yusuf, M.A.M., Zeuzem, S., Razavi, H., 2018. Global prevalence, treatment, and prevention of hepatitis B virus infection in 2016: a modelling study. Lancet Gastroenterol. Hepatol. 3, 383–403. https://doi.org/10.1016/S2468-1253(18)30056-6

Razavi, H., 2020. Global Epidemiology of Viral Hepatitis. Gastroenterol. Clin. North Am. 49, 179–189. https://doi.org/10.1016/j.gtc.2020.01.001

Ren, K., He, C., Cheng, Y., Li, G., Chen, X., 2012. Injectable Enzymatically-crosslinked Hydrogels Based on Poly (L-glutamic acid) Graft Copolymer. Polym. Chem. 00, 1–8. https://doi.org/10.1039/x0xx00000x

Rizwan, M., Yahya, R., Hassan, A., Yar, M., Azzahari, A.D., Selvanathan, V., Sonsudin, F., Abouloula, C.N., 2017. pH sensitive hydrogels in drug delivery: Brief history, properties, swelling, and release mechanism, material selection and applications. Polymers (Basel). 9, 1–37. https://doi.org/10.3390/polym9040137

Saboktakin, M.R., Tabatabaie, R.M., Maharramov, A., Ramazanov, M.A., 2011. Development and in vitro evaluation of thiolated chitosan-Poly(methacrylic acid) nanoparticles as a local mucoadhesive delivery system. Int. J. Biol. Macromol. 48, 403–407.

https://doi.org/10.1016/j.ijbiomac.2010.12.014

Sanjay, S.T., Zhou, W., Dou, M., Tavakoli, H., Ma, L., Xu, F., Li, X.J., 2018. Recent advances of controlled drug delivery using microfluidic platforms. Adv. Drug Deliv. Rev. 128, 3–28. https://doi.org/10.1016/j.addr.2017.09.013

Sarah, S., Vellozzi, C., Reingold, A., Harris, A., Haber, P., Ward, J.W., Nelson, N.P., 2018. Prevention of Hepatitis B Virus Infection in the United States: Recommendations of the Advisory Committee on Immunization Practices, Center for Disease Control and Prevention NMWR. https://doi.org/10.1111/j.1468-0289.1991.tb01269.x

Savoji, M.T., Pourjavadi, A., 2006. Carrageenan — Polyacrylonitrile as a Novel Biopolymer-Based Superabsorbent Hydrogel : Synthesis , Characterization , and Swelling Behaviors. Polym. Eng. Sci. 1779–1786. https://doi.org/10.1002/pen

Shi, W., Dumont, M., Babacar, E., 2014. Synthesis and properties of canola protein-based superabsorbent hydrogels. Eur. Polym. J. 54, 172–180. https://doi.org/10.1016/j.eurpolymj.2014.03.007

Silva, J.P.A., Figueirêdo, C.B.M., de Medeiros Vieira, A.C.Q., de Lyra, M.A.M., Rolim, L.A., Rolim-Neto, P.J., de La Roca Soares, M.F., Albuquerque, M.M., Soares-Sobrinho, J.L., 2017. Thermal characterization and kinetic study of the antiretroviral tenofovir disoproxil fumarate. J. Therm. Anal. Calorim. 130, 1643–1651. https://doi.org/10.1007/s10973-017-6477-z

Singhal, R., Gupta, K., 2015. A Review : Tailor-Made Hydrogel Structures (Classifications and Synthesis Parameters). Polym. Plast. Technol. Eng. 2559. https://doi.org/10.1080/03602559.2015.1050520

Sokker, H.H., Abdel Ghaffar, A.M., Gad, Y.H., Aly, A.S., 2009. Synthesis and characterization of hydrogels based on grafted chitosan for the controlled drug release. Carbohydr. Polym. 75, 222–229. https://doi.org/10.1016/j.carbpol.2008.06.015

Song, J.E., Kim, D.Y., 2016. Diagnosis of hepatitis B. Ann. Transl. Med. 4, 1–6. https://doi.org/10.21037/atm.2016.09.11

Sood, N., Bhardwaj, A., Mehta, S., Mehta, A., 2016a. Stimuli-responsive hydrogels in drug delivery and tissue engineering. Drug Deliv. 23, 758–780. https://doi.org/10.3109/10717544.2014.940091

Sood, N., Bhardwaj, A., Mehta, S., Mehta, A., Sood, N., Bhardwaj, A., Mehta, S., Mehta, A., 2016b. Stimuli-responsive hydrogels in drug delivery and tissue engineering. Drug Deliv. 23, 748–770. https://doi.org/10.3109/10717544.2014.940091

Spearman, C.W., Afihene, M., Ally, R., Apica, B., Awuku, Y., Cunha, L., Dusheiko, G., Gogela, N., Kassianides, C., Kew, M., Lam, P., Lesi, O., Lohouès-Kouacou, M.J., Mbaye, P.S., Musabeyezu, E., Musau, B., Ojo, O., Rwegasha, J., Scholz, B., Shewaye, A.B., Tzeuton, C., Sonderup, M.W., 2017. Hepatitis B in sub-Saharan Africa: strategies to achieve the 2030 elimination targets. Lancet Gastroenterol. Hepatol. 2, 900. https://doi.org/10.1016/S2468-1253(17)30295-9

Sun, D., Zhu, L., Yao, D., Chen, L., Fu, L., Ouyang, L., 2018. Recent progress in potential anti-hepatitis B virus agents: Structural and pharmacological perspectives. Eur. J. Med. Chem. 147, 205–217. https://doi.org/10.1016/j.ejmech.2018.02.001

Tan, M., Bhadoria, A.S., Cui, F., Tan, A., Van Holten, J., Easterbrook, P., Ford, N., Han, Q., Lu, Y., Bulterys, M., Hutin, Y., 2021. Estimating the proportion of people with chronic hepatitis B virus infection eligible for hepatitis B antiviral treatment worldwide: a systematic review and meta-analysis. Lancet Gastroenterol. Hepatol. 6, 106–119. https://doi.org/10.1016/S2468-1253(20)30307-1

Tang, C., Yau, T.O., Yu, J., 2014. Management of chronic hepatitis B infection : Current treatment guidelines , challenges , and new developments. World J. Gastroenterol. 20, 6262–6278. https://doi.org/10.3748/wjg.v20.i20.6262

Tiollais, P., Pourcel, C., Dejean, A., 1985. The hepatitis B virus. Nature 317, 489–495.

Tong, S., Pan, J., Lu, S., Tang, J., 2018. Patient compliance with antimicrobial drugs: A Chinese survey. Am. J. Infect. Control 46, e25–e29. https://doi.org/10.1016/j.ajic.2018.01.008

Ulijn, R. V., Bibi, N., Jayawarna, V., Thornton, P.D., Todd, S.J., Mart, R.J., Smith, A.M., Gough, J.E., 2007. Bioresponsive hydrogels. Mater. Today 10, 40–48.

https://doi.org/10.1016/S1369-7021(07)70049-4

Ullah, F., Othman, M.B.H., Javed, F., Ahmad, Z., Akil, H.M., 2015. Classification, processing and application of hydrogels: A review. Mater. Sci. Eng. C 57, 414–433. https://doi.org/10.1016/j.msec.2015.07.053

Valaydon, Z.S., Locarnini, S.A., 2017. The virological aspects of hepatitis B. Best Pract. Res. Clin. Gastroenterol. 31, 257–264. https://doi.org/10.1016/j.bpg.2017.04.013

Varaprasad, K., Raghavendra, G.M., Jayaramudu, T., Yallapu, M.M., Sadiku, R., 2017. A mini review on hydrogels classification and recent developments in miscellaneous applications. Mater. Sci. Eng. C 79, 958–971. https://doi.org/10.1016/j.msec.2017.05.096

Wang, Y., Wang, J., Yuan, Z., Han, H., Li, T., Li, L., Guo, X., 2017. Chitosan cross-linked poly(acrylic acid) hydrogels: Drug release control and mechanism. Colloids Surfaces B Biointerfaces 152, 252–259. https://doi.org/10.1016/j.colsurfb.2017.01.008

Wang, Y., Yang, N., Wang, D., He, Y., Chen, L., Zhao, Y., 2018. Poly (MAH-β-cyclodextrin-co-NIPAAm) hydrogels with drug hosting and thermo/pH-sensitive for controlled drug release. Polym. Degrad. Stab. 147, 123–131. https://doi.org/10.1016/j.polymdegradstab.2017.11.023

Woraphatphadung, T., Sajomsang, W., Rojanarata, T., Ngawhirunpat, T., Tonglairoum, P., Opanasopit, P., 2018. Development of Chitosan-Based pH-Sensitive Polymeric Micelles Containing Curcumin for Colon-Targeted Drug Delivery. AAPS PharmSciTech 19, 991–1000. https://doi.org/10.1208/s12249-017-0906-y

Yang, J.A., Yeom, J., Hwang, B.W., Hoffman, A.S., Hahn, S.K., 2014. In situ-forming injectable hydrogels for regenerative medicine. Prog. Polym. Sci. 39, 1973–1986. https://doi.org/10.1016/j.progpolymsci.2014.07.006

Yao, K., Li, J., Yao, F., Yin, Y., 2012. Chitosan-based hydrogels: functions and Applications. Taylor & Francis.

Zhang, K., Feng, W., Jin, C., 2019. Protocol Efficiently Measuring the Swelling Rate of Hydrogels. MethodsX 1–13. https://doi.org/10.1016/j.mex.2019.100779

Zhang, Y.-Y., Hu, K.-Q., 2015. Rethinking the Pathogenesis of Hepatitis B Virus (HBV) Infection. J. Med. Virol. 87, 1989–1999. https://doi.org/10.1002/jmv

Zhou, K., Terrault, N., 2017. Management of hepatitis B in special populations. Best Pract. Res. Clin. Gastroenterol. 31, 311–320. https://doi.org/10.1016/j.bpg.2017.06.002

Zrinyi, N., Pham, A.L.T., 2017. Oxidation of benzoic acid by heat-activated persulfate: Effect of temperature on transformation pathway and product distribution. Water Res. 120, 43–51. https://doi.org/10.1016/j.watres.2017.04.066